Adipose tissue dysfunction in obesity: modulation of cellular stress responses by melanocortins.

Nádia da Silva Fernandes Lucas
Master´s student in Cell and Molecular Biology - FCUP

Biomedicine Department, Unit of Experimental Biology, Faculty of Medicine, University of Porto
Ageing & Stress Group, i3S/IBMC – Instituto de Investigação e Inovação em Saúde/Instituto de Biologia Celular e Molecular, University of Porto

2020

Advisor
Adriana Raquel Rodrigues, Junior Researcher

Biomedicine Department, Unit of Experimental Biology, Faculty of Medicine, University of Porto
Ageing & Stress Group, i3S/IBMC – Instituto de Investigação e Inovação em Saúde/Instituto de Biologia Celular e Molecular, University of Porto

Co-advisor
Alexandra Maria Gouveia, Assistant Professor

Faculty of Medicine and Faculty of Nutrition and Food Science of Porto´s University.
Ageing & Stress Group, I3S/IBMC – Instituto de Investigação e Inovação em Saúde/Instituto de Biologia Celular e Molecular, University of Porto

U.PORTO
FACULDADE DE CIÊNCIAS
UNIVERSIDADE DO PORTO

Todas as correções determinadas pelo júri, e só essas, foram efetuadas.

O Presidente do Júri,

Porto, _____/_____/_____

CONFERENCE COMMUNICATIONS

The work developed in this dissertation has been presented partially or integrally in the following scientific meetings:

1) National and international oral communications

October 30th, 2019

11th Symposium on Metabolism – Ageing & Metabolism
University of Porto

Silva, N.; Salazar, M. J.; Silva, E.; Neves, D.; Almeida, H.; Gouveia, A. M.; Rodrigues, A. R. (2019) Beneficial effects of melanocortins on obesity-related metabolic dysfunction: a focus on the adipose tissue features of premature ageing. Abstract book pp. 44.

February 13th, 2020

13th Encontro de Jovens Investigadores da Universidade do Porto (IJUP20)
University of Porto

Silva, N.; Salazar, M. J.; Silva, E.; Neves, D.; Almeida, H.; Gouveia, A. M.; Rodrigues, A. R. (2020) Melanocortins act as stress-response modulators in adipose tissue of obese mice. Book of Abstracts, number 16921.

Presentation distinguished in the "Health Science" session.

September 17th – 20 th, 2020

15th YES Meeting Digital Experience
University of Porto

Silva, N.; Salazar, M. J.; Silva, E.; Neves, D.; Almeida, H.; Gouveia, A. M.; Rodrigues, A. R. (2020) Melanocortins repress stress-specific responses to attenuate oxidative damage of adipose tissue in obesity

September 28th – 30th, 2020

1st EUGLOH Annual Student Research Conference – Global Health Challenges: Diseases of Modern Life
University of Szeged

Silva, N.; Gouveia, A. M.; Rodrigues, A. R. (2020) α-MSH reestablishes homeodynamics of obese adipose tissue by modulating cellular stress responses.

Presentation invited by the University of Porto.
Presentation distinguished in the "Noncommunicable and pandemic diseases" session.

2) Poster communication

November 28th - 30th, 2019

8th I3S annual meeting
University of Porto

Silva, N.; Salazar, M. J.; Silva, E.; Neves, D.; Almeida, H.; Gouveia, A. M.; Rodrigues, A. R. (2019) Alfa-MSH decreases cellular stress responses in ingWAT of obese mice. Abstract Book pp. 317.

"Imagination is everything.

It is the preview of life's coming attractions."

- Albert Einstein

À minha mãe.

AGRADECIMENTOS

A elaboração desta dissertação não seria possível sem o contributo de enumeras pessoas, com quem muito aprendi este ano, e aqui quero humildemente agradecer.

Começo por agradecer aos que mais de perto trabalharam comigo para a elaboração desta dissertação de mestrado. Começo por agradecer ao Professor Doutor Henrique Almeida pela oportunidade de integrar o seu grupo "Ageing and Stress". Agradeço à minha orientadora, Doutora Adriana Rodrigues, por todo o incentivo e por todo o préstimo neste trabalho. Adicionalmente, agradeço também à minha coorientadora, Professora Doutora Alexandra Gouveia, por todo o apoio prestado nesta dissertação. Deixo também uma palavra de reconhecimento aos restantes membros do grupo, por todo o apoio e alegria que trouxeram aos meus dias. O meu maior abraço também vai para todos aqueles que me apoiaram no departamento de biomedicina da FMUP, em especial à técnica Anabela Silvestre, que mesmo sem obrigatoriedade sempre me auxiliaram quando necessitava.

Em seguida, gostaria de agradecer à direção do mestrado em Biologia Celular e Molecular pelo apoio prestado durante estes dois anos. Assim, à Professora Doutora Conceição Santos e ao Professor Doutor José Américo Sousa agradeço toda a dedicação e estima. Sem vós, e todos os nossos professores de mestrado, não teria encontrado o meu rumo profissional tão celeremente.

A amizade e apoio incondicional daqueles que a nós são mais próximos revelam-se fulcrais nos momentos determinantes da nossa vida. De facto, sou uma mulher afortunada por ter um grupo de amigos tão benevolente. Dito isto, gostaria de começar por agradecer ao grupinho das mitocôndrias, que tem sido uma das mais importantes fontes de energia para mim nesta jornada. Ao Luís Póvoas agradeço todo o encorajamento, todo o carinho, todas as conversas infinitas sobre tudo e sobre nada; e acima de tudo, pelo seu inigualável companheirismo (e paciência... existem dias em que não é fácil conviver comigo). À Ana Patrícia Gomes agradeço todos as palavras reconfortantes e todos os sorrisos contagiantes. À Catarina Príncipe agradeço as suas palavras sábias e todo o incentivo. À Marta Ramos reconheço toda a serenidade que consegue trazer a qualquer situação e todo o seu apoio. O nosso grupinho foi um dos melhores presentes que o mestrado me trouxe. Gostaria também de agradecer às minhas amigas e companheiras de casa no Porto (Marina Pimentel, Melissa Abreu, Mariana Sá, Tânia Carvalho e Patrícia Nogueira), por toda a alegria, apoio e afeição. Obrigado por transformarem a nossa casa num lar feliz. Aos meus amigos de longa data agradeço todo

o companheirismo e carinho, que felizmente nem a distância foi capaz de atenuar. À Susana Fernandes, Susana Castro, Nicolau Correia, Jovita Freitas, Mariana Franco e Luísa Rodrigues agradeço toda a paciência, amparamento e amizade incondicional.

A todos vós amigos, obrigada por acreditarem em mim, mesmo quando nem já eu acreditava. A vossa amizade foi muito importante para mim neste ano, e sem vocês, esta dissertação provavelmente não veria a luz do dia.

Não podia também deixar de agradecer à minha família, por tudo o que sempre fizeram por mim. Somos poucos, mas somos bons. Queria agradecer à minha avó Maria por todo o carinho e por todo o encorajamento. É uma das pessoas mais inteligentes e determinadas que conheço, sendo por isso para mim uma grande fonte de inspiração na minha vida. Outro grande exemplo de vida, e a quem muito tenho de agradecer, é à minha mãe. Exemplarmente todos os dias me mostra que com uma boa dose de paixão, uma pitada de destemor e outras duas de resiliência; temos tudo o que necessitamos para seguir os nossos sonhos. Agradeço todo amor e por sempre me incentivar a seguir em frente sem medos (mesmo nas minhas ideias mais malucas). Por tudo isto, e muito mais, estou a si eternamente grata.

Termino agradecendo à vida por todas as pessoas e situações com que me presenteou. Sinto-me grata. Todos os dias são a prova, que os milagres, realmente existem.

RESUMO

A progressiva disfunção do tecido adiposo (TA) é um processo chave na patologia da obesidade. À medida que o TA perde a capacidade de armazenar adequadamente o excesso de energia, os mecanismos de resposta ao stresse e reparação celular ficam gravemente comprometidos; contribuindo assim para a destabilização sistémica da homeodinâmica metabólica e redox.

O sistema das melanocortinas tem sido amplamente estudado pela sua ação no sistema nervoso central, onde regula mecanismos de controlo de apetite. No entanto, o sistema das melanocortinas também contribui para a modulação da homeodinâmica energética em tecidos periféricos, tais como o TA. Recentemente, o nosso grupo mostrou que a hormona alfa-estimuladora de melanócitos (α-MSH), há muito conhecida por promover sinais de saciedade no sistema nervoso central, promove o dispêndio energético através da estimulação de "browning" do TA em ratinhos obesos. Além disso, ratinhos obesos tratados com α-MSH perderam peso e massa gorda; e exibiram um perfil lipídico e glicêmico melhorado [1]. Assim, tendo em consideração a melhora geral do perfil metabólico de animais tratados com α-MSH, tentamos compreender na presente dissertação, se essa melhoria ocorre concomitantemente com a modulação de respostas celulares ao stresse e mecanismos de autofagia; sendo que estes se encontram comumente desregulados na obesidade.

Para o efeito, ratinhos C57BL/6 cuja obesidade foi induzida por uma dieta hiperlipídica, foram injetados intraperitonealmente com α-MSH (150μg/Kg/dia) ou solução salina por duas semanas. Em seguida, o tecido adiposo branco subcutâneo inguinal (ingTAS) foi colhido, e na presente dissertação, utilizado na análise de biomarcadores de stresse de retículo endoplásmico, stresse oxidativo e autofagia; através das técnicas de western-blot e qPCR. Adicionalmente, os níveis de peróxido de hidrogénio foram avaliados com a kit Amplex® Red e a carbonilaçáo proteica através da técnica de Oxyblot.

Os dados obtidos no âmbito desta dissertação demonstraram que a α-MSH modula de forma distinta as três principais vias de sinalização de stresse do retículo endoplasmático: apesar de ser capaz de atenuar as vias de sinalização da PERK e IRE1α, foi incapaz de modular a via da ATF6α. Em concordância com a atenuação destes dois mecanismos de stresse de retículo endoplasmático no TA obeso, também se notou a benfeitoria das respostas de stresse oxidativo em animais tratados com α-MSH. Foi possível observar o contributo da α-MSH para atenuação das defesas antioxidantes em ingTAS, bem como nos níveis de ativação do fator de transcrição geral de stresse NF-κB,

possivelmente associados com a diminuição tendencial dos níveis de peróxido de hidrogénio neste tecido. Mais marcante, suportando a atenuação mediada por α-MSH do estresse oxidativo em ingTAS, níveis reduzidos de proteínas carboniladas foram observados em animais tratados com esta melanocortina. Juntamente com o esmorecimento das respostas de estresse de ER e oxidativo, e níveis diminutos de biomoléculas danificadas; ingTAS de animais tratados com α-MSH exibiram uma atenuação das respostas de autofagia, conforme demonstrado pelos níveis diminuídos significativos de proteínas relacionadas à autofagia (por exemplo, ATG16L1β e LAMP1 glicosilado).

Em suma, a presente dissertação enfatiza um novo potencial terapêutico para a melanocortina α-MSH; que através da modulação das vias de estresse celular e mecanismos de autofagia, parece ajudar no restabelecimento da homeodinâmica redox no ingTAS na obesidade.

Palavras-chave:

Obesidade, tecido adiposo, melanocortinas, homeodinâmica celular, stresse ER, stresse oxidativo, autofagia e dano das biomoléculas.

ABSTRACT

The progressive dysfunction of adipose tissue (AT) constitutes a key process in the pathogenesis of obesity. As AT loses the ability to properly store energy surplus, adipose stress responses and cellular repair mechanisms become severely compromised, further contributing to impaired whole-body metabolic and redox dynamics.

The melanocortin system has been extensively studied for its action in the central nervous system, where it controls feeding behavior. However, this conserved pathway also modulates energy homeodynamics in peripheral tissues, as in AT. Recently our group has demonstrated that the melanocortin α-melanocyte stimulating hormone (α-MSH) induces energy expenditure by stimulating AT "browning" in obese mice. In addition, α-MSH-treated mice lost weight and fat mass, and exhibited an improved lipid and glycemic profile [1]. We therefore attempted to comprehend in the present dissertation, if the overall amelioration of the metabolic profile of obese α-MSH-treated mice occurs alongside with the modulation of cellular stress responses and autophagy mechanisms in AT, which are commonly dysregulated in obesity.

To do so, subcutaneous white adipose tissue from diet-induced obese C57BL/6 mice, intraperitoneally injected with α-MSH (150μg/Kg/day) or saline solution for two weeks was used for the analysis of ER-stress, oxidative stress and autophagy biomarkers through western-blotting and qPCR techniques. Also, levels of hydrogen peroxide were measured using the Amplex® Red kit and protein carbonylation through the Oxyblot technique.

Data obtained in the scope of this dissertation demonstrated that α-MSH modulates the three main ER-stress responses distinctively: while it attenuated both PERK and IRE1α signaling pathway, it was unable to alter ATF6α signaling. Concordantly with the attenuation of these two arms of the UPR in obese adipose tissue, it was observed the amelioration of oxidative stress responses in α-MSH treated animal. It was possible to show that α-MSH decreased the antioxidant defenses of obese ingWAT, as well as the activation of general stress transcription factor NF-κB, which possibly correlates with the tendency to observe reduced levels of hydrogen peroxide in this tissue. Most importantly, adding evidence for an α-MSH-mediated attenuation of oxidative stress in ingWAT, decreased levels of carbonylated proteins were found in α-MSH-treated obese mice. Alongside with the modulation of both ER-stress and oxidative stress responses, and diminished levels of damaged biomolecules, obese adipose tissue of α-MSH-treated

animals exhibited an attenuation of autophagy responses, as demonstrated by the significant diminished levels of autophagy-related proteins (e.g. ATG16L1β and glycosylated LAMP1).

In sum, the present thesis emphasizes a new potential therapeutic role for melanocortin α-MSH, suggested to aid in the reestablishment of redox homeodynamics of obese ingWAT through the modulation of cellular stress response pathways and autophagy mechanisms.

Keywords:

Obesity, adipose tissue, melanocortins, cellular homeodynamics, ER stress, oxidative stress, autophagy and biomolecule damage.

TABLE OF CONTENTS

TABLE OF INDEX

FIGURE INDEX

ABBREVIATIONS

•OH	Hydroxyl radical
•NO	Nitrogen monoxide
•NO_2	Nitrogen dioxide
ACTH	Adrenocorticotropic hormone
AgRP	Agouti-related protein
AKT	Protein kinase B
ARC	Arcuate nucleus of the hypothalamus
ASIP	Agouti-signaling protein
AT	Adipose tissue
ATF	Activating transcription factor
ATG	Autophagy-related proteins
ATP	Adenosine triphosphate
BAT	Brown adipose tissue
BiP	Glucose-regulated protein 78 / immunoglobulin-heavy chain-binding protein
BMI	Body mass index
cAMP	Cyclic adenosine monophosphate
CART	Cocaine-and-amphetamine-regulated transcript
CHOP	CCAAT/enhancer-binding protein homologous protein
CLS	Crown-like structure
Clu	Clusterin / Apolipoprotein J
CNS	Central nervous system
DIO	Diet-induced obese

DMH	Dorsomedial hypothalamic nucleus
DNPH	2,4-Dinitrophenylhydrazine
DUOX	Dual oxidase relatives
ECM	Extracellular matrix
ER	Endoplasmic reticulum
ERK1/2	Extracellular signal-regulated kinase 1/2
ETC	Electron transport chain
$FADH_2$	Reduced flavin adenine dinucleotide
Fe^{2+}	Ferrous iron
Fe^{3+}	Ferric iron
FOXC2	Forkhead box protein C2
GC	Golgi complex
GPCR	G-coupled protein receptor
GPx	Glutathione peroxidase
H_2O_2	Hydrogen peroxide
HIF1	Hypoxia-inducible factor 1
HNE	4-hydroxinonenal
HO-1	Heme oxygenase 1
HOCl	Hypochlorous acid
HSP90	Heat shock protein 90
IRE1α	Inositol requiring enzyme 1 alpha
JAK	Janus protein kinase
JNK	Jun-N-terminal kinase
LAMP	Lysosome-associated membrane glycoprotein

LH	Lateral hypothalamus
MAPK	Mitogen-activated protein kinase
MCR	Melanocortin receptor
mDNA	Mitochondrial DNA
MRAP	Melanocortin receptor associated protein
mTORC1	Mammalian target of rapamycin complex 1
NADH	Reduced nicotinamide adenine dinucleotide
NADPH	Reduced nicotinamide adenine dinucleotide phosphate
NEFA	Non-esterified fatty acid
NF-κB	Nuclear factor kappa B
NOS	Nitric oxide synthase
NOX	Nicotinamide adenine dinucleotide phosphate oxidase
Nrf2	Erythoid 2–related factor 2
NTS	Nucleus of the solitary tract
NPY	Neuropeptide Y
$O_2^{\bullet-}$	Superoxide anion
ONO_2^-	Peroxynitrite anion
OxPhos	Oxidative phosphorylation
p62	Sequestosome-1
PC	Pro-hormone-converting enzyme
PERK	Protein kinase R-like endoplasmic reticulum kinase
p-H2AX	Phosphorylated H2A histone family member X
PI3K	Phosphatidylinositol-3-kinase
PI3P	Phosphatidylinositol-3-phosphate

PKA	Protein kinase A
PKC	Protein kinase C
POMC	Pro-opiomelanocortin hormone
PVH	Paraventricular nucleus of the hypothalamus
Q	Ubiquinone
R•	Reactive species
RNS	Reactive nitrogen species
ROS	Reactive oxygen species
SAT	Subcutaneous white adipose tissue
STAT	Signal transducers and activators of transcription
SOD	Superoxide dismutase
TG	Triglyceride
TLR	Toll-like receptors
UCP-1	Uncoupling protein 1
ULK	Atg1–unc-51-like kinase
VAT	Visceral white adipose tissue
VMH	Ventromedial hypothalamus
WAT	White adipose tissue
WHO	World Health Organization
Xbp1	X-box binding protein 1
α-MSH	Alpha-melanocyte stimulating hormone
β-LPH	β-lipotropin

1. INTRODUCTION

Obesity prevalence has increased considerably in the past couple of decades, nearly tripling since 1975, according to the World Health Organization (WHO) [2]. At the present time WHO estimates that more than 1.9 billion adults are overweight worldwide, of which at least 650 million are obese [2]. Despite all public and individual health efforts to halt obesity, its prevalence shows no sign of slowing down. If post-2000 trends continue, by 2025, obesity is expected to affect 18% of men and surpass 21% of woman worldwide [3].

Regrettably, this global trend is also beheld in Portugal, as epidemiological studies demonstrated that in only 10 years (2005-2015), obesity prevalence nearly doubled [4]. At the present date, both overweight and obesity affect more than 2/3 of the Portuguese population, putting Portugal at the top of the list of European countries with the highest prevalence of these pathologies [4, 5].

Even more startling, as obesity is considered a major risk factor for the development of other diseases, the incidence of these are also expected to increase. Besides significantly reduce life expectancy, obesity and related disorders negatively influence the life quality of those affected. Beyond impairing health, the sociological and socioeconomic impacts of obesity cannot similarly be overlooked.

Even though the obesity research has improved in the past couple of decades, we are still losing the battle against this pandemic. Still, a deeper knowledge on the molecular mechanisms of obesity pathophysiology is necessary, in order to strengthen the foundations for the development of new efficient therapeutic strategies.

1.1 AN EVOLUTIONARY PERSPECTIVE OF OBESITY PANDEMIC

The rising prevalence of obesity in our society is a recent phenomenon on *Homo sapiens* evolution. Large-scale genome-wide association studies have identified more than 405 genes in humans which contribute to obesity development; however, it is known that not all “obesity genes” carriers become overweight or obese [6, 7]. In fact, monogenic causes of obesity are relatively rare and cannot explain the current observed trend [7, 8]. Instead, the recent increased incidence of obesity seems to positively correlate with the “Westernization” of lifestyle in our civilization, which propensities an obesogenic environment by stimulating the consumption of energy-dense foods whilst

encouraging a sedentary lifestyle [8-10]. Thereby, genetic predisposition to accumulate fat, alongside with the modern obesogenic environment, seem to be the leading cause underlying the recent spread of obesity pathology [6]. The genetic, environmental and psychosocial factors act through a wide range of physiological mediators of food intake and energy expenditure, which are known to affect fat deposition, further contributing to obesity development and progression [11]. Indeed, it is becoming increasingly evident that obesity aetiology is remarkably complex.

1.2 EAETHIOLOGY AND DEFINITION OF OBESITY

Newton´s first law of thermodynamics states that energy cannot be created or destroyed. Therefore, the energy required for the fuelling of body functions must be acquired from ingested food. In order to ensure that whole-body energy homeodynamics is not compromised, regulation of energy intake, expenditure and storage is tightly under the control of interconnected neuronal and endocrine systems [11]. Nonetheless, when consumed energy exceeds metabolic expenditure rates, energy surplus is stored in the form of high-energy molecules: (1) generally in the form of glycogen in the liver and muscle and (2) specially in the form of triglycerides (60-80%) in the adipose tissue (AT) [12]. A continuous positive energy balance fuels the excessive accumulation of fat in AT, leading to overweight and obesity development.

Obesity has been recognized as a complex chronic progressive disease, defined by WHO as “an abnormal or excessive fat accumulation that may impair health” [2]. Clinically, weight excess is commonly appraised by the body mass index (BMI) [Weight (kg)/ Height^2 (m)], with overweight and obesity being characterized by a BMI ≥ 25 Kg/m^2 and ≥ 30 Kg/m^2, respectively. Frequently, BMI measurements are complemented with waist circumference and waist-hip ratio measurements, in order to more realistically stratify health risks [13]. Notwithstanding other methods are available to assess body fat content, which vary on their: accuracy, convenience, cost and safety requirements. These include densitometry, bioelectrical impedance analysis, anthropometry, dual-energy X-ray absorptiometry and advanced imaging-based methods (such as computed tomography and magnetic resonance techniques) [14, 15].

Obesity is a major risk factor for the development of more than 200 chronic diseases [16], such as: metabolic diseases (e.g., type 2 diabetes mellitus and fatty liver disease) [17], cardiovascular diseases (e.g., hypertension, atherosclerosis, myocardial

infraction) [18, 19], musculoskeletal disorders (e.g., osteoarthritis) [20] and some types of cancers (e.g., breast, liver, ovarian, prostate, kidney, gallbladder, colon among others), just to name a few [21, 22].

Intriguingly, it was observed that one subset of obese individuals seems to be protected against obesity-induced metabolic complications [23]. Hence, excessive fat accumulation and obesity are *per se* insufficient to explain the incidence of obesity-related comorbidities. Instead, it is suggested that the development of the aforementioned diseases are primarily related with regional distribution of fat and how adipocytes expand to accommodate energy surplus [24, 25], demonstrating the importance of AT for obesity pathophysiology progression.

1.3 ADIPOSE TISSUE BIOLOGY

The days when AT was considered an inert organ are long gone. Classically, AT has been viewed as responsible for the protection of internal organs and sensible regions against mechanical stress. But AT is now recognised as an essential player in energy metabolism and thermoregulation processes [26, 27]. Indeed, AT has been acknowledged as an important endocrine organ, responsible for the production and secretion of adipokines (mainly leptin and adiponectin); as well as other biological active compounds, such as: lipids, proteins, microRNAs and growth differentiation factors [28, 29]. Through the synthesis and secretion of bioactive molecules, AT aptly communicates and coordinates cellular responses with other organs in the body. In fact, it is so important that studies on pathologies characterized by either a deficit (lipodystrophy) or excess (overweight and obesity) adiposity have demonstrated that a certain amount of AT is necessary to maintain heath and a normal metabolism [30].

1.3.1. Adipose tissue heterogeneity and adipocyte dynamics

In mammals, distinct AT depots are distributed throughout the body, occupying specific anatomical locations and performing well-determined biological functions. Albeit different, AT depots architecture is characterized by a complex 3D poly-lobular structure, which exhibits signature functionality [31]. Each AT lobule is constituted by adipocyte and non-adipocyte cells embedded in a matrix of loose connective tissue.

Data acquired from lineage tracing approaches has demonstrated that adipocytes exhibit an heterogeneous nature (derive from distinct precursor populations), although the majority can be traced back to the mesoderm [28]. In fact, discrete sub-populations of adipocytes, with specific metabolic and secretory properties, have not only been described in distinct fat depots but also within a specific depot [29]. Although adipocytes predominate in AT, representing nearly 1/3 of all AT cells [26, 32], other cell types contribute to the structural integrity and function of this organ. These comprise blood cells, endothelial cells, mast cells, pericytes, vascular smooth muscle cells, resident immune cells (such as monocytes, macrophages and lymphocytes), neuronal cells, mesenchymal stem cells, fibroblasts, adipose precursor cells among others [33, 34].

Each fat type, due to genetic and development events, exhibits specific histological and metabolic features, which ultimately dictates it's function [32]. Till today, at least four distinct types of AT have been described in both humans and rodents: white AT (WAT), brown AT (BAT), “browned”/”brite”/”beige” (brown-in-white) AT and pink AT [28]. In the present dissertation, special attention has been given to WAT.

1.3.1.1 White adipose tissue

Even though humans and rodents share several fat depots, some are specific for each specie. However, in both species, the most prominent fat type is WAT. Based on the anatomical distribution, WAT depots can be classified into two main groups: subcutaneous (SAT) and visceral (VAT) AT (Figure 1). SAT is positioned beneath the skin and it is representative of 80% - 90% of body fat. In humans, it is predominantly found in the abdominal and gluteo-femoral regions. Abdominal AT can be further subdivided into superficial and deep AT, being anatomically separated by Scarpia's fascia, exhibiting distinct morphological and metabolic characteristics [28]. Similarly, in rodents, SAT can be classified into subcutaneous anterior fat (including axillary, cervical, interscapular and subscapular fat depots) and subcutaneous posterior fat (dorsolumbar, inguinal and gluteal AT depots) [35]. On the other side, only accounting for roughly 10% of body fat, VAT is located within the intra-abdominal compartment surrounding internal organs, such as: the digestive organs (mesenteric and omental fat depots), the paravertebral position between the spine and posterior abdominal wall (retroperitoneal fat depot), in-between the heart and pericardium (epicardial/pericardial fat depot) and the kidney (perirenal fat depot). Besides the latter, humans also possess an additional fat

depot localized superficially to the renal fascia, called the pararenal AT. Furthermore, while humans have omental AT, mice exhibit VAT surrounding the reproductive organs (perigonadal AT) [26, 28, 36]. In addition to the outlined AT depots, other WAT depots exist in both species, such as: dermal WAT and bone marrow WAT [28]. It should also be noted that, in conditions such as obesity and lipodystrophy, depositions of fat can also occur ectopically, which is responsible for the triggering of deleterious effects on non-AT organs (e.g., liver, skeletal muscle and heart) – commonly defined as lipotoxicity [37].

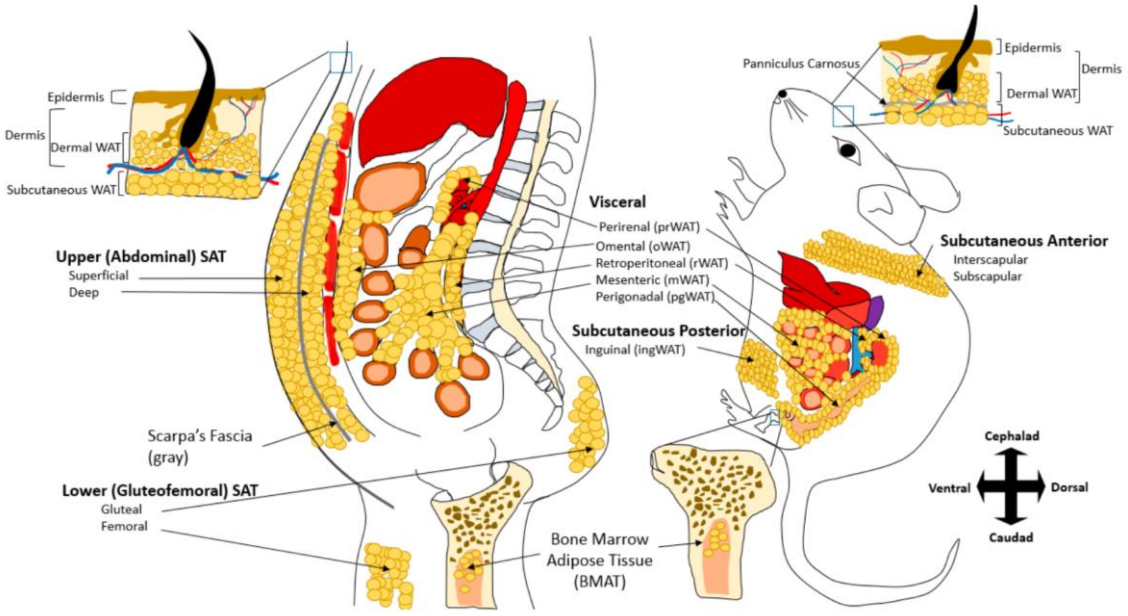

Figure 1 | Comparison of distinct subcutaneous and visceral WAT depots present in humans and rodents. Scheme obtained from [28].

WAT has traditionally been defined as a long-term energy reservoir. In WAT depots, white adipocytes store energy in unilocular lipid vacuoles with varying size, which determines the white adipose cell diameter (ranging typically from 10-20 µm to 70-80 µm) [38]. Moreover, in unilocular adipocytes the cytoplasm occupies only a small rim around the lipid droplet and the nucleus is typically squeezed onto the cellular membrane [38]. Notwithstanding, other physiological functions are also operated by this fat tissue (e.g. mechanical protection of tissues, inflammatory processes and innate immunity). Most notably, WAT is also responsible for the coordination of systemic metabolism and energy homeodynamics, and because of that, in conditions as obesity and lipodystrophy, it possesses a key role in the whole-body metabolic impairment [27]. However, current data point to a dissimilar contribution of SAT and VAT depots for the development of metabolic dysfunction in obesity, which point to a greater contribution of VAT to these

complications [27, 39]. The aforementioned differences are conjectured to be intrinsically associated with distinct morphological, metabolic and functional characteristics of the two depots; as well as the specific anatomical location occupied by each (due to the aided venous drainage through the liver and pancreas and increased intra-abdominal pressure applied by VAT) [39, 40]. On the other side, up to a certain limit of fat accumulation, SAT has been hypothesised to have a protective role against certain features of metabolic dysfunction. However, this hypothesis has been disputed in the literature, as deep layers of SAT have been strongly associated with insulin resistance, similarly to what is observed in VAT [41].

1.3.1.2 Brown adipose tissue

Another well-characterized AT type is BAT. As the name implies, BAT exhibits a brownish appearance, which can be explained by the dense network of mitochondria and vasculature noticed within the tissue, and consequent higher content in iron and cytochromes [42].

In mammals, BAT has been implicated as central in the maintenance of whole-body energy homeodynamics, mainly due to its importance in thermoregulation processes [43, 44]. Due to the latter, BAT assumes an important function during the neonatal developmental phase, as maintenance of body temperature is challenging [27]. However, in adult individuals, BAT exists in a lesser extent in the human body, constituting only small discrete and relatively homogenous fat depots present within the cervical, axillary and paraspinal regions [26, 43]. Central to the characteristic thermogenic activity of BAT are brown adipocytes, which exhibit a multilocular nature and abundant cristae-dense mitochondria expressing uncoupling protein-1 (UCP-1). The UCP-1 is found in the inner membrane of the mitochondria and it is responsible for the leakage of protons across the mitochondrial membrane, thus decreasing the proton-motive force generated in the process of oxidative phosphorylation (OxPhos). Consequently, it allows the uncoupling of oxidative respiration and synthesis of adenosine triphosphate (ATP), enabling the energy acquired from substrate oxidation to be dissipated in the form of heat [44].

1.3.1.3 WAT plasticity

Histological analysis of WAT have revealed the existence of several regions where adipocytes with hybrid phenotypic and functional features of those exhibited by white and brown adipocytes emerge – termed beige adipocytes [38, 44]. The origin of beige adipocytes is not consensual in the literature, with some authors suggesting these cells arise from *de novo* differentiation of specific precursors, while others suggest these originate though the direct transdifferentiation of mature white adipocytes. Beige adipocytes appear to contribute to a unitary role regarding energy metabolism, whereas energy derived from substrate oxidation is partitioned to both metabolism and thermogenesis, similarly to white and brown adipocytes, respectively. It has been well established that during periods of energy surplus, similarly to white adipocytes, beige adipocytes predominantly aid in the storage of energy excess. Yet, e.g. upon cold exposure, beige adipocyte exhibit brown-like features [e.g. elevated expression of uncoupling protein 1 (UCP-1)] , allowing the increase dissipation of heat [30, 44]. Beige adipocytes are one of the most evident profs of adipocyte remarkable phenotypic plasticity, being able to shift its structure and metabolism, to better adapt to the physiological conditions of the organism and to the environmental conditions to which it is exposed.

Another example of the remarkable plasticity exhibited the adipose organ is the pink AT. During pregnancy, lactation and post-lactation periods; subcutaneous AT from the female mammary region is remodelled and acquires a pinkish tonality, in which pink adipocytes become responsible for the production and secretion of milk, giving rise to a new organ: the mammary gland [45]. Increasing evidence from lineage tracing data suggests that pink adipocytes derive from the reversible transdifferentiation of white adipocytes from the subcutaneous WAT into mammary gland alveolar epithelial cells [46]. Pink adipocytes exhibit an adipocyte-like morphology, with abundant accumulation of lipids in the cytoplasm, roundish nucleus located at the centre of the cell and milk-containing granules [45, 46]. Strikingly, recent evidences suggest that besides the white-to-pink and vice-versa transdifferentiation processes, pink-to-brown and brown-to-myoepithelial and vice-versa cellular conversions can also occur in AT, once more enhancing the incredible plasticity of the adipose organ [47, 48].

1.4 ADIPOSE TISSUE REMODELLING IN OBESITY

The contribution of AT to obesity progression and the development of obesity-related comorbidities is anything but meek. As AT fails to properly store energy surplus, improper remodelling of AT occurs, which is considered to be a hallmark of obesity development and progression [49].

As a strategy to accommodate energy surplus, AT can expand though two distinct mechanisms: hypertrophy (enlargement of pre-existing adipocytes) and hyperplasia (increase of adipocyte number). In early-onset obesity, storage of energy excess occurs mainly through hypertrophy mechanisms. In hypertrophic adipocytes, cell size is determined by the amount of accumulated triglycerides (TGs) in lipid droplets [32]. As obesity progresses, the capacity of adipocytes to break down lipids and renew TGs becomes significantly compromised, promoting the increased accumulation of fat in adipocytes [50]. The excessive accumulation of fat in hypertrophic adipocytes has been typically associated with impaired cellular function and dysmetabolism [51, 52]. However, hypertrophic adipocytes produce and secrete factors known to induce the proliferation and differentiation of adipocyte precursors into mature adipocytes, allowing the expansion of AT through hyperplasia mechanisms (adipogenesis). This is considered to be a recovery mechanism to overnutrition, since smaller adipocytes are often described in the literature as less dysfunctional when in comparison with bigger equivalents, even though some studies contest this remark [37, 49]. Withal, hyperplasia mechanisms are often impaired in obese AT. Thus, energy surplus is stored commonly in hypertrophic adipocytes, as well as in ectopic regions.

In obesity, the improper remodelling of AT induces a chronic low-grade sterile inflammation state in the organ – called metainflammation [53]. Although inflammation is initially an adaptive response to stress conditions in obese AT; an abnormal higher synthesis and liberation of pro-inflammatory factors, chemo attractants along with immune-related genes in circulation is potentiated [37, 53, 54]. The *culprit* of obesity-induced inflammation is the accumulation of classically activated M1-macrophages in AT, which it is estimated to be 4 times higher in obese subjects when in comparison with lean individuals [53, 55]. In obese AT, macrophages are usually observed forming crown-like structures (CLS) surrounding dead adipocytes, contributing to its removal and serving as a buffer for lipid excess [56]. Although macrophage infiltration in the expanding AT is initially considered a protective mechanism, whose main objective is to restore AT homeodynamics, it is becoming clear that as obesity progresses it clearly

becomes out of balance. The excessive enlargement of obese AT, mainly ensued from adipocyte hypertrophy, also provokes hypoxia, as capillary density cannot follow the demands of the expanding AT in obesity. In its turn, hypoxia further exacerbates inflammation. In an attempt to physically restrict the expeditious expansion of obese AT, overproduction of extracellular matrix (ECM) components occurs [57]. Consequently, obese AT presents an increased fibrotic profile and reduced plasticity.

Thus, when in comparison with AT from lean individuals, improper remodelling of AT in obesity potentiates impaired metabolic and redox homeodynamics; which are ultimately reflected in increased inflammatory, fibrotic and hypoxic responses (Figure 2). Indeed, the improper remodelling of AT in obesity has been considered as an aggravating factor for the development of obesity-related complications.

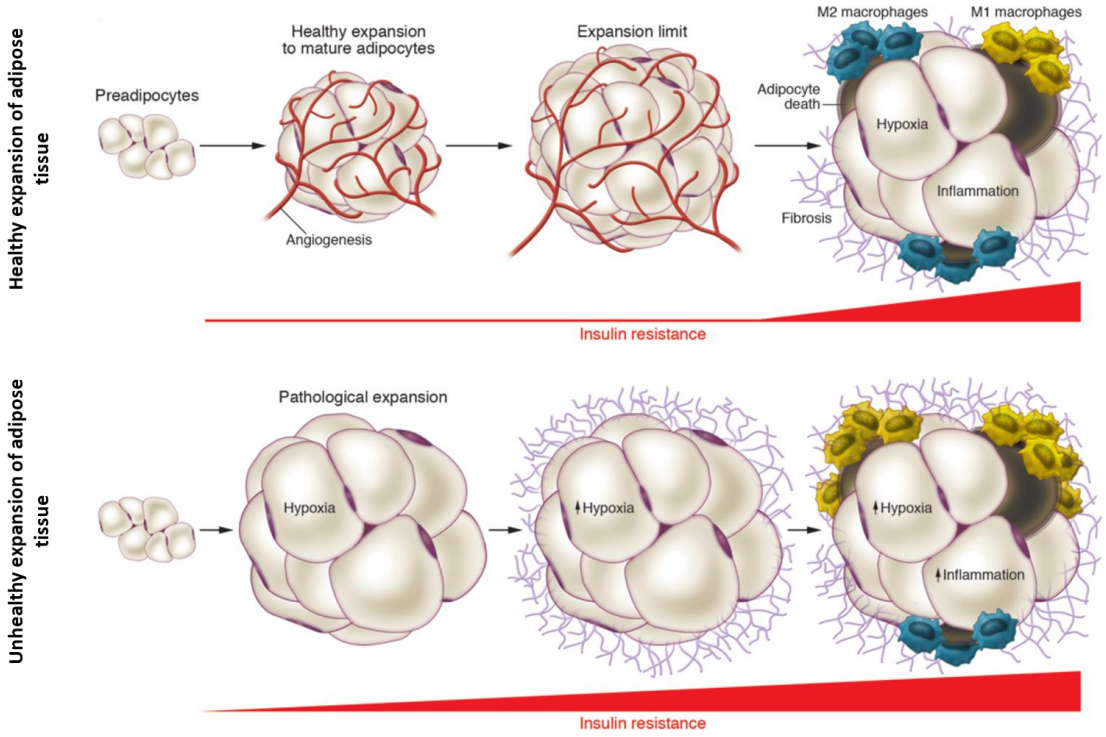

Figure 2 | AT remodeling mechanisms can be considered healthy or unhealthy. Healthy expansion of AT is considered to occur mainly though hyperplasia mechanisms, alongside with an adequate angiogenic response and apt ECM remodeling. In contrast, unhealthy expansion of adipose tissue is ensued predominantly though hypertrophic mechanisms. Furthermore, enhanced hypoxia, fibrosis and inflammatory responses are observed in the dysfunctional AT. Image acquired from [58].

1.5 THE MELANOCORTIN SYSTEM IN ENERGY HOMEODYNAMICS

The melanocortin system is considered to be one of the most complex neuro-hormonal systems in mammals [59]. It has been recognized for its pivotal role in the

regulation of whole-body energy homeodynamics, though the modulation of feeding behaviour in the CNS [60].

The modulatory effect exercised by this conserved pathway is assimilated not only in the CNS, but also in peripheral tissues, thus assisting in a large number of other physiological processes. The melanocortin system was firstly discovered for its role in skin pigmentation and adrenal steroidogenesis. Today, it has been demonstrated that the influence of melanocortins on peripheral tissues is even more embracing, affecting the: modulation of energy expenditure, immunomodulation, steroidogenesis, temperature control, sexual function, exocrine gland secretion, cardiovascular regulation and neuromuscular regeneration processes [61]. The melanocortin system has also demonstrated to also have important anti-inflammatory activities. Furthermore, this conserved pathway is also capable of modulating cellular glucose uptake, triglyceride synthesis, lipid deposition and lipid mobilization; in the liver, muscle and adipose tissue [62].

1.5.1. Components of the melanocortin system

The melanocortin system is composed by (1) melanocortin agonist peptides; (2) endogenous antagonists; (3) Melanocortin receptors (MCRs) and (4) melanocortin receptor associated proteins (MRAPs) [59, 63].

1.5.1.1 Melanocortin peptides

The melanocortin system integrates several melanocortin agonists, derived from a 31 KDa multiplex precursor – pro-opiomelanocortin (POMC) protein. POMC processing is a highly regulated physiological process, as POMC post-translational modifications occur in a cell- and tissue-specific manner [64].

POMC peptide is cleaved by pro-hormone-converting enzymes (PCs), and the resulting peptides, can be further modified by a variety of other enzymes (e.g. endoproteases, exopetidases, acetylation and amidation enzymes) [64]. POMC is initially cleaved in adrenocorticotropic hormone (ACTH), β-lipotropin (β-LPH) and the N-POMC intermediate. Then, the originated peptides give rise to even smaller biological relevant peptides: ACTH is further cleaved in α-melanocyte stimulating hormone (α-MSH), β-LPH originates β-MSH and β-endorphin, while from N-POMC derives γ-MSH

(Figure 3) [65]. Although not under the scope of the present work, it is worth noting that the post-translational processing of the POMC peptide originates besides melanocortins another type of peptides, the β-endorphins.

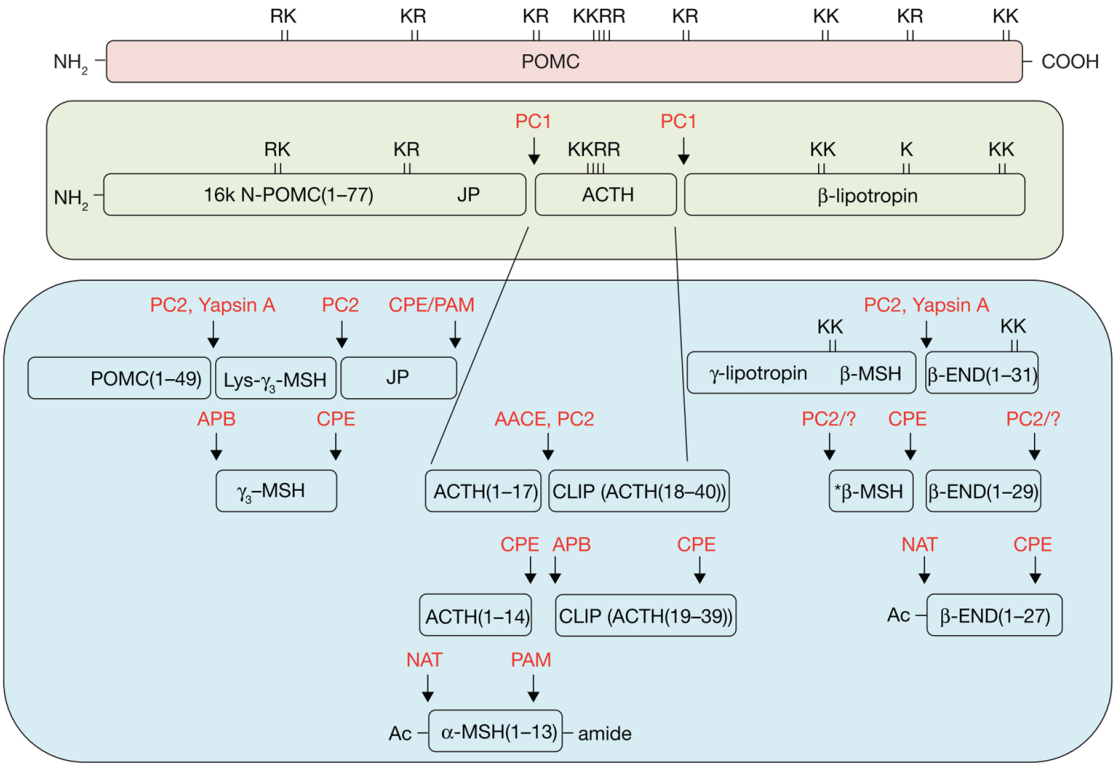

Figure 3 | Processing of POMC pro-hormone occurs in a cell- and tissue-specific manner. The post-translational cleavage of POMC occurs by the sequential action of proteases, commonly named prohormone convertases (PCs). ACTH sequential cleavage gives rise to α-MSH whereas β-LPH sequential cleavage originates β-MSH and β-endorphin. Schematic representation of POMC processing obtained from [64].

The present dissertation is focused on the role of α-MSH peptide, which is derived from the first 13 amino acids of the N-terminal region of ACTH, corresponding to the acetyl ACTH (1→13)-amide (Ac-ACTH(1–13)-NH_2). Melanocortin α-MSH presents the conserved heptapeptide core (Met^4-Glu^5-His^6-Phe^7-Arg^8-Trp^9-Gly^{10}), which is responsible for the binding to MCRs [66]. Three distinct variation of α-MSH exist: desacetyl α-MSH (N-terminal serine is free), α-MSH (monoacetylated at the N position) and diacetyl α-MSH (diacetylated at the N and O positions), whereas the carboxyl terminal is in the amide form [67]. These are postulated to have distinct physiological roles. Previous studies have demonstrated that, consistently with the diminished levels of acetylating enzymes α-N-acetyltransferase found in extracts of the hypothalamus, the deacetylated form of α-MSH predominates in the hypothalamus [68]. It has been also reported that both α-MSH and desacetyl α-MSH are necessary to regulate appetite, metabolism and body weight, presenting an important role in the maintenance of energy

balance, whose effects are not necessarily analogous [69]. Previous studies demonstrated that although α-MSH and desacetyl α-MSH present a similar affinity for MC3R and MC4R, in order to reduce food intake, desacetyl α-MSH would have to be intracerebroventricular injected in a concentration 25 times higher than that required to see the same effect with α-MSH [70]. The role of diacetyl α-MSH in mammals is still to be understood. In fact, elucidation of the biological functions of each variant of α-MSH in mammals needs to be further deepened.

1.5.1.2 The melanocortin receptors

The MCRs are G-coupled protein receptors (GPCRs), which belong to the Class A rhodopsin-like family. Hitherto, five MCRs have been described and numbered from 1 to 5 (MC1–MC5R), accordingly with the order of their cloning.

Upon activation by melanocortins, the MCRs suffer conformational changes, which are ultimately responsible for the induction of both dependent and independent G-protein signalling pathways [71]. Stimulation of dependent G-protein signalling pathways is known to involve the activation of $G_{\alpha s}$, $G_{\alpha q}$, $G_{\alpha i}$ and $G_{\alpha 12}$ subunits, depending on the G-protein subtype that is coupled to the receptor [72]. All the MCRs are known to couple to more than one G-protein subtype, but the most well described pathway involves the activation of G_s protein, through which $G_{\alpha s}$ subunit dissociates from the βγ heterodimer, leading to the activation of adenylyl cyclase (AC) and to the subsequent increase on cAMP levels and activation of protein kinase A (PKA) [72]. MCRs can also inhibit PKA if coupling to G_i or even switch to the activation of protein kinase C (PKC) when coupling to the G_q protein [72]. Moreover, $G_{\alpha 12}$ signalling culminates in the modulation of both PKA and PKC [72].

Succinctly, activation of MC1R coupled to the G_s protein has been implicated in the (1) stimulation of AC and consequent increase in cAMP (2) increased Ca^{2+} levels and (3) the stimulation of extracellular signal-regulated kinase 1/2 (ERK1/2). MC2R and MC3R are suggested to act similarly to MC1R, however they are able to activate PKC signalling pathway. MC4R, besides being able to couple to G_s activating AC, it also couples to G_q and G_i, activating PKC, ERK1/2 and phosphatidylinositol-3-kinase (PI3) kinase pathways. Lastly, MC5R through coupling to G_s can activate PKA pathway, while through the coupling to G_i it is known to stimulate the ERK1/2 pathway. GPCRs have also been found to mediate signal pathways by the stimulation of G-protein independent processes, namely through Janus protein kinase / signal transducers and activators of

transcription (JAK/STAT), Src-family tyrosine kinases, β-arrestins, and PDZ domain-containing proteins [73].

Activity of MCRs is further regulated through receptor internalization. Although mechanisms for MCR internalization are specific, generally upon binding of melanocortin to MCR, β-arrestins are recruited to the plasma membrane, which facilitates the recruitment of clathrin complexes. Thus, internalization of the receptor occurs though clathrin-coated pits [72]. After internalization, the MCR can be (1) targeted for degradation, through lysosome dependent mechanism; (2) recycled back to the cellular membrane, through endosomes or (3) it can persist in the cytoplasm, aiding in the perpetuation of the signal throughout time. Furthermore, the activity of MCR can be further modulated through: (1) the regulation of its transport to the plasma membrane by chaperones, (2) the modulation of its intracellular trafficking and signalling by MRAP proteins and (3) and the inhibition of its activity by natural endogenous antagonist [72].

Depending of the specific interaction of melanocortins-MCR, distinct physiological processes can be stimulated, with the most significative being summarized in Table 1.

Table 1 | Summarized characterization of the function and tissue expression pattern of MCRs. The specific interaction of melanocortins with MCRs occurs with varied affinities, and modulated by different accessory proteins, which play an important role in prompting specific responses in distinct tissues. Adapted from [65, 72, 74].

MCR	Affinity of the melanocortin agonists	MCR expression	Physiological function
MC1R (α-MSH classical receptor)	α-MSH = ACTH > β-MSH > γ-MSH	Skin (Melanocytes), adipocytes, immune cells; pituitary; placenta; testis	Melanogenesis/Pigmentation; Inflammation; Pain Perception.
MC2R (ACTH receptor)	ACTH	Adrenal cortex; adipocytes; skin	Adrenal steroidogenesis; Cellular proliferation;
MC3R	α-MSH = β-MSH = γ-MSH = ACTH	Hypothalamus; limbic system; placenta; digestive tract; heart; mammary glands; muscle cells; immune cells; kidney	Energy homeodynamics; Inflammation.

MC4R	α-MSH = ACTH > β-MSH > γ-MSH	Hypothalamus; limbic system; cerebrum; brain stem; muscle cells	Energy expenditure and food intake; Homeodynamics and glucose concentration; Sexual Function; Blood pressure; Pain perception.
MC5R	α-MSH > ACTH > β-MSH > γ-MSH	Muscle; liver; spleen; lung; brain; adipocytes; skin; gastrointestinal tract; kidney; ovary; uterus: adrenal gland; β-lymphocytes; testis; exocrine glands	Exocrine gland secretion; Immunomodulation in B and T cells; Adipocyte cytokine release; Thermogenesis; Glucose uptake in muscle; Controls fatty acid oxidation in skeletal muscle and adipose tissue.

1.5.1.3 Melanocortin receptor associated proteins

The MRAP family consists of small single transmembrane proteins. Heretofore, only two MRAP members have been described: MRAP1, which in humans possess two splice-isoforms (MRAP1α and MRAPβ) and MRAP2.

The main function of MRAP proteins is to regulate the trafficking, signalling and ligand binding affinity of melanocortins-MCR, aiding in the regulation of the pharmacological profile and function of MCR [75]. In the particular case of MRAP1, it has been established that it is important for the trafficking of MC2R to the plasma membrane, as well as to ATCH binding and consequent activation of MC2R; and its deficiency has been associated with the loss of functional ACTH receptors [76]. On the other side, besides being implicated in the modulation of MC3R, MC4R and MC5R; MRAP2 has been demonstrated to be required in growth and development processes and metabolism regulation [77, 78].

1.5.1.4 Melanocortin antagonist

The melanocortin system is unique, since its activity is regulated though the expression of endogenous antagonists – agouti-signalling protein (ASIP) and agouti-related peptide (AgRP) – that compete with melanocortin peptides for binding to MCRs [59].

Both ASIP and AgRP are structurally similar yet exhibit distinct tissue expression profile and receptor binding affinities. Typically, ASIP is associated with pigmentation

regulation and its expression was thought to be limited to the skin [79]. Mice with the yellow mutation at the agouti locus present an ectopic overexpression of ASIP, resulting on a pleiotropic phenotype in these animals, which not only affects coat colour, but also increased tumour susceptibility and induced late-onset obesity associated with hyperphagia [80]. Thus, the latter phenotypic effect could suggest the presence of an ASIP-like protein in the brain [79]. On the other side, the AgRP is expressed mainly in the CNS, where it antagonizes the effect of α-MSH through the binding to MC3R and MC4R [81].

1.5.2. Central regulation of food intake by the melanocortin system

The central melanocortin system is composed by distinct complex neural network, responsible for the interpretation and integration of a wide range of peripheral inputs, and consequently responsible for the establishment of a coordinated central response.

In first-hand, the central response to food intake is triggered by two-main neural populations, which are chemically and anatomically distinct. Both are found predominantly within the arcuate nucleus of the hypothalamus (ARC), but also in the nucleus of the solitary tract (NTS), in the brainstem and striatum. The two neural populations coexist in the CNS and are classified according with the peptides they express as POMC and AgRP neurons. In rodents, POMC neurons have been found to co-express cocaine-and-amphetamine-regulated transcript (CART), which is post-transcriptionally cleaved though a distinct splicing mechanisms as in Humans [82]. Similarly, about 90% of the neural population expressing AgRP also expresses neuropeptide Y (NPY) [83]. These two discrete neural populations are called first-order neurons, attending their ability to sense neural signals from higher brain centres and external clues from peripheral organs. Within the hypothalamus, POMC and AgRP neurons receive inputs from other hypothalamic nuclei [e.g. paraventricular nucleus of the hypothalamus (PVH), dorsomedial hypothalamic nucleus (DMH), ventromedial hypothalamus (VMH) and lateral hypothalamus (LH)] and from extrahypothalamic brain regions (e.g. lateral septum and bed nucleus of the stria terminalis)] [84]. Moreover, through the expression of specific receptors at cell surface, both POMC and AgRP neurons are able to perceive: (1) long-term signals, mostly humoral clues (e.g.; insulin and leptin) and (2) short-term signals, namely gut hormones (e.g. peptide YY (3-36), ghrelin and cholecystokinin).

Attending the peripheral signal detected by the first-order neurons, stimulation of either POMC or AgRP production occurs, thus triggering opposite responses regarding feeding behaviour. In the fed state, food consumption is inhibited. Peripheral organs, such as the AT and the pancreas, secrete onto the blood circulating clues (leptin and insulin, respectively) with the ability to cross the blood-brain barrier, and interact with specific receptors present at the surface of both POMC and AgRP neurons, promoting the activation of POMC neurons through its depolarization, while inhibiting AgRP neurons [85, 86]. Thereafter, POMC-derived peptides interact with MC3R and MC4R expressed by the second-order neurons, being able to decrease food intake. In contrast, in the "starved" state, AgRP neurons are stimulated by increased concentrations of orexigenic circulating clues (such as ghrelin) and low concentration levels of insulin and leptin. In this case, AgRP antagonize the activity of hypothalamic MC3R and MC4R induced by melanocortins, thus stimulate feeding.

Hence, POMC and AgRP neurons work in coordination to regulate feeding behaviour accordingly with the biological requirements. Several studies have demonstrated that defects in melanocortin system components (e.g., POMC, MCRs and MRAP proteins) promote the development of obesity, as well as of its associated comorbidities, in both humans and mice [87-89]. Their importance in the regulation of metabolic disorders is mainly evidenced by mutations in the hypothalamic melanocortin system. More than 150 mutations of MC4R gene have been described in obese patients [90], accounting for the most frequent cause of monogenic obesity (2-5% of all cases) [83, 91]. MC4R deficient individuals exhibit severe obesity, a higher lean mass, higher bone mineral density and higher linear growth early childhood [91]. MC4R variants are known to be inherited in a codominant manner and to have incomplete penetrance [91, 92]. Thus, MC4R mutation carriers exhibit distinct obesity syndromes, with homozygotes exhibiting severer symptoms when in comparison with heterozygotes [91]. Indeed, homozygotes individuals present a more pronounced hyperinsulinemia and increased hyperphagic behaviour than the heterozygotes [91]. Attending the pivotal role of this receptor in the regulation of feeding behaviour at the CNS, the MC4R has been a target for the development of anti-obesity drugs [95, 96]. However, so far, no satisfactory results have been obtained since the undesirable effects largely surpass the any beneficial effects.

Preservation of energy homeodynamics is also regulated though the action of MC3R, which possess a non-reductant role with the function of MC4R [93]. Being so, mutations in this receptor have also been linked with obesity development. It has been

postulated that in the course of Human evolution, as populations went through periods of famine, mutations on MC3R seem to have been acquired, which diminished the sensitivity of this receptor to melanocortins [94]. MC3R is suggested to be primarily involved in the regulation of feeding efficiency (ratio of weight gain to food intake), since $MC3R^{-/-}$ mice present an increased fat mass and reduced lean mass, despite the maintenance of food intake levels or even though its reduction. It is thus hypothesized that when MC3R is absent, nutrients are stored preferentially in the form of fat at the expense of lean mass [93].

Attending that the activity of MC3R and MC4R are known to be modulated by MRAP family of enzymes, it is not surprising that mutations in these proteins also enable the development and progression of obesity pathology. MRAP2 disruption has been associated with obesity, as three distinct mutation in MRAP2 have been observed in obese individuals [77]. MRAP2 knock-out models have demonstrated to exhibit a similar phenotype to those exhibited by MC3R knock-out. However, since MRAP2 is expressed broadly throughout the hypothalamus and other metabolic active tissues; and it can interact with many other GPCR targets [95]; it is possible that the obese phenotype displayed by these animals arises from the deregulation of several mechanism beyond the melanocortin system [96]. MRAP1 has also a role in weight regulation in humans but, it has not yet been established if MRAP1 deficiency is associated with obesity, since only one isolated case has been reported in the literature [97].

Although relatively rare, mutations in the POMC peptide, as well as its derivatives, are also implicated in the development of obesity. These individuals typically develop an hyperphagic behaviour and become obese at an early age [98]. Concordantly with its orexigenic effect, it has also been demonstrated that overexpression of both AgRP and agouti contributes to obesity development. Furthermore, mutations in components of the leptin-melanocortin pathway, are known to propensity the development of obesity: LEP, LEPR, prohormone-convertase-1 gene, adenylate cyclase-3 gene [99].

1.5.3. Regulation of adipocyte function by the melanocortin system

The melanocortin system has also been implicated in the regulation of metabolic pathways in the adipose tissue. However, the exact cellular signalling mechanisms triggered are still not fully comprehended.

Our group is particularly focused on the role of the melanocortin α-MSH on the direct modulation of cellular responses in adipocytes. A previous study from our group, in murine 3T3-L1 adipocyte cell line, demonstrated that α-MSH modulates lipid metabolism by binding to MC5R [100]. It was shown that α-MSH (1) impairs fatty acid esterification through ERK1/2 pathway and (2) promotes lipolysis through cAMP / PKA-dependent mechanisms [100]. The latter fatty acid oxidation mechanism was also observed by Gan *et al.* [101]. Additionally, upon exposure to α-MSH, 3T3-L1 adipocytes developed "brown-like" thermogenic properties, presented a higher mitochondrial content, in association with increased basal and uncoupled mitochondrial respiratory rates [1]. Subsequent studies carried out in diet-induced obese (DIO) mice confirmed the results obtained *in vitro*, showing that intraperitoneal administration of α-MSH stimulated the expression of genes associated with the thermogenic program, inducing browning of inguinal subcutaneous WAT (ingWAT), accompanied by a greater mitochondrial oxygen consumption rates [1]. In addition, it also reduced mice body weight and fat mass in a time-dependent manner, without being observed any alteration in food intake. Altogether, these data are suggestive of a direct action of α-MSH in adipocytes. Remarkably, α-MSH-treated mice also exhibited an ameliorated lipid and glycaemic serum profile [1], demonstrative of α-MSH potential as a novel anti-obesity drug.

1.6 REDOX BALANCE AND STRESS SIGNALLING PATHWAYS

Primitive life forms evolved in a highly reducing environment, but as oxygen (O_2) and it´s reduction intermediates become more abundant in the atmosphere, life had to adapt to it or it would have become extinct [102]. Due the high reactivity of O_2, this molecule is able to participate in high-energy generating processes, such as the OxPhos, enabling the sustenance of the physiological demands of complex life forms. However, attending the oxidizing capacity of O_2, the negative effects induced by this molecule on biological systems cannot be neglected. Notwithstanding, organisms not only developed protective antioxidant systems, but also redox-sensitive signalling pathways which aid in cellular homeodynamics [102].

1.6.1 The ROS paradox

The Paracelsus *dictum* "The dose makes the poison" can be properly applicable to the concentration of O_2 and free radical species in biological systems [103]. Free

radicals can be formed by several elements, but oxygen and nitrogen have been recognized as the most important in biological systems. The term reactive oxygen species (ROS) has been characteristically defined as partially reduced metabolites of O_2 which possess strong oxidizing capabilities, while reactive nitrogen species (RNS) derive from •NO [104]. These species encompass two distinct classes: free radicals and non-free radicals. Free radicals are defined as species which can have an independent existence and contain an incomplete electron shell. This class includes species such as: hydroxyl radical (•OH), superoxide anion ($O_2^{\bullet-}$), •NO, peroxynitrite (ONO_2^-) and nitrogen dioxide ($\bullet NO_2$). Regarding non-free radicals, these are mainly characterized by its high oxidant potential and allow the rapid formation of species with a high power of oxidation in biological systems. This class includes species such as hydrogen peroxide (H_2O_2), hypochlorous acid (HOCl), ONO_2^- and oxygen singlet ($^1\Delta gO_2$) [105].

Indeed, maintenance of redox homeodynamics has been phrased as "the golden mean of the healthy living", as preservation of adequate physiological concentrations of ROS is necessary for redox signalling – termed oxidative eustress [103, 106]. On the other side, conditions where the increased abnormal concentration of oxidants in the cell exceeds the capacity of the antioxidant systems, which can cause potential damage in the biological systems, through the damage of biomolecules and the disruption of cellular signalling pathways – termed oxidative stress [96, 120].

1.6.2 Exogenous and endogenous sources of reactive species in the cells

Oxidative stress can be induced in biological systems upon exposure to a huge heterogeneity of environmental factors, including pollutants (e.g. chemicals and xenobiotics) and high-energy radiation (e.g. UV and ionizing radiation). Additionally, attending the multiple valence states, metals can promptly react with oxygen and originate ROS, mainly via the Fenton- and Haber–Weiss-type reaction mechanisms [107, 108]. The first step of the Fenton reaction involves the reduction of ferric iron (Fe^{3+}) into ferrous iron (Fe^{2+}) (eqn (1)). Subsequently, in the second step of Fenton-reaction, Fe^{2+} reacts with H_2O_2, originating Fe^{3+}, •OH and OH^- (eqn (2)). Then, •OH can react with H_2O_2, generating $O_2^{\bullet-}$ (eqn (3)). Subsequently, through the Harber-Weiss reaction, $O_2^{\bullet-}$ reacts again with H_2O_2, generating •OH and OH^-, through the reduction of Fe^{3+} to Fe^{2+} (eqn (4)).

$$Fe^{3+} + O_2^{\cdot -} \rightarrow Fe^{2+} + O_2 \quad (1)$$

$$Fe^{2+} + H_2O_2 \rightarrow Fe^{3+} + OH^{\cdot} + OH^{-} \quad (2)$$

$$OH^{\cdot} + H_2O_2 \rightarrow O_2^{\cdot -} + H^{+} + H_2O \quad (3)$$

$$O_2^{\cdot -} + H_2O_2 \xrightarrow{Fe^{+3}/Fe^{+2}} OH^{\cdot} + OH^{-} + O_2 \quad (4)$$

Nevertheless, it is worth noting that ROS are continuously produced as a consequence of aerobic metabolism, through redox reactions carried out under physiological conditions. Recent studies postulate that 0.2% of consumed oxygen is converted in ROS. Production of free radical species has been proved to occur in several organelles. However, the main site of ROS production has been demonstrated to change according to the cell type and even throughout time. Yet, of all intracellular sites, the following three are highlighted typically as the main source of ROS in the cell: the mitochondria, the endoplasmic reticulum (ER) and cellular membranes [109].

The mitochondria is commonly described in the literature as the powerhouse of the cell, as it is able to generate two distinct types of energy: heat and ATP. Plus, it is also considered to be the main site of ROS production in the cell, as approximately 90% of cellular ROS can be traced back to this organelle [110]. The production of free radical species in mitochondria is primarily associated with the process of OxPhos, where reducing equivalents [Reduced nicotinamide adenine dinucleotide (NADH) and dihydroflavine-adenine dinucleotide ($FADH_2$)] reaped from catabolic pathways are progressively oxidized, as electrons are transferred across four cytochrome centres localized in the inner membrane of the mitochondria: NADH- ubiquinone (Q) oxidoreductase (complex I), succinate-Q reductase complex (complex II), Q-cytochrome C oxidoreductase (complex III) and cytochrome c oxidase (complex IV) [111]. The electron flow from NADH and $FADH_2$ is responsible for the reduction of O_2 into H_2O, and it occurs concomitantly with the transference of protons from the mitochondrial matrix to the intermembrane mitochondrial space by complex I, III and IV. As the pumping of protons from the matrix to the intermembrane mitochondrial space occurs concomitantly with the movement of electrons, an electrochemical gradient is generated. The generated redox energy provides a chemiosmotic and electromotive forces, which upon return of protons to the mitochondrial matrix, is exploited by F1F0 ATP synthase (Complex V) to drive ATP synthesis [111, 112].

The process of electron transference along the cytochrome chain is imperfect, as electrons derived from NADH and $FADH_2$ can react with other electron acceptors, such as free O_2, giving rise to radical molecules [110]. The two main sources of ROS production in the electron transport chain (ETC) are believed to be complex I and complex III, with these being able to release $O_2^{\bullet-}$ into the matrix and to both sides of the inner mitochondrial membrane (matrix and intermembrane space), respectively [113]. However, this idea has been disputed in the literature, as some authors have suggested that the main sites of electron leakage in the electron transport chain change attending the physiologic conditions of an organism. Just in the mitochondria, ROS production has been demonstrated to occur in at least 9 distinct sites, including also ETC independent sites, namely in cytochrome P450 [114, 115].

Other important organelle implicated in ROS synthesis is the ER, with the process of protein synthesis and folding being the main contributors to this effect. In the ER-lumen, and in combination with e.g. chaperones, co-factors and foldases; the oxidizing redox micro-environment for the correct folding, translocation and post-translational modification of secretory and transmembrane proteins is provided [116]. Most proteins require the formation of disulphide bridges, to acquire and stabilize their tertiary and quaternary structures, in a process highly sensitive to redox balance. Disulphide bridge formation occurs *via* protein-relay systems, through processes carried out by oxidoreductase enzymes residing in the ER, namely protein disulphide isomerases and endoplasmic reticulum disulphide oxidase 1 α and β [117]. Attending that the catabolic processes carried out by these enzymes have O_2 as their terminal electron acceptor, production of ROS occurs as a consequence of their function [118-121]. Nevertheless, generation of ROS in the ER is also possible through activation of other protein systems, such as: dihydronicotinamide-adenine dinucleotide phosphate (NADPH) oxidases (NOX), the glutathione /glutathione disulphide and the microsomal monooxygenase system [116].

Although special attention has been given to mitochondria and ER, perhaps one of the most important organelles in ROS balance is the cellular membrane [122]. Regarding ROS synthesis, two of the main sources of these species in the membrane include members of the NOX and the dual oxidase relatives (DUOX) family of enzymes, which are responsible for the generation of ROS both in the form of $O2^{\bullet-}$ or H_2O_2. Additionally, significant production of ROS is achieved in cellular membranes by xanthine oxidase, which liberates H_2O_2 to the outer part of the membrane, and the nitric oxide synthases (NOS), which synthetises and liberates •NO to the inner part of the membrane.

Furthermore, in a lesser extent lipoxygenase and cyclooxygenases, which are at least for a short period of their life cycle, close to the plasma membrane, are also known to produce ROS.

Even though the three intracellular sites aforementioned play an important role in the generation of ROS, free radical species can also be produced in significant quantities in other organelles or cellular compartments, such as a by-product of lysosomal and peroxisomal enzymatic reactions. In sum, the joint activity of all the described systems contributes to the redox macro- and microenvironment in cells, which consequently contribute to cellular mechanisms regulation.

1.6.3 Biomolecule damage by ROS and RNS

When concentration of ROS exceeds that to be considered to be physiologically adequate, cellular integrity and functioning is compromised, due to their ability to promptly react with all major classes of biomolecules, such as: lipids, proteins, DNA and even RNA. Accordingly, with the chemical nature of the radical species, distinct affinities and reactivity's towards the affected biomolecule have been described and extensively scrutinized in the literature. Even if impairment of physiological processes did not occur, the altered species are known to become a source of oxidative stress itself. Thus, the triggered redox impairment in the cell is perpetuated through a positive feedback mechanism.

Lipid oxidation was one of the first mechanisms, regarding the oxidative damage of biomolecules, to be described as these biomolecules are essential components of the cellular membrane. Thus, when the structure of these biomolecules is altered, the integrity of cellular membranes is compromised. Not all lipids react with ROS equally. ROS preferentially react with polyunsaturated lipids, due to the large number of double bonds in their structure, leading to their oxidation [123]. This process is called lipid peroxidation, and it involves the formation and propagation of lipid radicals in a cyclic manner, leading to the amplification of the reaction, ultimately compromising the stability of cellular membranes [124]. As a product of lipid peroxidation, about 32 aldehydes have been identified, which unlike free radicals, are highly stable and can diffuse out of the cell, attacking targets away from their production site [123]. Albeit the existence of non-enzymatic mechanisms aforementioned explained, lipid oxidation can also be carried out by enzymatic processes, mainly though lipoxygenases and photo-oxidation processes [125, 126].

As for the proteins, the oxidative modification of proteins by ROS and RNS has been recognized as a major post-translational modification. These modifications can either be reversible or irreversible, playing an important role in protein structure, and consequently in the regulation of it's physiologically function. For this reason, to some extent, the oxidative modification of proteins has been implicated to have beneficial roles in heath maintenance. However, when these processes are unregulated, these modifications have been linked with the structural decline of the affected biomolecules, and consequent impairment of cellular functioning [127]. In the present thesis, special focus has been given to protein carbonylation. Protein carbonylation describes the process responsible for the formation of reactive ketones or aldehydes, which is favoured by ROS and metals. Formation of these chemical groups occurs through the direct oxidation of side chains of amino acids (e.g. proline, arginine, lysine among others) [128]. Not a unique pathway is responsible for the conversion of proteins to carbonyl derivatives, but several: through the oxidation of the protein backbone, through the formation of protein-protein cross-linkages, through the oxidation of amino acid side chains and even through the fragmentation of protein carbonyl adducts [129]. Protein carbonylation is a marker for oxidative damage in the cells, and thus several sensitive methods have been developed for the determination of carbonyl groups. One of the most methods to detect carbonylated proteins is through 2,4-Dinitrophenylhydrazine (DNPH) detection.

Lastly, stability of RNA and DNA is also compromised by non-physiological concentrations of ROS, and even other metabolites in the cells. Alterations induced by these species not only include the direct modification of nucleotide bases, but also induce the breakage of single/double strands, apurinic/apyrimidinic sites, sister chromatid exchange, DNA-DNA and DNA-protein cross-links, and even in some cases it alters methylation patterns and compromises DNA/RNA repair mechanisms [130, 131]. However, it has been demonstrated that RNA is most pone to oxidation, when in comparison with DNA, as it is physically closer to ROS and RNS generation sites and molecularly is not as stable as DNA. Furthermore, of all nucleotide basis, guanosine is the most prone to oxidation, as it exhibits a lower reduction potential [132]. Indeed, the most studied DNA damage marker is the 2'-deoxy-8-oxo-7,8-dihydroguanosine, which is a product of guanosine oxidation by •HO and generates a GC/TA transversion upon replication [133]. Regarding RNA, the most common marker of oxidation is also a homologue of 2'-deoxy-8-oxo-7,8-dihydroguanosine, most specifically 8-Oxo-7,8-dihydroguanosine.

1.6.4 Antioxidant defence system

Organisms are equipped with complex antioxidant systems, which are capable of (1) reacting/quenching free radical species or (2) delay/inhibit damage of cellular structures by these highly reactive species, in an attempt to prevent the triggering of ROS-induced cascades of cellular damage [124].

Traditionally, an antioxidant has been defined as a molecule which is able at low concentrations, to delay or prevent the oxidation of an oxidizable substrate present at higher concentrations [134]. Each antioxidant presents intrinsic characteristics, differing in its nature and reducing power [135]. Primary antioxidant defences can scavenge reactive species, breaking the chain of destruction induced by ROS. Secondary antioxidant defences include singlet oxygen quenchers, molecules responsible for the decomposition of H_2O_2, chelators of metals, inhibitors of oxidative enzymes and absorbers of UV radiation [134]. Attempts have been made to categorize these compounds having into consideration their activity (enzymatic or non-enzymatic), solubility on water and lipids (hydrophilic or hydrophobic), endogenous or exogenous nature, natural or synthetic and preventative or repair-systems [134]. The listing of the main antioxidants found in living organisms is included in Table 2.

Table 2 | Summarization of the most common antioxidant compounds responsible for the maintenance of redox homeodynamics in living systems.

	Endogenous antioxidants	Exogenous antioxidants
Enzymes	Superoxide dismutase (SOD); Catalase; Glutathione peroxidase (GPx); Gluthathione reductase; Metallothionein.	Ferritin; Transferrin; Ceruloplasmin; Albumin.
Small antioxidants	Uric acid; Coenzyme Q; Lipoic acid.	Vitamin C; Vitamin E; Carotenoids; Phenolics (such as hydroxybenzoic acids and flavonoids; possessing a flavylium or 2-phenylchromenylium ion skeleton).

Working in coordination with the antioxidant systems, mechanisms responsible for the removal or repair of damaged biomolecules also exist, endeavouring that ROS-oxidation by-products do not significantly and continually compromise cellular

metabolism and homeodynamics. One of the most common cytoprotective mechanism is the enzymatic degradation of damaged biomolecules by: nucleases, proteases and lipases. Then, liberation of damaged components of biomolecules for secretion or recycling is accomplished, while promoting the reutilization of non-damaged components [131]. Recycling of damaged and dysfunctional cellular components is also aided by autophagy mechanisms [136].

Regarding oxidized lipids, a panoply of enzymes is responsible for the selective removal, repair and replacement of damaged lipid fragments. It includes peroxidases and glutathione S-transferase, which reduce lipid peroxides to the corresponding alcohol and inhibiting the further progression of the chain reaction of oxidized lipids [137]. Other enzymes, such as Gpx4, is responsible for the independent reduction of phospholipid peroxides. Inside the lipid bilayer, damaged lipids are specifically removed and substituted through phospholipase A2 and acyltransferase enzymes, respectively. Furthermore, lipid droplets have been found to sequester oxidized lipids and proteins, and also prevent lipid peroxidation. Then, oxidized lipids have been shown to migrate to the surface monolayer of lipid droplets [138], an area specially enriched with enzymes. Then, recycling of these organelles could occur by two distinct mechanisms: lipophagy and lipolysis [139]

On the other hand, protein repair mechanisms appear to be limited. Instead, even though some oxidized protein forms can be recognized and degraded by the cells, other tend to accumulate overtime in the cell, ultimately eliciting the dysfunction of cellular processes. Damaged proteins can be degraded by the cell through the activation of proteolytic enzymes (e.g. via the ubiquitin-proteasome system or though autophagy-dependent mechanisms), or can have its proteolytic susceptibility increased, or even a combination of both [131].

Since the genetic material is by its nature chemically unstable and vulnerable to damage, sophisticated mechanisms against DNA and RNA damage are present in cells. Several mechanism responsible for the direct repair of oxidative-damaged nucleic acid exist, namely: base excision repair, nucleotide incision repair, nucleotide excision repair, homologous recombination, mismatch repair and translesion DNA synthesis [137]. These mechanisms are used accordingly to the specific oxidative damage in the nucleic acid, and on the cellular condition, some of which are used preferentially over others.

However, cells possess other protection mechanisms against oxidative stress, which go far beyond those above described. Those can involve cellular architecture, which it is taken into advantage to protect essential components form oxidative damage.

1.6.5 Stress-induced signalling pathways

1.6.5.1 ER-stress and the unfolded protein response

Under conditions of cellular stress, such as: the accumulation of mutant and misfolded proteins, imbalanced calcium levels and even though alterations in lipid composition [140]; ER-equilibrium becomes compromised. In an attempt to re-establish equilibrium, the ER triggers an adaptive response called the unfolding protein response (UPR).

Alterations on ER-equilibrium are perceived by a variety of ER-stress transducers, which are tethered in the ER-membrane [141]. Three of these ER-stress transducers have been extensively described and characterized, as well as the respective signalling pathways triggered upon its induction, which are: protein kinase R-like endoplasmic reticulum kinase (PERK), inositol requiring enzyme 1 alpha (IRE1α) and activating transcription factor (ATF) 6α (Figure 4).

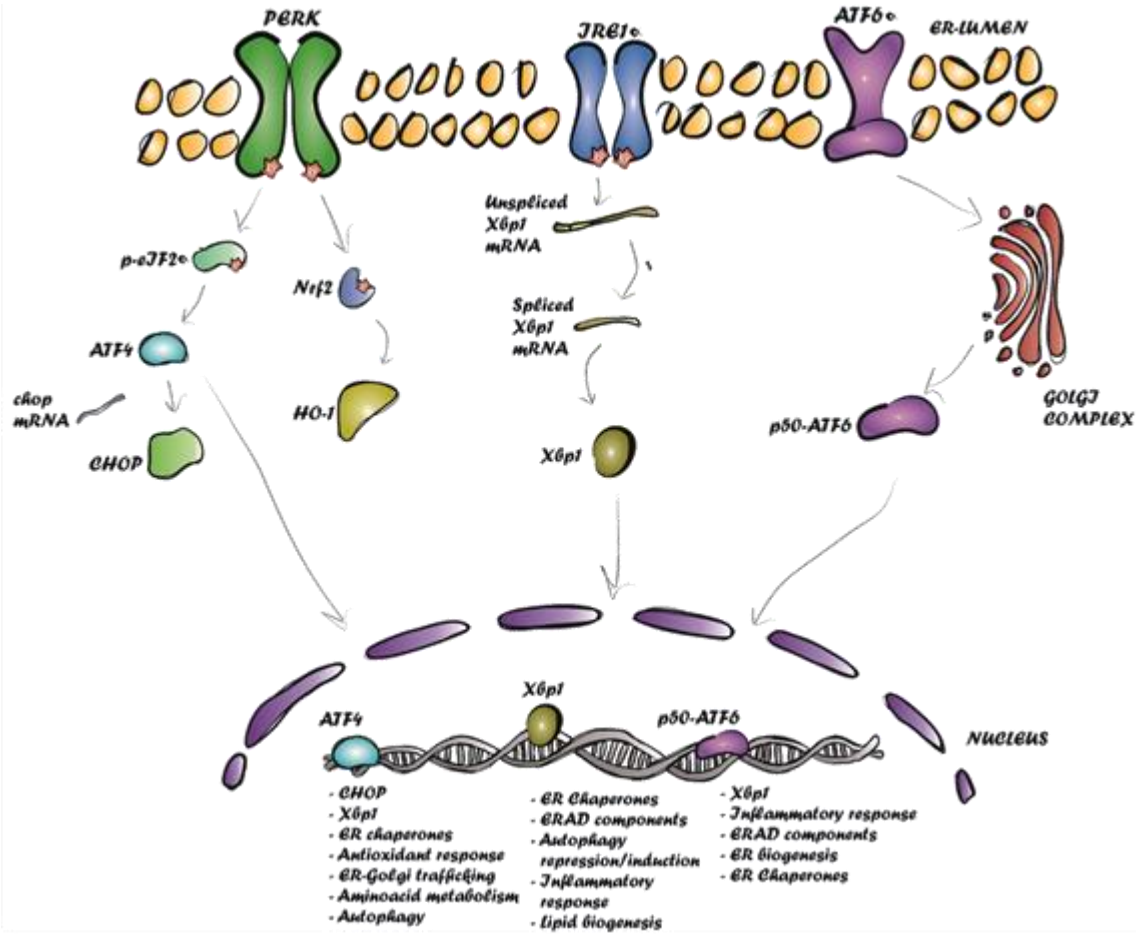

Figure 4 | Schematic representation of the three main ER-stress signalling pathways: PERK, IRE1α and ATF6α. The three ER-transducer work in coordination, triggering distinct signalling pathways, in an attempt to restore ER-homeodynamics.

The three ER-stress transducers are under normal conditions bound by their intra-luminal domain to molecular chaperone glucose-regulated protein 78/ immunoglobulin-heavy chain-binding protein (GRP78, also known as BiP). However, upon an impaired proteostasis environment, due to the increased accumulation of misfolded or aberrant proteins in the ER-lumen, BiP protein detaches from the ER-stress transducers and triggers their activation. Furthermore, lipid perturbation can also be accountable for the triggering of UPR responses, as PERK and IRE1α are known to perceive alterations on membrane fluidity or lipid packing, and more recently, ATF6α has been implicated in the sensing of specific sphingolipids [142-144].

ER-stress transducer PERK is a type I transmembrane protein, which is accepted to be activated through its dimerization and auto-phosphorylation. PERK activation can either result in cellular death or be cytoprotective, depending on which effectors are activated [145]. On one side, activated PERK promotes the phosphorylation of eukaryotic initiation factor 2 (eIF2α) in its Ser51 residue, attenuating global translational processes

[146]. Furthermore, the increased levels of phosphorylated eIF2α (p-eIF2α) aid in the expression of specific targets, namely of activating transcription factor 4 (ATF4). Consequently, ATF4 has been shown to stimulate ATF3 and CCAAT/enhancer-binding protein homologous protein (CHOP); which aid in metabolism regulation, cellular redox status and apoptosis [147]. Moreover, through the increased levels of p-eIF2α, activation of general stress transcription factors can be stimulated, as the steady-state levels of its regulatory proteins (namely its inhibitor) are lowered [147]. On the other side, PERK transducer also stimulates other well characterized signalling cascade – the erythoid 2–related factor 2 (Nrf2) pathway.

IRE1α is the most primordial ER-stress transducer so far described. It has been classified as a type I transmembrane protein, which exhibits intrinsic kinase and endoribonuclease activities. Upon detaching of BiP, the IRE1α transducer is activated upon dimerization, trans-autophosphorylation and binding of ADP co-factor [148, 149]. Upon induction and activation, IRE1α has site-specific endoribonuclease activity at the carboxyl end of its cytoplasmic domain and is responsible for the selective cleavage and degradation of specific mRNAs. One well characterized IRE1α-target involved in the UPR response is X-box binding protein 1 (*Xbp1*) mRNA. It is commonly accepted that upon IRE1α activation, due to its RNase activity, excision of a 26bp intron of unspliced-*Xbp1* (*uXbp1*) mRNA is possible [150]. Though this axis, the IRE1α signalling pathway contributes to the expression of ER-chaperones and to ER-biogenesis, which consequently lead to the enhancement of the secretory capacity of the ER.

Mammalian cells express two distinct ATF6 homologous proteins: the ATF6α and the ATF6β proteins; which exhibit specific physiological and biochemical characteristics. In the present thesis, we will be focusing on ATF6α, which on the contrary to both PERK and IRE1α, is a type II transmembrane glycoprotein [151]. ATF6α has been demonstrated to be expressed constitutively as a 90-kDa protein (p90ATF6α) [151], to which BiP protein is bound. In ER-stress cells, BiP dissociates from p90ATF6α, leading to the exposure of two golgi-localization sequences present in its ER-luminal domain [152]. p90ATF6α is then translocated to the golgi complex (GC), where upon action of site-1 protease and site-2 protease , cleavage of the luminal domain and the transmembrane anchor occurs, culminating in the formation of an active 50-kDa protein (p50ATF6α) [152]. However, in the literature, it has been demonstrated that this protein can suffer post-translational processing in other peptides, which also present biological activity. Upon its cleavage, p50ATF6α migrates to the nucleus, where it binds to ER-stress response elements, inducing the expression of several molecular chaperones

(e.g. BiP, GRP94 and calreticulin) and ER-degradation-enhancing α-mannosidase-like proteins. Furthermore, p50ATF6α also upregulates the expression of *Xbp1* gene [153], which after transcription is processed by IRE1α.

However, activation of these ER-stress transducers has been shown to occur via non-canonical pathways, known to play specific roles in the UPR response. But overall, it is accepted that the UPR response culminates in the reprogramming of the transcriptional and translation cell program to a pro-survival response, aiming to reduce ER-load through: (1) the increase on its folding capacity, (2) the promotion of the degradation of misfolded proteins and (3) autophagy triggering [154, 155]. Nonetheless, if ER-stress pursuits, the UPR can further increase the accumulation of ROS within the cells and switches to a pro-apoptotic response, which culminate in cell death.

1.6.5.2 General stress signalling responses

Stress signalling pathways have been evolutionary conserved throughout evolution and serve as a point of integration of several stimuli.

Besides the ER-stress response, both ROS generation and all the three branches of the canonical UPR have been associated with the activation of oxidative stress pathways. One of the most important general stress signalling pathways involves the activation of NF-κB. The NF-κB family of transcription factors is composed by 7-Rel related proteins. Under normal conditions, NF-κB is associated with members of the inhibitor of κB (IκB) protein family, which maintain NF-κB sequestered in the cytoplasm, thus controlling its DNA-binding affinity. Upon a large variety of stimulus, signalling adaptor engage IKK activity, which will consequently phosphorylate serine residues present in the signal responsive region of IκB proteins [156]. The post-translational modification of IκB proteins ultimately leads to its ubiquitination and proteasomal degradation. The NF-κB dimers are then free to translocate to the nucleus, where they can induce the transcription of specific target genes. The fine-tuning of the transcription process can be further modulated, though the constitution of the dimers formed and the post-translation modification of NF-κB proteins.

Albeit the induction of the NF-κB pathway has been most notorious, the panoply of signalling pathways activated upon oxidative stress are far more extensive and will not be here fully reviewed. However, special emphasis can be given to the subsequent

pathways, which are known to be upregulated in obesity, contributing to its progression and to the development of related comorbidities.

1.6.6 Autophagy mechanisms

Autophagy aids in cellular homeostasis, since it contributes to the regeneration of metabolic precursors and biomolecules, as well as to the clearance of damaged or unnecessary subcellular debris [136]. Furthermore, autophagy mechanisms also contribute to the selective delivery of mitochondria (mitophagy), ribosomes (ribophagy), bacteria/viruses (xenophagy), peroxisomes (pexophagy) and protein aggregates (aggrephagy) to the lysosome and/or vacuole [157].

Autophagy responses can be induced through a variety of regulatory factors, although its regulation occur predominantly by amino acids and hormones. Hitherto, three distinct types of autophagy have been described attending the modality by which autophagosomes are delivered into the lysosome, namely: macroautophagy, microautophagy and chaperone-mediated autophagy [158, 159]. Macrophagy, from now on termed autophagy, is the best characterized autophagy type. This process is characterized by the formation of autophagy vesicles, through: (1) membrane nucleation/ autophagy iniciation (2) vesicle elongation and cargo recruitment, (3) autophagosome maturation and (4) autophagosome cargo degradation [136, 160].

The autophagy machinery is complex. Thus far, about 35 autophagy-related proteins (ATG) have already been described in yeast through genetic screens. Most ATG genes found in yeast have homologous counterparts in mammals, which regulate autophagy mechanisms alongside with additional factors specific to higher eukaryotes [161]. The ATG proteins are evolutionary conserved in other species, and form several functional units: namely the Atg1–unc-51-like kinase (ULK), the class III PI3K complex, ATG9 vesicle, the ATG2-ATG8 complex, the ATG12 conjugation system and the microtubule-associated protein light chain 3 (LC3) conjugation system [161].

In canonical autophagy, in the initiation step, nucleation of cellular membranes occurs, to form a pre-autophagosome structure called the phagophore. The phagophore is constituted by a cup-shape membrane, which engulfs parts of the cytoplasm [160]. Cellular membrane nucleation is promoted by phosphatidylinositol-3-phosphate (PI3P), which is generated by a multimeric protein complex, composed of Beclin 1, class III phosphatidylinositol-3-kinase (PIK3C3, or VPS34), and ATG14L [136]. This process is

maintained under tightly control, including ultraviolet irradiation resistance-associated gene (UVRAG) and Bax-interacting factor 1 (BIF1), which substitute for ATG14L, autophagy/beclin-1 regulator 1, and the putative negative regulator Rubicon.

Upon membrane nucleation, elongation and sealing of the autophagosome membrane occurs, originating the autophagosome. The autophagosome possesses a unique double-membrane. Two important ubiquitin-like systems are known to intervene in autophagosome elongation: the ATG12 and the LC3 conjugation machineries. In the ATG12 conjugation, the ATG12 protein is conjugated with ATG5, by E1-like enzyme ATG7 and E2-like enzyme ATG10, giving rise to the ATG12-ATG5 complex. Conjugation of ATG12-ATG5 appears to occur constitutively in the cell, as no E3-like enzyme responsible for ATG12-ATG5 de-conjugation has been discovered [160]. Furthermore, the ATG12-ATG5 complex further conjugated with the coiled-coil protein ATG16L1 (following its oligomerization). The ATG12-ATG5-ATG16L1 complex functions as a E3-like enzymes, and aids in the formation and in the elongation of the autophagosome membrane [161]. Furthermore, the LC3 system is homologous of the ATG8 system in yeast. In this system, LC3 is cleaved by ATG4B protease, generating LC3-I isoform. To this isoform, as well as to other LC3 homologues, the phosphatidylethanolamine (PE) is added. Conjugation of LC3-I with PE occurs through the sequential action of E1-like enzyme ATG7 and E2-like enzyme ATG3, originating the LC3-II. Conversion of LC3-I into LC3-II is a key step in the regulation of autophagy membrane elongation.

Subsequently, the autophagosome matures as it fuses with endosomes and subsequently with lysosome, generating autophagolysosomes. Following fusion, degradation of the inner membrane of the autophagolysosome and the cargo sequestered occurs [161].

1.7 MODULATION OF STRESS SIGNALLING PATHWAYS IN OBESITY

In obesity, perhaps the most important factors contributing to the exacerbation of oxidative stress is the excessive supply of substrates to the metabolic pathways. Indeed, AT dysfunction is known to play an important role in the aggravation of systemic oxidative stress, which ultimately contribute to both obesity progression and related comorbidities [162, 163].

1.7.1 Mitochondrial signaling pathways become dysfunctional in obesity

The excessive supply of metabolic substrates is known to impair mitochondrial dynamics. Evidences suggest that mitochondrial number, distribution and morphology suffer alterations in obesity [164]. Many factors contribute to mitochondrial progressive dysfunction in obesity, which include: (1) impairment of lipid and glucose metabolism, (2) alterations of DNA methylation sites in adipocyte precursors which alter the metabolic phenotype of mature adipocytes [164].

Dysregulation of mitochondrial processes has also been implicated in the exacerbation of ROS synthesis that occurs primarily during the OxPhos. Undeniably, balanced production of ROS by mitochondria has been recognized as an important redox signal, which is responsible for the integration of the mitochondrial function with the rest of the cellular processes [165]. Furthermore, the mitochondria is capable of coordinate its functions with other organelles in the cell, such as the ER, through direct contact at multiple sites – mitochondria-ER associated membranes – enabling the regulation and interconnection of distinct processes in the cell [166]. For this reason, communication between these organelles is thought to be the link between mitochondrial dysfunction and ER stress. In the case of obesity pathology, this interconnection has a negative role in the progression of obesity, and to the development of metabolic disorders associated with obesity, as both exhibit impaired function in obesity [167].

1.7.2 ER-stress in obesity

Although the ER organelle has been typically seen as the organelle responsible for the correct folding of proteins, it also plays an important role in nutrient and energy sensing, aiding in the regulation of TG droplets formation and in the sensing of cholesterol levels [168]. Thus, it is no surprising that obesity has been extensively associated with UPR disturbances [140, 168]. Previous studies have demonstrated that obesity *per se* causes ER stress, predominantly in the liver and in the AT [169].

In the particular case of obesity, ER-stress induction can occur through the stimulation of classic ER-stress mechanisms involving the ER-lumen or through alterations on the ER-membrane environment [170]. However, in early-onset obesity, the UPR appears to exhibit a cytoprotective role. During obesity progression, ER-stress becomes chronic. The constitutive activation of ER-stress signalling pathways has been

shown to be one of the main causes of AT inflammation, since it stimulates the synthesis of a variety of inflammatory cytokines [171]. Thus, the constitutive activation of ER-stress signalling pathways, contributes to the development of obesity-induced co-morbidities. Thus, targeting of ER-stress signalling pathways has been postulated by many to be reasonable to halt, or at least attenuate, obesity-induced complications [171].

1.7.3 Oxidative stress pathway

The consumption of a high-fat diet (HFD) and obesity *per se* have not only been associated with the UPR activation, but also with the chronic activation of stress signalling pathways, ultimately contributing to the impairment of metabolism. Among these are included the activation of general stress transcription factor NF-κB in a time-dependent manner [172]. It is consensual in the literature that activation of the NF-κB pathway promotes inflammation, which ultimately contribute to the development of metabolic disorders. In fact, interfering with the NF-κB pathway has been demonstrate to alleviate type 2 diabetes, hyperglycemia and insulin resistance [173]. Further contributing to the inflammatory profile, obesity is also associated with the activation of: MAPK pathways [ERK, c-Jun N-terminal kinase (JNK) and p38] [174] and the NADPH oxidase (specially of NOX4 in AT) [175]. The constitutive activation of these signalling pathways, among others, have delineated the relationship between obesity and immunometabolism; and has been associated with the development of obesity-related complications.

Further contributing to this aggravation, in obesity, the antioxidant defences responsible for the maintenance of redox homeodynamics become compromised. Obese individuals are known to typically present diminished levels of antioxidant sources: SOD, catalase, vitamin A, vitamin C, vitamin E and β-carotene; which cannot compensate the increased concentration of ROS in the cells [176].

1.7.4 Autophagy in obesity

Autophagy mechanism are known to be unregulated in obesity [177]. However, it is not clear if stimulation or repression of this recycling mechanisms occurs in obesity pathophysiology [178]. What is known, is that adipocyte deregulation of autophagy has deleterious effects on both local and global metabolism, which contribute to the

development of metabolic disorders [178]. Supporting this, pharmacological modulation of autophagy has proven to be beneficial for the treatment of obesity and related comorbidities in pre-clinical studies [178]. However, autophagy might not be only an effect of obesity but also a cause, thus creating a vicious cycle which contributes to the further deterioration of systemic metabolism in obesity.

Nevertheless, how does this mechanism become unregulated in obesity? It has been extensively described that autophagy responses are highly sensitive to nutrient signals, in particular to high-fat diets and rich caloric food intake [178]. This mechanism predominantly occurs though the PI3K and protein kinase B (PKB, also known as AKT). The latter is known to activate mammalian target of rapamycin (mTOR), and it is postulated to contribute to the Beclin-1 phosphorylation [136]. Thus, through the activation of mTOR (consequently inhibition of ULK1 activity), as well as the phosphorylation of Beclin-1, these mechanisms serve as negative regulators for autophagy mechanisms. On the other side, inflammatory stimuli could also be accountable for the upregulation of autophagy in adipose tissue [178].

In sum, it is observed that in obesity, autophagy responses in AT are activated by multiple regulatory signalling pathways, which sometimes exhibit an opposing effect. In fact, understanding of the autophagy processes in obesity is quite confusing, since autophagy responses vary attending : (1) the studied model of obesity, (2) the obesity duration, (3) the tissue- and organ- studied, (5) the results obtained by distinct techniques when analysing the same tissue yield distinct results and (6) characteristic of the studied patient or animal (as the age) and the incidence of related comorbidities [178].

2. AIMS

Although the modulatory role of melanocortin α-MSH in the CNS has been extensively described in the bibliography, little is known about its role in the modulation of signalling pathways in peripheral tissue, namely AT. Previous results from our group demonstrated that the intraperitoneal administration of α-MSH promoted browning of adipose tissue while boosting energy expenditure in obese C57BL/6 mice. Furthermore, this melanocortin induced an overall amelioration of the metabolic profile of these animals [1].

Hence, the present work aims to ascertain if the observed amelioration occurred alongside with the modulation of stress signalling pathways and autophagy mechanisms in ingWAT of obese mice.

A previously established obesity-induced mice model will be employed in this work. After 14 days of treatment with α-MSH, ingWAT was collected and here used for the analysis of:

1. The effect of α-MSH in the three main UPR-induced mechanisms, which include the PERK, IRE1α and ATF6α signalling pathways;
2. The redox status of AT, through the direct detection of ROS, and also through the evaluation of the key antioxidant enzymes and transcription factors, which compose the antioxidant defence system;
3. The oxidative damage induced by ROS, in proteins and DNA;
4. The appraisal of cellular recycling mechanisms, through the determination of the expression levels of autophagy-related proteins.

3. METHODOLOGY

3.1 Animals and ingWAT processing

The animal model of obesity used in the present study was established in a previous work [1]. Briefly, 10-week-old C57BL/6 mice was fed with a high fat diet (HFD) (45% of total energy from fat) for 10 weeks. Then, obese mice were subjected to daily intraperitoneal injections of saline solution (control group) or α-MSH (150 µg/kg/day) for 2 weeks. Afterward, animals were sacrificed and ingWAT was harvested. The collected tissue was in part stored at -80 °C (RNA and protein extraction), immersed in formaldehyde (used as a fixative before inclusion on paraffin, which was used for the histological staining technique) and included in optimal cutting temperature (OCT, VWR, Pennsylvania, EUA) compound (used for the immunohistochemistry technique).

3.2 Masson's trichrome coloration

Paraffin-embedded ingWAT sections from standard and HFD fed mice were subjected to the Masson's trichrome stain. Firstly, sections were dewaxed in xylene for 10 minutes. AT sections were then hydrated with solutions containing successively lower concentration of ethanol (100%, 90% and 70% v/v), and finally were placed in water for a minimum of 20 minutes. Afterwards, AT was stained with aniline blue solution for 5 minutes, followed by staining with gill haematoxylin for the same period of time. Then, ingWAT sections were rinsed with picric alcohol 1% (w/v) for 15 minutes, and then washed abundantly with water. Next, ingWAT was stained with ponceau fuchsin for 15 minutes. After removing its excess with water, sections were placed for 10 minutes in the mordant phosphomolybdic acid 1% (w/v). The samples were afterwards washed with water, before staining with 0.5% w/v of light green SF yellowish for 10 minutes. Lastly, dye excess was removed with water, and then left for 2 minutes in a 1% v/v acetic acid solution. After this step, the slides were quickly passed though absolute ethanol and xylene, before assembly with Entellan® media (Merk, Darmstadt, Germany). Stained ingWAT was observed under the Zeiss Axioskop 40 microscope (Zeiss, Oberkochen, Germany), and digital images were captured with the coupled Leica EC3 camera (Leica, Wetzlar, Germany). Captured images were analysed using Axiovision Rel 4.8 software.

3.3 Protein extraction and quantification

Total protein content was extracted from 100 mg of frozen ingWAT. ingWAT portions were placed in an Eppendorf containing 1,4mm Precellys® Zirconium Oxide Beads (Bertin Corporation, Montigny-le-Bretonneux, France) and 200 μL of lysis solution (5mM Tris-base pH 7.5, 10 mM NaCl, 5 mM EDTA, 1 mM β-glycerophosphate, 0.25% Triton X-100, 1:200 phosphatase inhibitor and 1:100 protease inhibitor). Subsequently, the tissue was mechanically homogenised at 65000 RPM for 20 seconds, using the MagNA Lyser Instrument (Roche Life Science, Penzberg, Germany) and then subjected to sonication during 15 minutes at 4°C, using Bioruptor UCD-100 sonicator (Diagenode, Denville, USA) coupled with Huber Minichiller 300 (Huber, Berching, Germany). Following sonification, samples were centrifuged at 12000G, during 10 minutes at 4°C, using HeraeusTH FrescoTH 21 centrifuge (ThermoFisher Scientific, Massachusetts, EUA) and the supernatant containing the protein fraction was recovered and stored at -20°C. The quantification of ingWAT protein extracts was performed using the traditional Bradford method, using the Bio-Rad Protein Assay Dye Reagent Concentrate (BioRad, California, USA). Spectrophotometric readings were carried out at 595 nm, using Tecan Infinite M200 spectrophotometer (ThermoFisher Scientific, Massachusetts, EUA). Lastly, protein concentration was estimated through interpolation with data from a bovine serum albumin (BSA) standard curve previously established.

3.4 Antibodies

In the current work, the following primary antibodies were used for the Western Blotting (WB) technique: rabbit anti-PERK (C33E10) at 1:1000 for 4 O/N at RT(Cell signalling, 3192S), rabbit anti-p-eIF2α SER51 D9G8 at 1:1000 for 4 O/N at 4ºC (Cell signalling, 3398P), rabbit anti-ATF4 (D4B8) at 1:500 for 8 O/N at RT (Cell signalling, 11815S), rabbit anti-HO-1 at 1:1000 for 4 O/N at 4ºC (Protein tech, 10701-1-AP), rabbit anti-IRE1α (14C10) at 1:500 for 8 O/N at RT (Cell signalling, 3294S), goat anti-ATF6α (N-16) at 1:200 for 4 O/N at 4ºC (Santa Cruz Biotechnology, sc-14250), anti-HSP90 at 1:3000 for 4 O/N at 4ºC (Abcam, ab13495), rabbit anti-SOD1 (FL-154) at 1:1000 for 4 O/N at 4ºC (Santa Cruz Biotechnology, sc-11407), rabbit anti-SOD2 at 1:10000 for 2 O/N at 4ºC (FL-122) (Santa Cruz Biotechnology, sc-30080), rabbit anti-Gpx-1 at 1:1250 for 4 O/N at 4ºC (Abcam, ab22604), rabbit anti-NF-κB at 1:1000 for 7 O/N at RT (D14E12) p65 (Cell signalling, 8242), rabbit anti-phospho-NF-κB p65 Ser536 (93H1) at 1:1000 for 7 O/N at RT (Cell signalling, 3033), rabbit anti-p-H2AX SER139 (20E3) at 1:1000 for 7 O/N

at RT (Cell signalling, 9718S), rabbit anti-Beclin-1 (D40C2) at 1:500 for 4 O/N at 4ºC (Cell Signalling, 3495T),rabbit anti-ATG5 for 4 O/N at 4ºC (D5F5U) at 1:1000 (Cell signalling, 12994), rabbit anti-ATG7 for 4 O/N at 4ºC (D12B11) at 1:1000 (Cell Signalling, 8558), rabbit anti-ATG3 at 1:1000 for 4 O/N at 4ºC (Cell signalling, 3415), rabbit anti-α-LAMP1 (H4A3) at 1:2500 for 7 O/N at RT (Abcam, ab25630), rabbit anti-ATG16L1 (D6D5) at 1:1000 for 7 O/N at 4ºC (Cell signalling, 8089T), rabbit anti-LC3A/B (D3U4C) at 1:1000 for 7 O/N at RT (Cell signalling, 12741), anti-p62 at 1:1000 for 4 O/N at 4ºC (Abcam, ab109012), goat anti-β-actin at 1:5000 for 1 O/N at 4ºC (Santa Cruz Biotechnology, sc-1616). The secondary antibodies were the following: goat anti-rabbit IgG HRP-linked at 1:5000 (Cell signalling, 7074), donkey anti-goat IgG HRP-linked at 1:10000 (Santa Cruz Biotechnology, sc-2020) and goat anti-mouse IgG HRP-linked at 1:10000 (Santa Cruz Biotechnology, sc-2039). Detection of β-actin was, in membranes to be incubated by anti-ATF4 primary antibody, carried out using the hFABTH Rhodamine Anti-actin primary antibody at 1:1000 for 1 hour at RT (Bio-Rad, #12004164), as these membranes were blocked with NGS. Detection of p-H2AX was also carried out by immunofluorescence, having been used the same primary antibody as for western blot, subsequently detected with the donkey anti-rabbit IgG (H+L) highly cross-adsorbed secondary antibody, Alexa Fluor 488 (Invitrogen, A21206) at 1:500 at RT for 1 hour.

3.5 WB analysis

SDS-PAGE was used to separate ingWAT protein lysates. 10% and 14% acrylamide gels were assembled in the Mini-Protean® Tetra Vertical Electrophoresis Cell (BioRad, California, USA), to which Laemmli buffer (25 mM Tris, 250 mM Glycine and 3.5 µM SDS) was added. Circa 30 µg of protein from each sample were prepared in sample buffer [150 mM dithiothreitol (DTT) and gel loading buffer (75 mM Tris pH 7.5, 3 mM EDTA, 15% glycerol, 3% SDS and 0.02% Bromophenol blue)], and loaded into the gel. As well as the protein molecular weight standard – NZYColour protein marker II (NZYTech, Lisboa, Portugal). Each SDS-PAGE gel was run at 25 mA, until the samples reached the bottom of the gel. Then, the separated proteins were blotted into 0.45 µm nitrocellulose membrane (Bio-Rad, California, USA). The transfer reaction was carried out in transfer buffer (48 mM Tris, 38 mM Glycine and 1.3 µM SDS and 20% methanol) using the BioRad system (BioRad, California, USA), at 30 V for 90 minutes. Prior to the incubation with the primary antibody, membranes were blocked with a solution of 5% BSA diluted in TBS/0.1% Tween-20 (20 mM Tris, 137 mM NaCl and 0.1% Tween-20, pH

7.6), during 1 hour at room temperature (RT). All membranes were blocked with 5% BSA, except for membranes to be incubated with anti-IRE1α and anti-ATF4 protein, which were incubated with 5%milk powder and 5% NGS, respectively. Specific primary antibodies were then diluted in the respective blocking solution and the membranes were incubated under specific conditions referred in section 3.4. Membranes were then washed in TBS/ 0.1% Tween-20 solution at least 4 times for 20 minutes, before incubation with the respective secondary antibody conjugated with the horseradish peroxidase (HRP) enzyme. In the particular case of membranes incubated with anti-ATF4 antibodies, further detection of β-actin was conducted by incubation with a specific fluorescent-conjugated antibody for 1 hour at RT, using a concentration of 1:1000. Membranes were incubated with respective secondary antibodies at RT for 60 minutes. Then, membranes were washed at least 4 times during 20 minutes in TBS/0.1% Tween-20, followed by a 10-minute wash with TBS/0.1% Triton X-100 (20 mM Tris, 137 mM NaCl and 0.1% Triton X-100, pH 7.6). Membranes were then visualized by chemiluminescence or fluorescence (in the case of ATF4), and quantified by densitometric analysis using ChemiDoc™ XRS (Bio-Rad, California, USA) and β-actin as loading control. Values were normalized to the mean of the values obtained for the control group (mice intraperitoneally injected with saline solution).

3.6 Oxyblot for detection of carbonylated proteins.

After the transfer process, nitrocellulose membranes with immobilized ingWAT proteins were equilibrated in 20% methanol/TBS solution for 5 minutes, and then washed using a 10% 2,2,2-trifluoroacetic acid (TFA) solution for 5 minutes. Then, membranes were incubated with 10 mM DNPH diluted in 10% TFA during 10 minutes at RT protected from light. After derivatization, the membranes were washed at least 5 times during 10 minutes in 10% TFA, followed by a 5-minute wash with a 50% methanol solution. Afterward, the nitrocellulose membranes were washed in TBS-Tween-20, for at least 3 times for 5 minutes. In order to avoid unspecific binding of the primary antibody, membranes were blocked during 1 hour at RT with a 5% milk powder/ TBS-Tween-20 solution. Subsequently, membranes were incubated with rabbit anti-DNP at 1:7500 (Sigma, D9656) primary antibody, during 3 overnights at 4°C. Membranes were then washed for at least 4 times, 20 minutes each, before proceeding to their incubation with HRP-conjugated anti-rabbit secondary antibody at 1:5000, during 1 hour at RT. Then, membranes were washed 4 times with TBS/ 0.1% Tween-20 solution, for a total of 80

minutes, and during 10 minutes with TBS/Triton X-100. Finally, carbonylated proteins were visualized by chemiluminescence, and quantified by densitometry analysis using ChemiDoc™ XRS (Bio-Rad, California, USA).

3.7 Immunofluorescence microscopy

Samples of ingWAT embedded in OCT were fixed in PFA 4% diluted in phosphate-buffered saline (PBS) for 2 hours, and then left in 30% sucrose/PBS buffer for 4 ON at 4°C. Afterwards, the tissue was included in OCT again and sectioned in the Leica CM3050 cryostat (Leica, Wetzlar, Germany). Section were then used to detect p-H2AX through immunofluorescence microscopy. Briefly, 14 µM sections of ingWAT were made to adhere to microscope slides for 30 minutes at 60°C. OCT residues were removed from ingWAT slices by washing with PBS. Tissue permeabilization was achieved using PBS/1% Triton X-100 for 5 minutes. Afterwards, ingWAT sections were washed with TBS/ Tween-20 for 5 minutes. In order to diminish unspecific binding of the primary antibody, sections were blocked in a solution of 5% BSA in TBS/Tween-20 for 1 hour at RT. Subsequently, incubation with the primary antibody rabbit anti-p-H2AX occurred ON at 4°C. Tissue sections were then washed at least 4 times, each time for at least 5 minutes, with TBS/0.1% Tween-20. Incubation with secondary antibody anti-rabbit, conjugated with Alexa® 488, was carried out in the dark for 1 hour at RT. Afterwards, secondary antibody excess was removed with TBS/0.1% Tween-20. In order to stain cell nucleus, the ingWAT sections were briefly incubated with 4',6-diamidino-2-phenyl-indole (DAPI). Lastly, slides were mounted with coverslips in a glycerol-PBS solution. Tissue sections were analysed by fluorescence microscopy, using Carl Zeiss AxioImager Z1 Apotome (Carl Zeiss, Oberkochen, Germany) coupled with a Zeiss AxioCam MR (Zeiss, Oberkochen, Germany) digital camera. Image analysis was carried out using Axiovision Rel 4.8 software.

3.8 qPCR experiments

Total ingWAT RNA content was previously extracted using TripleXtractor RNA (Grisp, Porto, Portugal) commercial kit following the recommended fabricant instructions. Evaluation of its concentration and purity was carried out previously using NanoDrop 2000 spectrophotometer (Thermo Scientific, Massachusetts, USA), and accordingly, a total of 1 µg RNA was used for cDNA synthesis using NZY First-Strand cDNA Synthesis

kit (NZYTech, Lisboa, Portugal), following the manufacturer instruction. Quantitative real-time PCR (qPCR) was then carried out in StepOne™ Real-Time PCR System (Applied Biosystems, California, USA) using PowerUp™ SYBR® Green Master Mix (Life Technologies, California, USA) and 0.5 µM of specific primers for CLU (Forward 5' CCAGTTCCCAGACGTGGATTT 3' and reverse 5' TTTGATTCTTCCTCTTCGTTTCC 3') and CHOP (Forward 5' GCCAGAATAACAGCCGGAAC 3' and reverse 5' TTTGATTCTTCCTCTTCGTTTCC 3') genes. The present analysis included as a reference gene the 18S ribosomal RNA gene (Forward 5' CGCCGCTAGAGGTGAAATTC 3' and reverse 5' CATTCTTGGCAAATGCTTTCG 3').

3.9 Assessment of H_2O_2 concentration in ingWAT

Determination of H_2O_2 concentration in ingWAT was possible through the use of Amplex® Red Hydrogen Peroxide/Peroxidase Assay kit (Invitrogen, California, USA). For the assay, 20 mg of frozen ingWAT was homogenised mechanically in 40 µL of 1X Reaction Buffer for 1 minute. The supernatant was then recovered and evaluated regarding its protein content using the previously described Bradford method. A total of 3 samples for each group was tested, using 5 µg and 25 µg of total protein. Each well contained the appropriate protein content in a total volume of 100 µL, in which 100 µM of Amplex Red reagent and 0.2 U/mL HRP diluted in 1X reaction buffer was added. Then, the samples were allowed to incubate at RT for 40 minutes, after which fluorescence was measured using Synergy™ Mx instrument (BioTek, Vermont, USA). The microplate reader was calibrated for excitation in 530 nm, and fluorescence was measured at approximately 590 nm. Values were normalized to the mean of the values obtained for the control group (mice intraperitoneally injected with saline solution).

3.10 Statistical Analysis

The results presented in this work are exhibited as means ± standard error of the mean (SEM). All experiments, with the exception of H_2O_2 measurements, were repeated at least twice. Furthermore, statistical analysis was carried out in GraphPad PRISM 6 (V.6.01), applying the unpaired two-tailed Student´s *t* test. Outliers were detected in the dataset through the ROUT method (Q of 1.0%) and were removed from the present analysis. Results were considered to be statistically significant when the value of *p* was lower than 0.05 ($*p < 0.05$ and $**p < 0.01$).

4. RESULTS

4.1 Histological characterization of obese ingWAT

The excessive accumulation of fat mass, typically in the form of triglycerides, induces the enlargement of lipid droplets in the adipocytes. In obese AT, due to the excessive accumulation of energy, adipocytes are significantly enlarged when in comparison with adipocytes from AT of lean individuals (Figure 5). In obesity, in an attempt to physically restrict AT expansion, production of extracellular components is promoted. Thus, as evidenced though the Masson's trichrome staining, obese AT presents an enhanced fibrotic profile, characterized by the increased accumulation of collagen fibbers observed in a dark bluish-green tonality in Figure 5 (green arrows). Improper remodelling of AT in obesity also promotes an increased inflammatory profile. When analysing obese ingWAT stained by Masson's trichrome, an increased accumulation of structures resembling CLS were visualized; in which is possible to observe what appears to be macrophages (dark purple) surrounding a presumably dead adipocyte (Figure 5, yellow arrows). To confirm if indeed these structures are CLS, further studies are necessary. The observed morphological alterations were already expected since these modifications were extensively described in the literature.

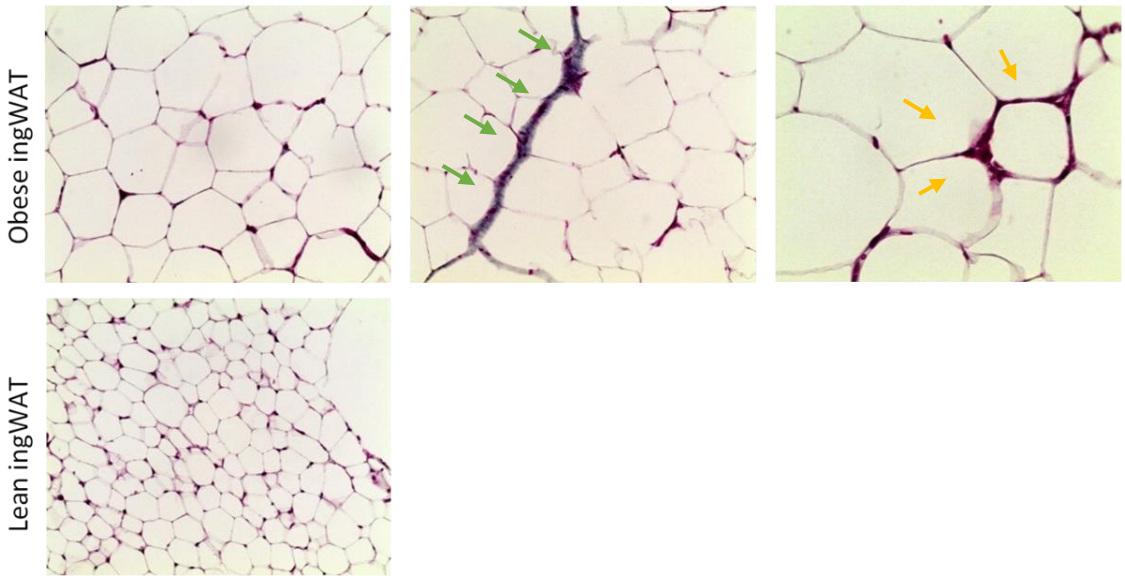

Figure 5 | Morphological analysis of inguinal SAT. Representative images of ingWAT sections, collected from obese and lean mice, stained using the Masson's trichrome technique. When in comparison with lean mice, obese mice present significantly enlarged adipocytes in ingWAT. Obese ingWAT also presented an increased fibrotic profile, as evidenced in green by the Masson's Trichrome stain (green arrows). Furthermore, obese ingWAT stained with Masson´s Trichrome also shows an increased prevalence of structures resembling CLS (yellow arrows), suggesting an increased inflammatory profile in obese ingWAT.

In fact, previous work carried out by our group demonstrated that intraperitoneal administration of α-MSH promoted a significant increase in the number of smaller adipocytes, whereas it diminished the number of enlarged adipocytes [1]. Attending that smaller adipocytes are typically depicted in the literature as less dysfunctional [49], these observations are in accordance with the ameliorated metabolic profile found in α-MSH-treated obese animals [1].

4.2 Melanocortin α-MSH modulates ER-stress signalling pathways in ingWAT of obese mice

It is consensual in the literature, that obesity is intrinsically associated with the development and maintenance of high ER-stress levels in AT [169]. Thus, we tried to comprehend if this neuropeptide was able to modulate the three main ER-stress signalling pathways: PERK, IRE1α and ATF6α signalling pathways.

4.2.1 PERK/ p-eIF2α/ ATF4 signaling pathways

WB analysis showed that obese mice treated with α-MSH exhibited lower expression levels of total PERK protein when compared to control animals (0.99±0.40 for control vs. 0.58±0.14 for α-MSH-treated groups, p=0.0211) (Figure 6, A). This occurs alongside with a decreased phosphorylation levels of its target, eIF2α on serine 51 (1.05±0.68 for control vs. 0.47±0.29 for α-MSH-treated groups, p=0.0333)(Figure 6, B). Attending the diminished levels of PERK and p-eIF2α in ingWAT of obese mice, it was expected a decreased expression of the PERK downstream mediator – ATF4. Unpredictably, it was demonstrated that the neuropeptide α-MSH does not alter the expression levels of ATF4 (1.00±0.20 for control vs 0.97±0.47 for α-MSH-treated groups, p=0.915) (Figure 6, C). Taking into consideration that ATF4 expression levels remain unchanged, we aimed to comprehend in the present work if transcript levels of the *Chop* gene, known to be induced by ATF4 were also similar in both experimental groups. Indeed, *Chop* mRNA levels did not vary between control and α-MSH-treated mice ($8.11\times10^{-5}\pm5.58\times10^{-6}$ for control vs $9.63\times10^{-5}\pm1.16\times10^{-5}$ for α-MSH-treated groups, p=0.311) (Figure 6, D).

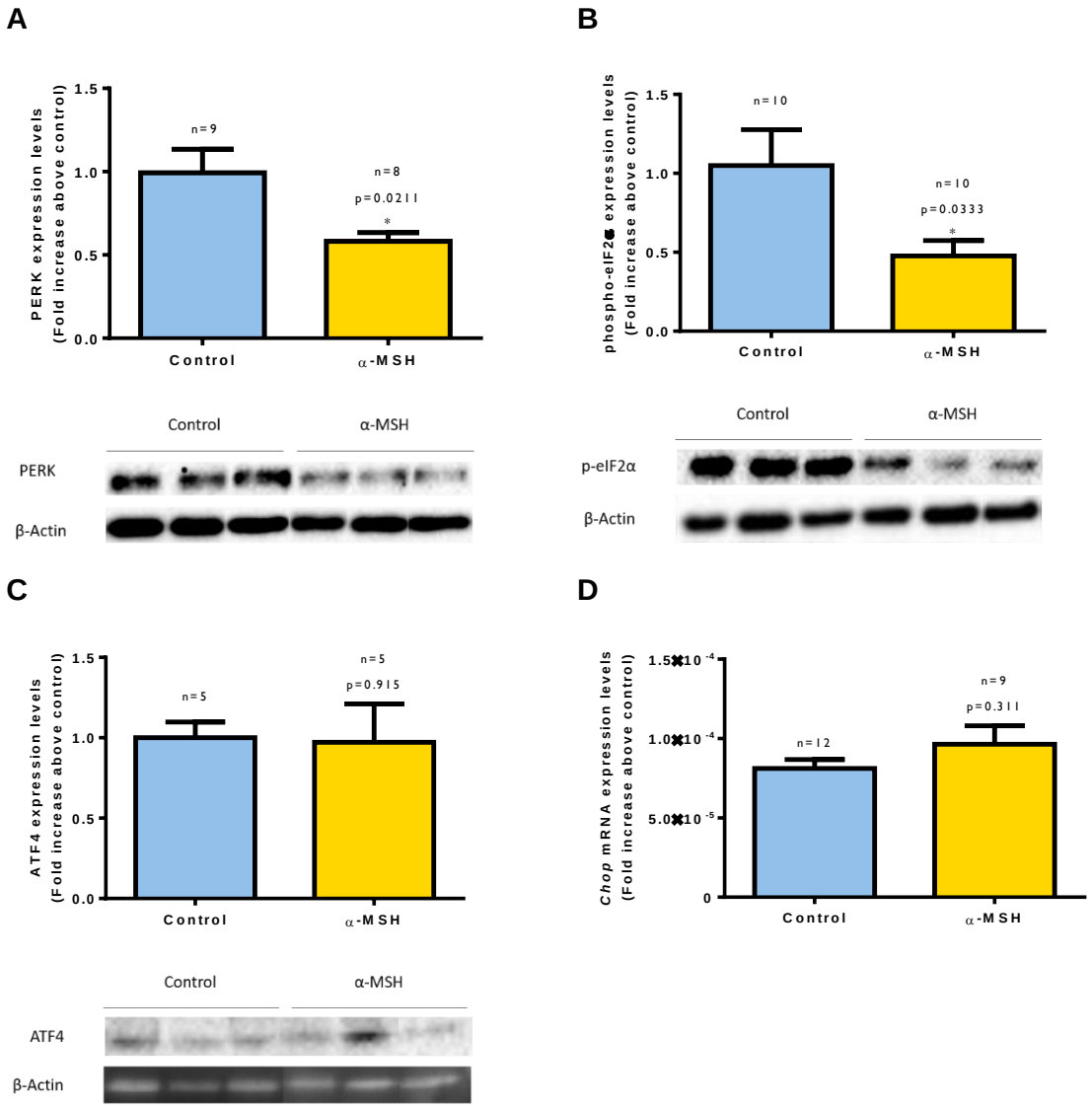

Figure 6 | **The PERK signalling pathway is modulated by melanocortin α-MSH in ingWAT of obese mice.** (**A**) WB analysis revealed that melanocortin α-MSH diminished the expression levels of PERK protein in ingWAT of C57BL/6 obese mice. WB bands are representative of 4 independent experiments. (**B**) α-MSH-treated mice presented lower levels of phosphorylated eIF2α at Ser51, as demonstrated in the blot accompanying the graph. (**C**) Albeit the diminished levels of p-eIF2α, downstream expression of ATF4 was unaltered. Data obtained by WB were analysed by densitometry, and the collected data used for graph construction (**D**) Accordingly, levels of *Chop* mRNA, whose expression is induced by ATF4, were similar in-between both experimental groups. Values represents means ± SEM, * $p < 0.05$, student's t test.

4.2.2 α-MSH does not alter IRE1α expression levels

The most conserved UPR-branch is the IRE1α signaling pathway. Recently it has been acknowledged the critical contribution of IRE1α for adipocyte differentiation [179]. Furthermore, IRE1α pathway is also known to play an important role in metabolism regulation, namely in glucose and lipid metabolism [148]; which were shown to be improved in α-MSH-treated mice [1]. Thus, we attempted to comprehend the effect of α-MSH on this signaling pathway, using the WB technique. We demonstrated that ingWAT

of α-MSH-treated obese mice exhibited similar levels of IRE1α expression, when in comparison with untreated counterparts (0.96±0.54 for control vs. 1.00±0.57 for α-MSH-treated groups, p=0.866) (Figure 7).

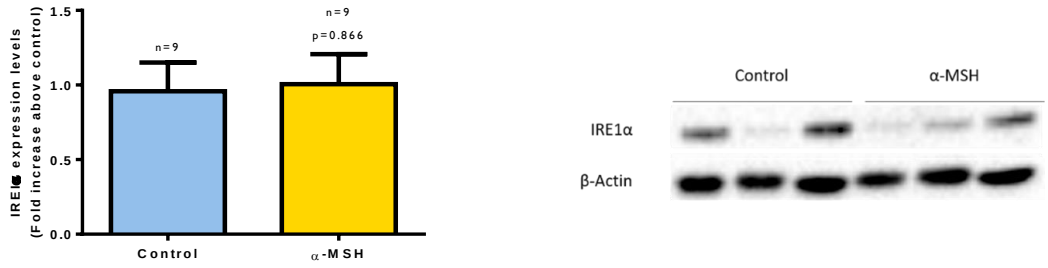

Figure 7 | Melanocortin α-MSH does not alter the expression of IRE1α in ingWAT of obese mice. Quantification of WB bands was carried out by densitometry and the exhibited blot is representative of 4 independent experiments. Values represents means ± SEM, student's t test.

4.2.3 ATF6α signalling pathway is not affected by α-MSH

Although ATF6α signalling pathways is best known for its role as a signal transducer in the ER-stress response, it has been recognized as a major regulator of tissue homeostasis [180]. The ATF6α is a transmembrane protein, with approximately 90 KDa. Upon stimulus, its activation is carried out by proteolysis, giving rise to 50KDa amino-terminal cytoplasmic fragment (p50-ATF6). p50-ATF6 acts as a transcription factor, migrating to the nucleus where it binds to ER-stress response and ATF/cAMP response elements, stimulating the selective expression of ER-stress related genes (e.g. *Chop*, *Xbp1* and *Bip*). In the present study, through the WB technique, we analysed the levels of active p50-ATF6α and found that these do not considerably change upon peripheral administration of α-MSH in DIO mice (0.98±0.38 for control vs. 1.06±0.34 for α-MSH-treated groups, p=0.649) (Figure 8).

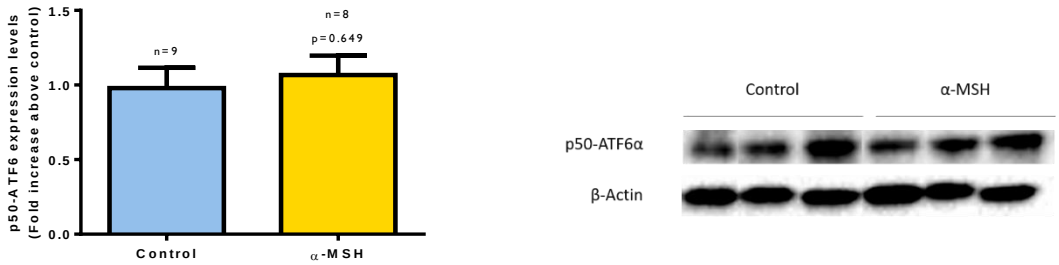

Figure 8 | α-MSH does not significantly alter p50-ATF6α protein expression levels in ingWAT of obese mice. The present graph was constructed with data obtained through the densitometry analysis of protein bands obtained in 4 independent experiments, for which the displayed blot is the representative. Values are means ± SEM, * p < 0.05, student's t test.

4.3 Expression of molecular chaperones is not altered upon exposure to α-MSH

The PERK, IRE1α and ATF6α signalling pathways are known to work in coordination with several stress response mechanisms, which intent to restore protein homeodynamics, in part through the enhanced expression of molecular chaperones. Having this into consideration, we evaluated the expression levels of two distinct chaperones: the extracellular protein clusterin (CLU) and the ATP-dependent molecular chaperone heat shock protein 90 (HSP90), by qPCR and WB, respectively. The present study showed that α-MSH did not significantly contributed to alterations on *Clu* mRNA levels (1.00±0.29 for control vs. 2.09±0.83 for α-MSH-treated groups, p=0.199) in ingWAT of obese mice (Figure 9, A). Similarly, levels of HSP90 protein did not significantly change in-between the two experimental groups (1.02±0.35 for control vs. 1.04±0.23 for α-MSH-treated groups, p=0.875) (Figure 9, B).

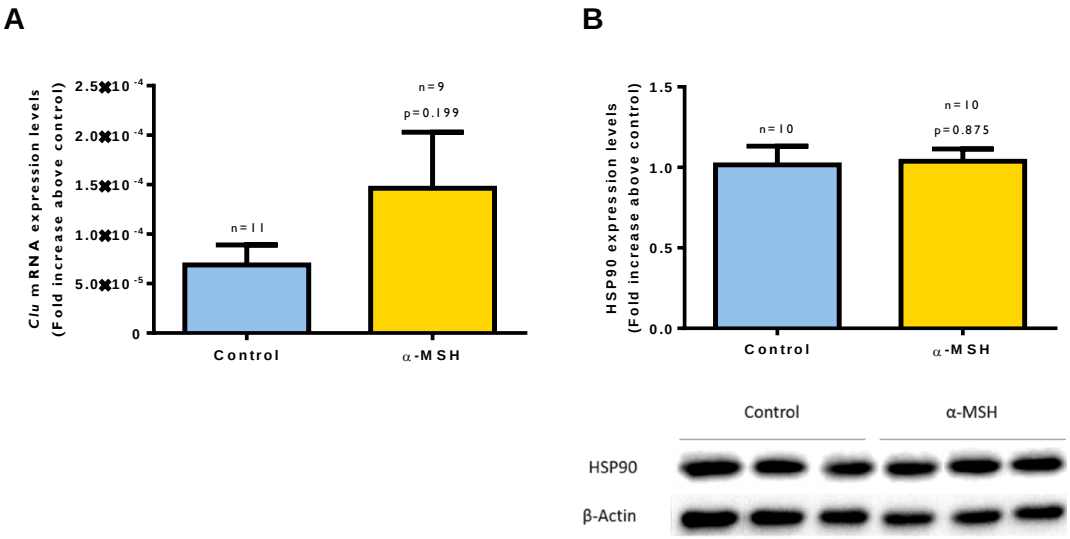

Figure 9 | **α-MSH did not modulate the expression of molecular chaperones HSP90 and Clu in obese ingWAT** (**A**) qPCR data showing that α-MSH did not alter transcript levels of *Clu* gene. (**B**) Protein expression levels of molecular chaperone HSP90, as accessed by WB, remain similar in ingWAT of animals of both experimental groups. The accompanying blot is representative of 4 distinct experiments, and the graph obtained through the densitometry analysis of the protein bands. Values are means ± SEM, * $p < 0.05$, student's t test.

4.4 α-MSH improves antioxidant defence mechanisms in ingWAT of obese mice

Having into consideration the intricate relationship between oxidative stress and ER stress responses, we tried to comprehend if the intraperitoneal administration of α-MSH in DIO-mice could also ameliorate redox homeodynamics in ingWAT. For this

purpose, we tried to evaluate the expression levels of antioxidant enzymes: superoxide dismutase 1 (SOD1), superoxide dismutase 2 (SOD2), GPx-1 and Heme oxygenase-1 (HO-1). Additionally, cellular levels of H_2O_2 and NF-κB activation were also accessed, as a by-product and biomarker of cellular oxidative stress, respectively.

Antioxidant enzymes are distinctly regulated by α-MSH. SOD isoforms catalyse the conversion of $O_2^{\bullet-}$ into H_2O_2 and are known to occupy specific cellular locations. The SOD1 isoform is widely expressed in the cell, and although it is predominantly found within the cytoplasm, it also exists in the nucleus, ER and mitochondria (within the intermembrane mitochondrial space) [181, 182]. Regarding SOD2, this isoform is exclusively located within the mitochondrial matrix [181]. Intriguingly, we found that α-MSH modulated the expression of both SOD isoforms distinctly: while being unable to alter SOD1 expression levels (1.04±0.083 for control vs. 0.96±0.24 for α-MSH-treated groups, p= 0.464) (Figure 10, A), it significantly diminished the expression of SOD2 isoform (1.00±0.18 for control vs 0.72±0.15 for α-MSH-treated groups, p= 0.0.0008) (Figure 10, B).

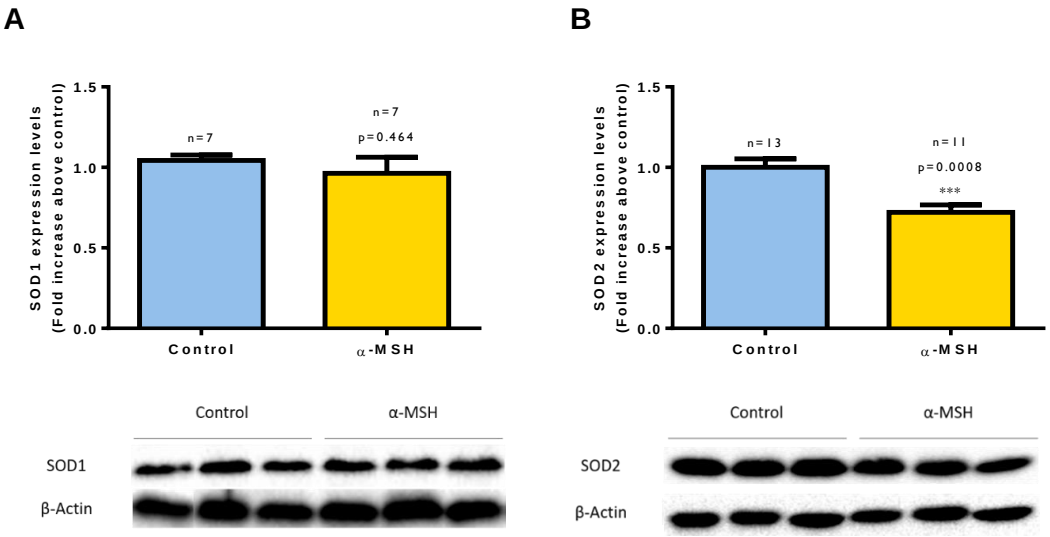

Figure 10 | Expression of SOD enzymes was modulated distinctively by melanocortin α-MSH. (**A**) Neuropeptide α-MSH did not alter the expression levels of SOD1 in ingWAT of DIO-mice, as accessed through WB. The representative blot of 2 independent experiments is shown, and the graph obtained through the densitometry analysis of bands. (**B**) Expression levels of isoform SOD2, were significantly diminished in ingWAT of α-MSH-treated mice. Data was obtained through the densitometry analysis of 2 independent experiments. Values are means ± SEM, *** $p < 0.001$, student's t test.

It is important to note that SOD family members are only responsible for the interconversion of different ROS species, producing H_2O_2 through the dismutation of $O_2^{\bullet-}$, which is less harmful than $O_2^{\bullet-}$. Further cellular detoxification of H_2O_2 is carried out by other antioxidant enzymes, such as catalase and GPx. Till date, the Gpx family of isoenzymes is known to be composed by 6 isoforms, with GPx-1 being the most

abundant isoenzyme. It is responsible for the detoxification of organic hydroperoxides and H_2O_2, using glutathione as a substrate. We therefore aimed to comprehend if α-MSH could modulate the expression of the enzyme GPx-1 in ingWAT of DIO-mice. It was found that levels of Gpx-1 were similar in both control and α-MSH-treated mice (0.97±0.22 for control vs. 0.95±0.36 for α-MSH-treated groups, p=0.880) (Figure 11).

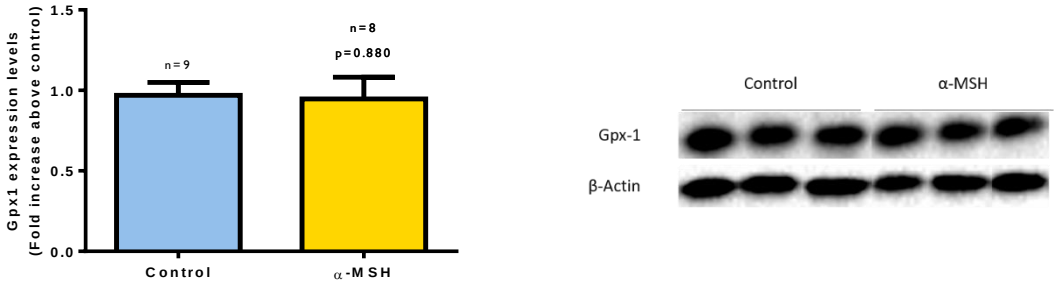

Figure 11 | Expression of Gpx-1 remains unaltered in ingWAT of obese mice upon peripheral administration of α-MSH. Assessment of Gpx-1 levels were carried out through 2 independent WB experiments and data plotted in the graph represent the densitometry analysis of the respective bands. A representative blot is shown. Values are means ± SEM, * p < 0.05, student's t test.

One of the major oxidant-inducible stress proteins is HO-1 proteins. The HO-1 is well known for its role in the degradation of heme; yielding carbon monoxide, free iron and biliverdin (which exhibits anti-oxidative properties). In the obese state, expression of HO-1 was been shown to be diminished, albeit an increased oxidative stress is observed [183-185]. Upregulation of HO-1 in adipocytes has been considered to be beneficial in the amelioration of obesity-induced metabolic complications, such as hypertension and glucose intolerance [185, 186]. Attending this pivotal cytoprotective role, HO-1 expression levels was evaluated in obese mice upon α-MSH treatment. However, it was observed that HO-1 expression levels (0.96±0.50 for control vs. 0.80±0.41 for α-MSH-treated groups, p=0.513) were similar in both experimental groups (Figure 12).

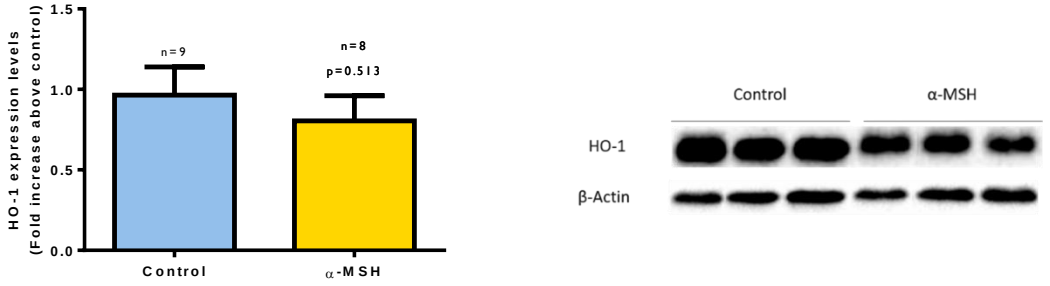

Figure 12 | Expression of HO-1 was maintained unaltered upon a 2-week long treatment with α-MSH in ingWAT of obese mice. WB analysis demonstrating similar HO-1 expression levels in both experimental conditions. Experiments were repeated only one time, and the graph obtained through the densitometry analysis of the obtained bands. Values are means ± SEM, * p < 0.05, student's t test.

4.5 Levels of H_2O_2 tend to decrease with α-MSH treatment

The preferable method to access oxidative stress in the cell is through the direct determination of ROS concentration. In the current dissertation, it was evaluated the effect of α-MSH in the levels of the most important second messenger in redox signalling: H_2O_2.

Although H_2O_2 is considered to be one of the simplest peroxides, it has demonstrated to be key to the regulation of several cellular pathways, involved in growth, proliferation, metabolism and angiogenesis [187]. Furthermore, assessment of H_2O_2 is preferable in detriment of other ROS (e.g. $O_2^{\bullet-}$), since it presents an increased chemical stability. Furthermore, in the scope of this dissertation, evaluation of H_2O_2 is key, as we evaluated the effect of α-MSH not only in the modulation of antioxidant enzymes responsible for its production (namely SOD1 and SOD2), as well as other responsible for its detoxification (specifically Gpx-1).

Determination of H_2O_2 concentration was possible using the Amplex® Red kit. We demonstrated that levels of H_2O_2 tended to decrease in ingWAT of α-MSH-treated animals (1.00±0.17 for control vs. 0.72±0.19 for α-MSH-treated group, p=0.178), as accessed through fluorescence spectroscopy (Figure 10, C). Statistical significance was not achieved, most likely due to the diminished number of samples (n=2) accessed in the current study.

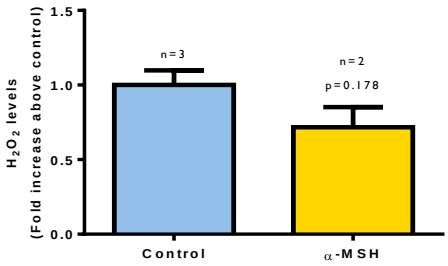

Figure 13 | Levels of H_2O_2 tended to decrease in ingWAT of α-MSH-treated mice, although statistical significance was not achieved. Concentration of H_2O_2 in ingWAT was estimated through the Amplex® Red kit, through spectrofluorimetry. Experiments were carried out only 1 time. Values are means ± SEM, * $p < 0.05$, student's t test.

4.6 α-MSH attenuates the NF-κB pathway

General stress transcription factors nuclear factor kappa B (NF-κB) is a primary regulator of oxidative stress and cell survival. Attending the overall importance of NF-κB for health and disease, this pathway has been pointed many times as a target for the

treatment of metabolic disorders. We therefore aimed to comprehend if α-MSH can modulate the activation of NF-kB signalling pathway in obese ingWAT. NF-κB activation occurs primarily via IKK-dependent phosphorylation and degradation of IκB proteins, followed by nuclear translocation of the released NF-κB dimers [156]. Dependent on cellular context, the nuclear function of NF-κB subunits occurs by post-transduction modification, enabling the fine-tuning of gene transcription [188, 189]. Indeed, the functional consequences of these modifications highly depend on the physiological condition of the organisms.

The most abundant and best characterized form of NF-κB is the p50/p65 heterodimer and the phosphorylation of p65 is a pivotal point for optimal NF-κB activation. Specifically, its phosphorylation on SER536 will be evaluated in the current study, as it represents the most inducible site of phosphorylation in response to inflammation and since it is highly conserved among distinct species [190]. Our data demonstrated that peripheral administration of α-MSH reduced the levels of phosphorylated p65 NF-κB at Ser 536 (1.00±0.56 for control vs. 0.35±0.32 for α-MSH-treated groups, p=0.0360) (Figure 14, A and D). Total expression levels of this transcription factor also tend to decrease (1.00±0.81 for control vs. 0.39±0.27 for α-MSH-treated groups, p= 0.084) (Figure 14, B and D), although significance is not achieved attending the large variance observed in both experimental conditions. In order to comprehend how this melanocortin could modulate both the phosphorylation and the expression, the ratio phospho-NF-κB/NF-κB was accessed and demonstrated to not change when comparing both experimental groups (1.00±0.64 for control vs. 0.96±0.92 for α-MSH-treated groups, p=0.94) (Figure 14, C and D).

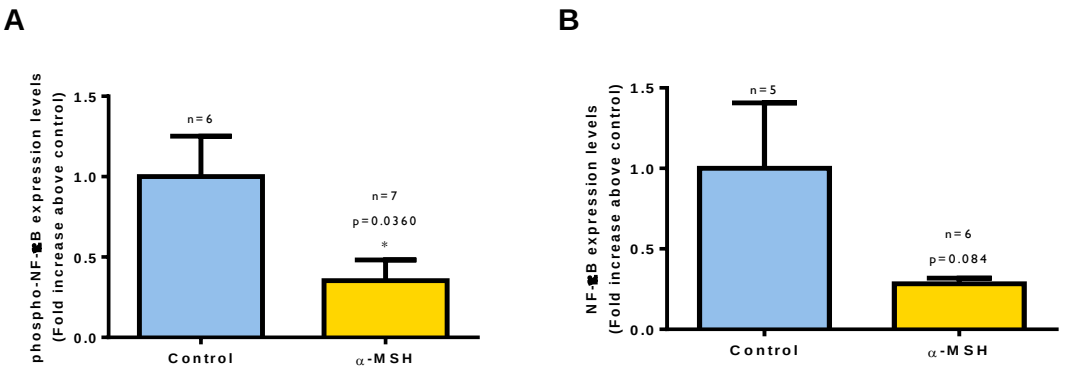

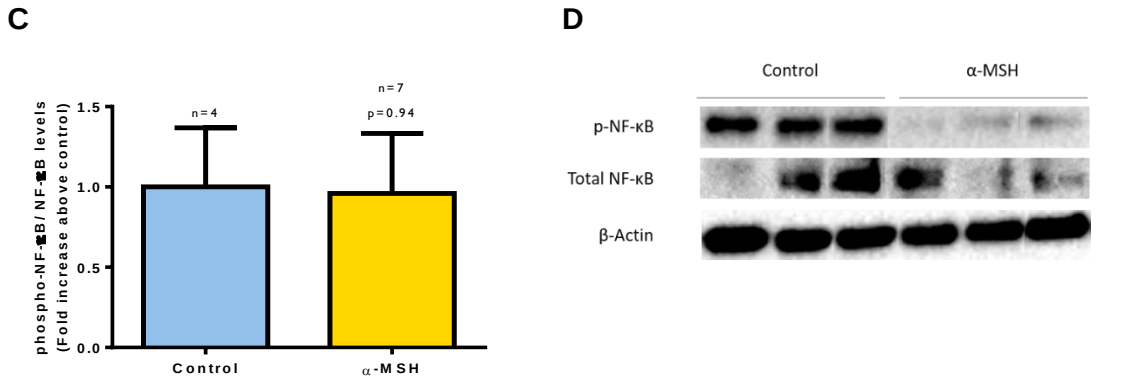

Figure 14 | α-MSH modulates p65 NF-κB phosphorylation in ingWAT of obese mice. (**A**) In obese mice, it was demonstrated that α-MSH significantly diminished the expression levels of phosphorylated p65 NF- κB. (**B**) Levels of total NF-κB protein tended to decrease in α-MSH treated animals, even though statistical significance was not achieved. (**C**) Ratio of p-NF-κB/ NF-κB were similar in both experimental groups. (**D**) WB experiments were repeated one time, and the graphs were obtained through the densitometry analysis of the bands. Values are means ± SEM, * $p < 0.05$, student's t test.

4.7 Biomolecule damage is diminished in ingWAT of α-MSH treated mice

In the present work, the melanocortin α-MSH was shown to significantly attenuate specific ER-stress and oxidative stress responses. We therefore may speculate the presence of a diminished number of oxidized biomolecules in ingWAT after α-MSH treatment. With this in mind, we tried to investigate if significant alterations in the damage of proteins and DNA occurred. In the present dissertation, protein oxidation was evaluated by measuring the levels of carbonylated proteins in ingWAT of control and α-MSH treated mice, through oxyblot. In fact, our results demonstrated that upon exposure to this melanocortin, obese mice exhibited significant lower levels of carbonylated proteins in ingWAT (0.98±0.080 for control vs. 0.80±0.14 for α-MSH-treated groups, p= 0.00863)(Figure 15, A). On the other side, DNA damage was evaluated through the assessment of levels of phosphorylated H2AX at Ser139, whose phosphorylation is induced in response to DNA double-strand breaks in mammals. WB analysis showed no significant differences in the levels of p-H2AX in ingWAT between controls and animals treated with α-MSH (0.97±0.40 for control vs. 0.68±030 for α-MSH-treated groups, p= 0.396)(Figure 15**,** B). By immunofluorescence, it was also possible to confirm the presence of p-H2AX in the nucleus as demonstrated by the colocalization of p-H2AX green fluorescence (AlexaFluor 488) with DAPI (blue) showed in Figure 15 (C).

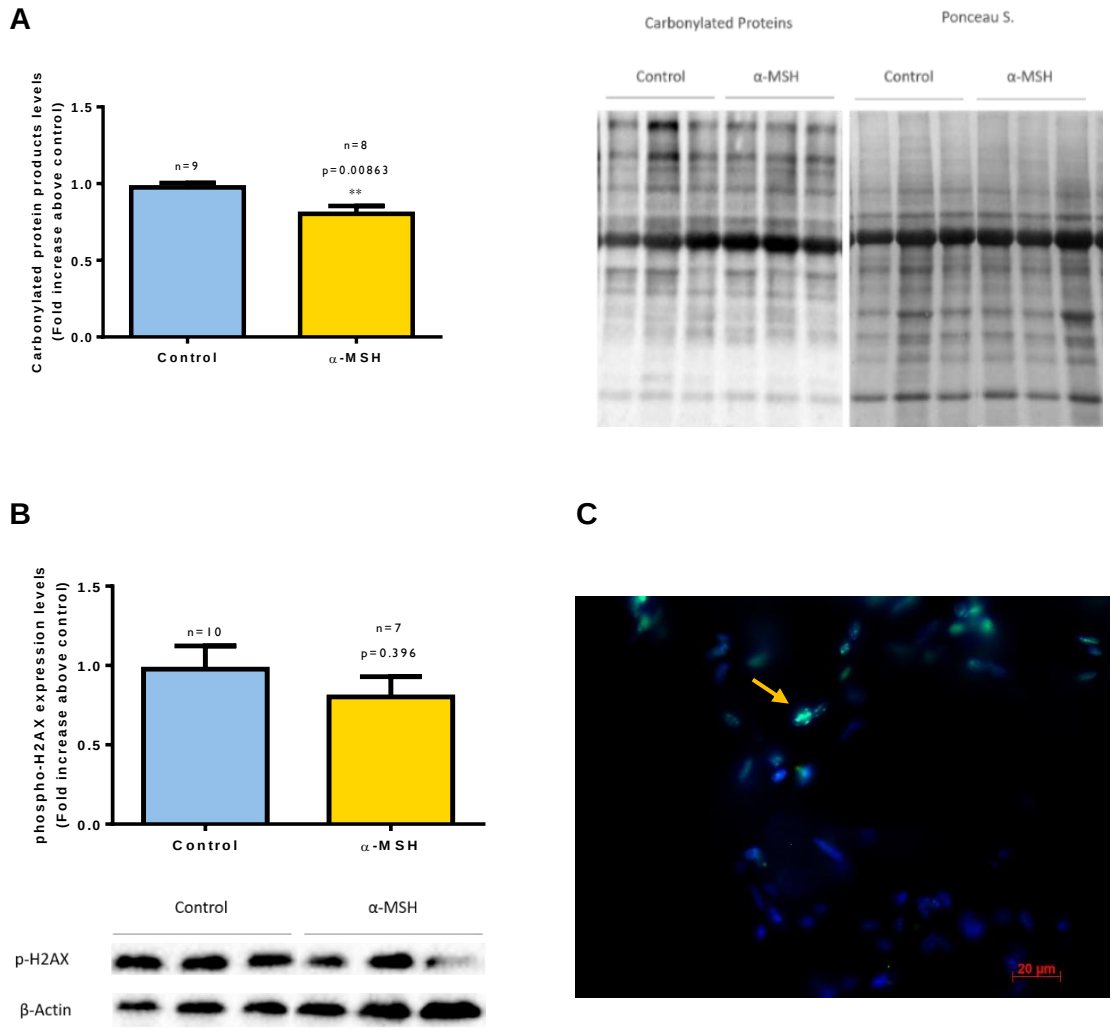

Figure 15 | Melanocortin α-MSH attenuated protein carbonylation in ingWAT of obese mice, without any changes regarding DNA damage (**A**) Melanocortin α-MSH significantly reduced the levels of carbonylated protein in ingWAT of obese mice, as evaluated by OxyBlot. The displayed oxyblot is representative of 3 independent experiments, and the data analysed through densitometry using the Ponceau S as loading control. (**B**) Albeit the differences in the levels of carbonylated proteins, no significant changes were observed in the levels of p-H2AX, as accessed by WB. The experiments were carried out 2 times independently, with a representative blot being displayed, and the data analysed through densitometry. Values are means ± SEM, ** $p < 0.01$, student's t test. (**C**) Immunofluorescence microscopy for p-H2AX protein showing the presence of pH2AX in the nucleus of adipocytes from obese ingWAT. Cellular nuclei are exhibited in blue (DAPI stain), shown in some case to colocalize with p-H2AX, whose signal exhibit a bright green colour and are indicated by a yellow arrow in the photograph.

4.8 α-MSH modulates autophagy responses in ingWAT of obese mice

Both ER- stress and oxidative stress signalling pathways are known to be implicated on the activation of autophagy responses. Autophagy is an essential process, responsible for the maintenance of cellular homeodynamics, through the mediated recycling of biomolecules and organelles in a lysosome-dependent manner [191]. Some studies suggest that these processes are upregulated in obesity, while other contradict

these, stating that autophagy mechanisms are inhibited in this pathology. Nonetheless, it is consensual that autophagy is compromised in obesity and contribute to the aggravation of obesity-induced dysfunction of AT [178]. Having this in consideration, the present work evaluated the expression of several autophagy-related proteins, in an attempt to comprehend the effect of α-MSH on this essential recycling mechanisms.

4.8.1 Autophagy initiation

Autophagy initiation is a complex mechanism, which requires the coordinated action of a variety of proteins, namely of Beclin-1 [192]. Here Beclin-1 expression was evaluated by WB technique, and its levels in ingWAT where shown to be neither enhanced nor reduced upon treatment of obese mice with α-MSH (0.92±0.42 for control vs. 0.81±0.26 for α-MSH-treated groups, p= 0.561) (Figure 16, B).

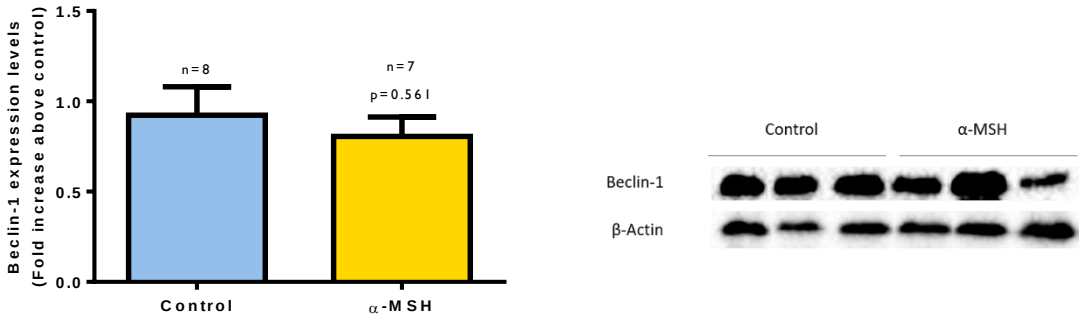

Figure 16 | Melanocortin α-MSH does not affect the expression of the autophagy-related protein Beclin-1. Similar levels of Beclin-1 protein were observed in both experimental conditions, as accessed through WB, by 2 distinct experiments. The graph was constructed by the densitometry analysis of the bands. Values are mean ± SEM, * $p < 0.05$, student's t test.

4.8.2 Autophagy elongation

In the autophagy elongation phase, two distinct conjugation system are triggered: the ATG12 and the LC3-I conjugation system.

The ATG12 signalling pathway is known to play an important role in the autophagy process by regulating elongation of membranes that evolve into autophagosomes. This mechanism is initiated by the conjugation of ATG12 with ATG5 by ATG7. The ATG5–ATG12 complex then interacts with ATG16L1 resulting in a multimeric complex that remains associated with phagophores but dissociated from fully

formed autophagosomes [191]. Even though it was not possible to access the expression levels of ATG12, the present study demonstrated that levels of ATG5 do not considerably change in obese ingWAT, upon treatment with α-MSH (1.01±0.14 for control vs. 1.08±0.23 for α-MSH-treated groups, p= 0.0858) (Figure 17, A). Furthermore, expression of ATG7 also presented similar levels in both experimental groups (1.00±0.40 for control vs. 1.32±0.62 for α-MSH-treated groups, p= 0.564)(Figure 17, B). Intriguingly, our data reveal that while α-MSH repressed the expression of ATG16L1β , with 68KDa (1.00±0.64 for control vs. 0.24±0.16 for α-MSH-treated groups, p= 0.0275), it does not significantly alter the protein levels of its isoform ATG16L1α, with 66 KDa (1.00±0.40 for control vs. 1.10±0.32 for α-MSH-treated groups, p= 0.678) (Figure 17, C).

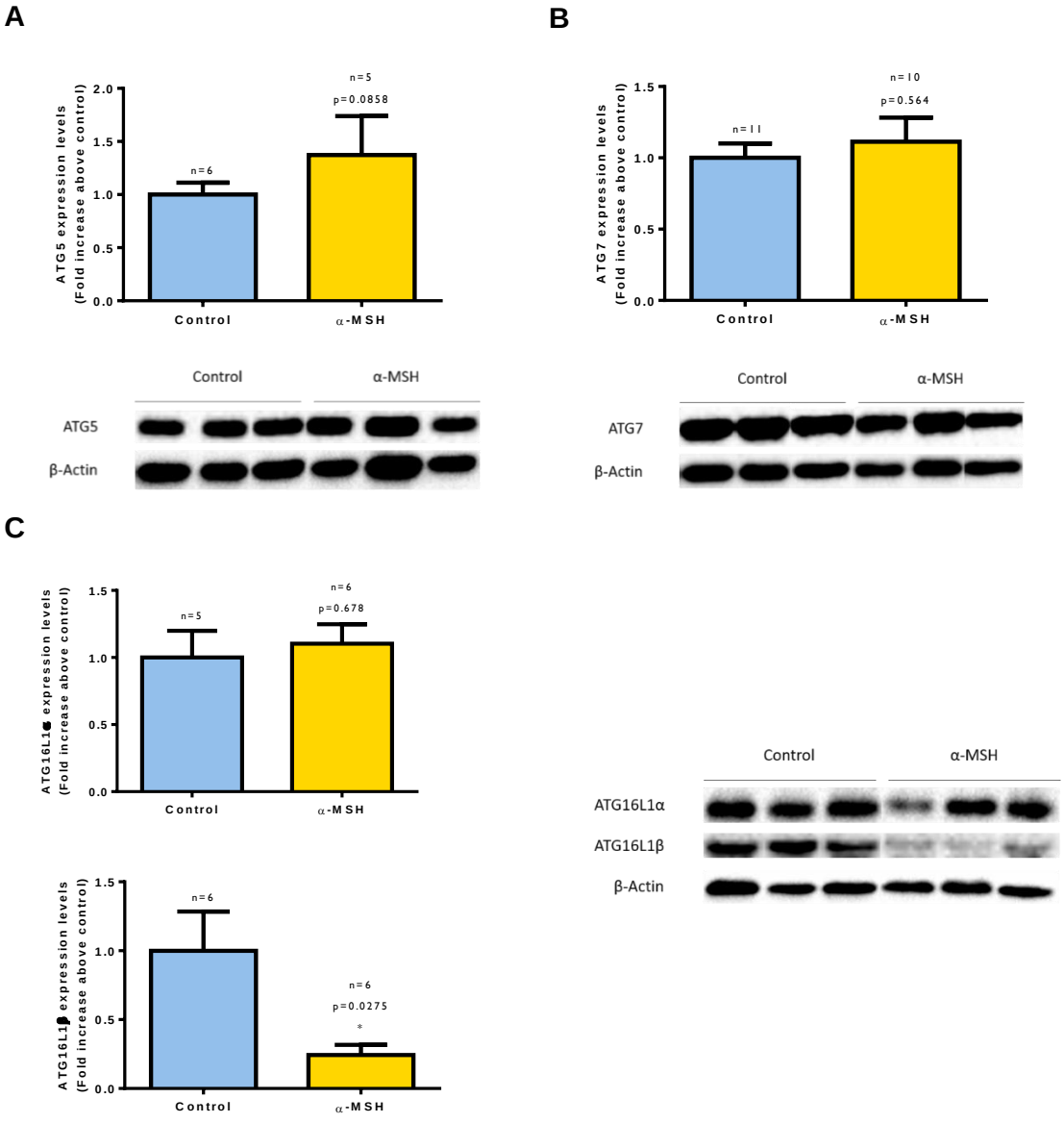

Figure 17 |α-MSH was able to modulate the ATG12-ATG5-ATG16 conjugation system in obese ingWAT. (**A**) After a2-week treatment with α-MSH, levels of ATG5 do not considerably change in ingWAT, as demonstrated through WB. Experiments were repeated 3 times and data was analysed through densitometry. (**B**) E1-like ubiquitin ligase ATG7

expression levels also remained unaltered upon α-MSH stimulus. The displayed blot is representative of 2 distinct experiments. (**C**) While α-MSH repressed the expression of ATF16L1β, it maintained unaltered the levels of ATG16L1α in ingWAT of obese mice, as accessed by WB. Experiments were repeated one time. Quantification of the bands were carried out through densitometry. Values are means ± SEM, * $p < 0.05$, student's t distribution.

The second reaction of autophagosome elongation involves the binding of LC3 to the autophagosome membrane by its conjugation to the lipid phosphatidylethanolamine, in a process called lipidation and regulated by autophagy conjugation systems: ATG12 (ATG5, ATG7, ATG10, ATG12, ATG16L1) and LC3 systems (LC3 family proteins, ATG3 and ATG7) [161]. The so formed LC3-II (lipidated form) remains associated with autophagosomes until after their fusion with lysosomes (in both inner and outer membrane). Once in the autolysosomes, LC3-II is degraded, while the LC3-II on the cytoplasmic surface can be delipidated back to LC3-I (non-lipidated form) [193] .Since LC3-II is conjugated with PE, it presents a bigger molecular weight when in comparison with LC3-I, and consequently it would be expected to migrate slower in the SDS-PAGE. However, the exact opposite is observed, probably because of its extreme hydrophobicity. In fact, after LC3 immunoblotting, it is possible to observe two distinct bands: one around 16 KDa corresponding to LC3-I and the other around 14 KDa corresponding to LC3-II [194]. A similar pattern was observed here using ingWAT proteins (Figure 18). We demonstrated that the levels of LC3-I (1.09±0.973 for control vs. 1.14±0.529 for α-MSH-treated groups, p= 0.927) and LC3-II (0.939±0.372 for control vs. 0.715±0.537 for α-MSH-treated groups, p= 0.429) remain similar in both experimental conditions (Figure 18, A). Concordantly, ratio of LC3-I/LC3-II did not significantly differ in between both experimental conditions (0.751±0.506 for control vs. 1.39±0.607 for α-MSH-treated groups, p= 0.143). It should be noted, however, that levels of this protein varied considerably in the animals tested, making it difficult to correctly interpret them in our physiological context. Furthermore, our results showed that melanocortin did not considerably changed the protein expression levels of ATG3 (1.12±0.63 for control vs. 1.68±1.04 for α-MSH-treated groups, p= 0.236)(Figure 18, B).

A

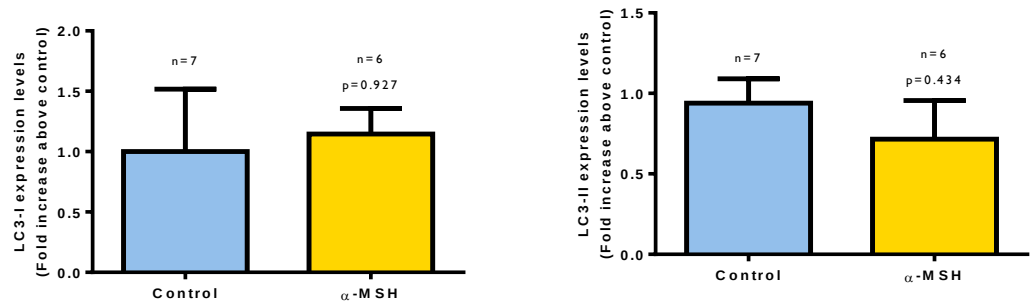

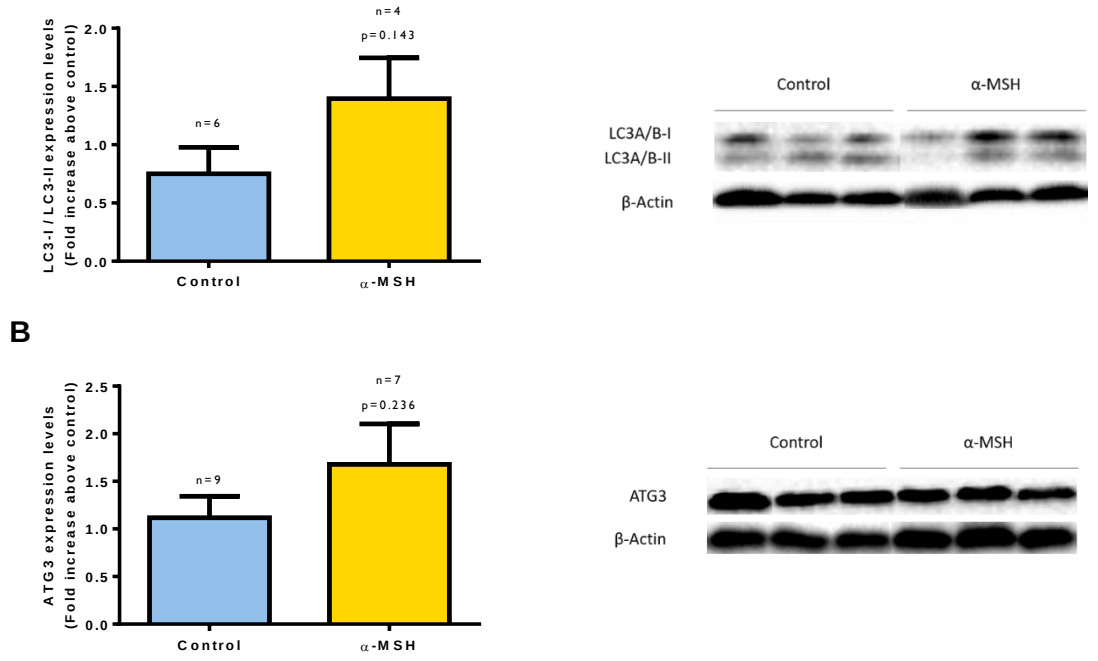

Figure 18 | **Expression of proteins involved in the LC3 ubiquitin-like conjugation system are not modulated in ingWAT by α-MSH**. (**A**) WB technique showing that neuropeptide α-MSH did not considerably change the expression of either LC3-I and LC3-II. Concordantly, ratio of LC3-I/LC3-II was also similar in both experimental conditions. Experiments were carried out 2 times independently, being the representative blot here shown. Quantification of the bands was carried out though densitometry. (**B**) Expression of E2-like enzyme ATG3 remained similar in control and α-MSH-treated mice, as evaluated by WB. The exhibited blot is representative of 2 independent experiments. Bands were analysed though densitometry. Values are means ± SEM, * $p < 0.05$, student's t test.

4.8.3 Autophagy Maturation phase

The lysosome-associated membrane proteins (LAMP)-1 and LAMP-2 constitute nearly 50% of all the lysosomal-associated membrane proteins [195]. Both proteins are known to share some common functions *in vivo*, although their roles are predicted to be non-redundant. Both proteins have been found to be highly glycosylated and can be found predominantly in the lysosome membrane. The oligosaccharides form a lining on the inner leaflet of the lysosome, which can contribute to: (1) the maintenance of lysosomal acidity, (2) the protection of lysosomal membrane components form degradation and (3) the fusion of this cellular structure with autophagosomes.

Due to the important role of the lysosome integrity, and consequently in the autophagy process, we ought to comprehend if α-MSH is able to modulate the expression of LAMP protein. Upon synthesis, the LAMP proteins are targeted to the cellular membranes, where they become glycosylated. N-glycosylation appears to have an important role for the maintenance of lysosomal integrity. It was possible to observe that even though this melanocortin did not significantly changes the levels of non-

glycosylated LAMP1 (0.92±0.38 for control vs. 0.65±0.39 for α-MSH-treated groups, p=0.186), it significantly diminished the levels of glycosylated LAMP1 (0.96±0.48 for control vs. 0.42±0.12 for α-MSH-treated groups, p= 0.0106) (Figure 19). On the other side, levels of *Lamp2* mRNA were found to be also significantly diminished in ingWAT of α-MSH-treated mice (unpublished data).

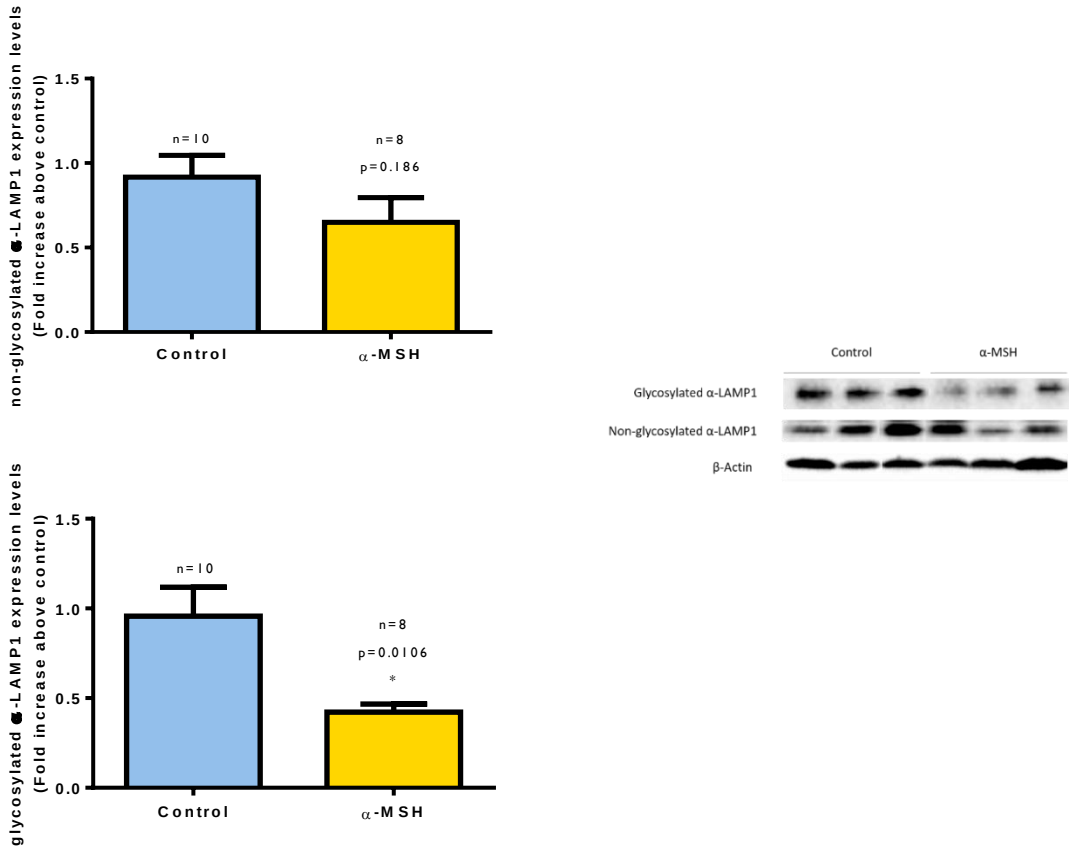

Figure 19 | Levels of glycosylated and non-glycosylated LAMP1 were modulated distinctly in obese ingWAT by α-MSH. Levels of glycosylated LAMP1 were significantly decreased in ingWAT of HFD-mice, while levels of non-glycosylated LAMP1 did not considerably change, as demonstrated through WB. Bands were quantified through densitometry. WB experiments were repeated 2 times independently, and the blot here exhibited is representative of these experiments. Values are means ± SEM, * $p < 0.05$, student's t distribution.

One of the most common markers for autophagy influx is the classical receptor of autophagy – protein sequestosome 1 (p62). P62 is a multifunctional adaptor protein located in the lysosome, which can interact with a variety of proteins, acting mainly as a cargo receptor for the autophagic degradation of ubiquitinated substrates. In obesity, p62 has demonstrated to have an important role in the regulation of adipogenesis, thus allowing the healthy expansion of AT [196]. This dissertation demonstrated that α-MSH did not considerably change p62 levels in ingWAT of obese animals (1.00±0.46 for control vs. 0.90±0.41 for α-MSH-treated groups, p= 0.758) (Figure 20).

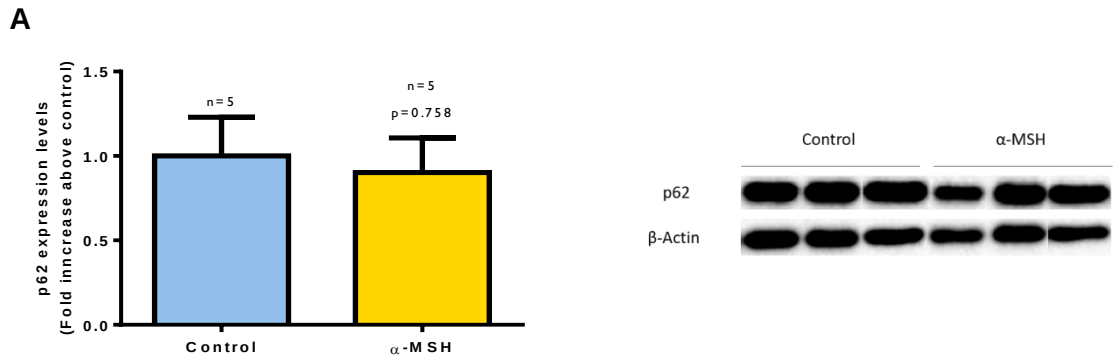

Figure 20 | Melanocortin α-MSH did not alter the expression levels of p62 in ingWAT of obese mice. Data was obtained through 2 distinct experiments, through the densitometric analysis of the obtained bands. The representative WB is here shown. Values are means ± SEM, * $p < 0.05$, student's t test.

5. DISCUSSION

The present work attempted to comprehend the modulatory effect of the melanocortin α-MSH on: (1) the three main ER-stress signalling pathways, (2) oxidative stress signalling pathways and (3) autophagy mechanisms in ingWAT of obese mice. Ultimately, we aimed to comprehend how these alterations impacted on biomolecule damage in ingWAT of α-MSH-treated mice.

5.1 ER stress pathways

It has been recognized that ER-stress is aggravated in obesity and contributes to the development of metabolic disorders [169]. The melanocortin α-MSH was shown to specifically attenuate ER-stress signalling pathways in ingWAT of obese mice (Figure 21).

In obesity, the PERK/p-eIF2α axis of UPR is known to be upregulated in AT [170]. Our results demonstrated that α-MSH-treated mice present lower expression levels of total PERK protein, alongside with diminished phosphorylation levels of its target, eIF2α. eIF2α integrates a wide number of signalling pathways, and thus its phosphorylation can be carried out by distinct kinases [147]. Although it was not possible to access which kinase is mainly responsible for the phosphorylation status of eIF2α, it is likely that activation of this translation initiation factor occurred predominantly by PERK. Even though PERK phosphorylation levels were not evaluated, a significant reduction in its total expression levels were observed in the ingWAT of α-MSH-treated mice, suggestive of an attenuation of the PERK arm of the UPR. In agreement, α-MSH significantly attenuates protein carbonylation and lipid peroxidation (unpublished results) in ingWAT of DIO mice, which are known triggers of the PERK/p-eIF2a arm of the UPR [140, 197]. Further supporting our results, Gan *et al.* demonstrated that neuropeptide α-MSH enhances the expression of forkhead box protein C2 (*foxc2*) mRNA in AT, which has been associated with the stimulation of AKT / mammalian target of rapamycin complex 1 (mTORC1) pathway [101, 198]. In ER-stressed cells, activation of AKT pathway has been shown to induce the phosphorylation of residue THR799 of PERK, leading to its inactivation, and consequently to the inhibition of eIF2α phosphorylation [199]. Thus, we may speculate that stimulation of the AKT/mTORC1 pathway by α-MSH, which consequently inhibits PERK, could at least in part explain the diminished levels of p-eIF2α in ingWAT. The reduced levels of activated eIF2α in ingWAT of obese mice

implicate that global translation processes are not as attenuated in α-MSH treated mice as in control individuals. By contrast, attending that p-eIF2α induces the transcription of specific mRNA encoding protein related with the stress response, it would be expected to observe an attenuated expression of these stress genes in ingWAT of α-MSH-treated animals.

Attending the diminished expression of p-eIF2α in ingWAT of α-MSH treated mice, it was expected to observe a significant diminution of ATF4 levels. It was demonstrated that ATF4$^{-/-}$ mice were significantly leaner when in comparison with control equivalents, due to increased energy expenditure rates, although these presented similar food intake levels [200]. Additionally, ATF4 has been recognized as an important modulator of lipid metabolism, and previous studies carried out *in vitro* and *in vivo* demonstrated that its attenuation prompts the expression of β-oxidation genes while repressing the expression of lipogenic related genes, enabling a reduction in the accumulation of fat in adipocytes [200, 201]. Previously demonstrated by our group, α-MSH-treated obese mice lost weight and fat mass, due to higher energy expenditure and lipid mobilization rates, without being observed any changes in food intake [1, 100]. In accordance, a previous study in murine 3T3-L1 adipocyte cell line, demonstrated that α-MSH modulated lipid metabolism, by binding to MC5R: (1) impaired NEFA esterification through MAPK / ERK1/2 pathway and (2) promoted lipolysis through cAMP/ PKA pathways [100]. Despite all the similarities between ATF4$^{-/-}$ andα-MSH-treated mice, data obtained in the scope of this dissertation demonstrated that α-MSH did not considerably changed the expression levels of ATF4, suggesting that the maintenance of ATF4 expression levels does not crucially prejudice the reestablishment of ingWAT homeodynamics. In fact, the maintenance of ATF4 expression levels in an ameliorated cellular redox profile can be considered a protective mechanism, since ATF4 elicits the expression of cytoprotective genes which aid in the restoring of cell homeodynamics [202].

Albeit for long time, ATF4 induction has been associated primarily with the UPR, it is now known that its expression can be induced by several ER-stress independent mechanisms [203, 204]. One important eIF2α-independent mechanism capable of inducing ATF4 activation depends on energetic and redox sensor mTORC1 [205], known to be upregulated by FOXC2 , Akt and ERK1/2 signalling [198]. Indeed, α-MSH has been shown to enhance the expression of *foxc2* mRNA levels in ingWAT [101] and to activated ERK1/2 in 3T3-L1 adipocyte cell line [100]. According to this, unaltered levels of ATF4 observed in the animals treated with α-MSH could result from a balance between ATF4

downregulation by p-eIF2a and ATF4 upregulation by mTORC1. In agreement, it has been described that mTORC1 activation stimulates glucose uptake [206], which has been found to be enhanced in ingWAT of α-MSH treated mice [1, 206], thus reinforcing the hypothesis that mTORC1 can be activated in ingWAT of α-MSH treated obese mice.

Hence, it would be interesting to confirm if α-MSH could indeed enhance the activation of mTORC1 in ingWAT of obese mice. But still, what would be the advantage on triggering an eIF2α-independent stress response? The answer to this question is not clear. However, we can speculate that it would allow the fine-tuning of the ER-stress signalling response, favouring the expression of ATF4-inducible genes while inhibiting p-eIF2α-inducible genes, without halting translational attenuation. The results obtained within the scope of the present dissertation highlights a putative model capable of explaining the modulatory effect of α-MSH in the PERK-arm of the UPR, by which levels of ATF4 are maintained (Figure 21).

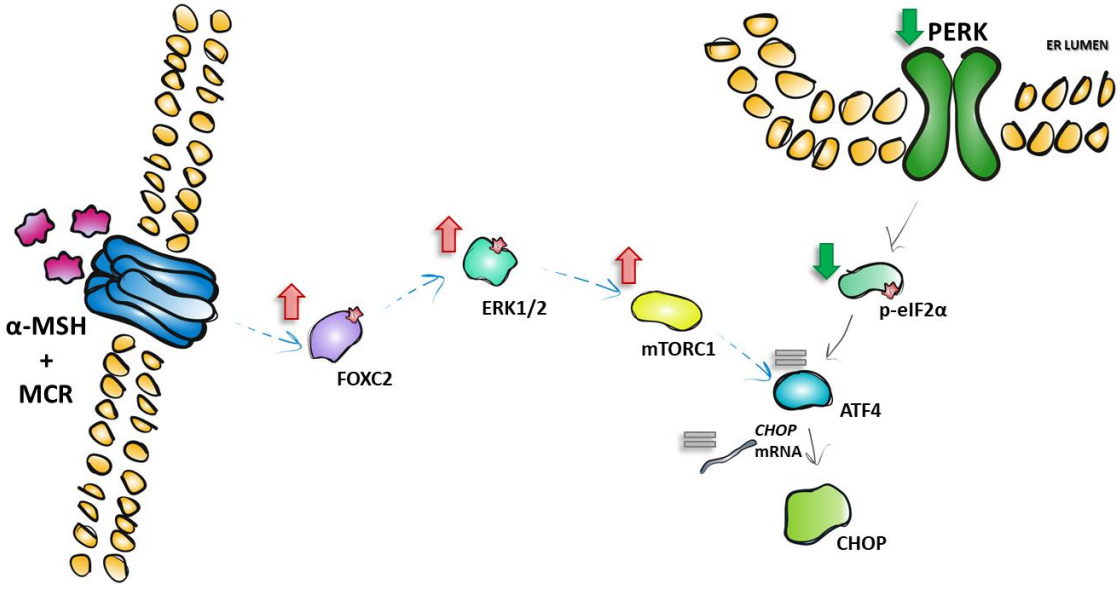

Figure 21 | It was established in the present work that α-MSH significantly diminished eIF2α phosphorylation, without altering the expression levels of its downstream target, ATF4. Thusly, the existence of a compensatory mechanisms responsible for ATF4 expression induction is hypothesized to be stimulated by α-MSH (blue intermittent arrows), which could indeed play an important role in obese ingWAT homeodynamics reestablishment. Accordingly, with previous studies, it is here suggested that activation of melanocortin receptors by this melanocortin, could putatively stimulate foxc2 and downstream effector ERK1/2. Consequently, activation of mTORC1 would be expected to occur in ingWAT of obese mice, and contribute to the maintenance ATF4 levels, albeit the diminished levels of phosphorylated eIF2α.

Although ATF4 elicits the expression of cytoprotective genes, upon prolonged ER-stress, this transcription factor is known to trigger the expression of pro-apoptotic transcription factors, namely CHOP [154]. In agreement with data obtained for ATF4,

Chop mRNA levels did not vary with α-MSH treatment. Palam *et al.* demonstrated that translation of *Chop* mRNA occurs preferentially when cellular levels of p-eIF2α are high, as a result of the easier passage of the ribosomes through the upstream open reading frame (uORF) located in the 5´ leader of the *Chop* mRNA [207]. Having into consideration the diminished levels of p-eIF2α observed in α-MSH-treated mice, it is possible that diminished levels of CHOP protein exist in ingWAT of α-MSH treated mice, even though similar transcript levels were observed. Supporting this conjecture, similarities in-between $CHOP^{-/-}$ and α-MSH-treated rodents were found in the literature. Indeed, like for obese mice intraperitoneally injected with α-MSH [1], CHOP deficient mice did not only present an improved adipocyte function, but also improved glucose tolerance and insulin sensitivity [208].

In contrast to the PERK arm of the UPR, IRE1α expression levels in ingWAT does not considerably change upon α-MSH treatment. It is commonly accepted that upon IRE1α activation, due to its RNase activity, [150], splicing of u*Xbp1* mRNA occurs resulting in the formation of spliced-*Xbp1* (s*Xbp1*), which can be effectively translated into a 371 amino acid protein. It was demonstrated that α-MSH-treated mice exhibited lower levels of $Xbp1^S$ mRNA (unpublished data). Attending that Xbp1 transcription is regulated by the nuclear form of ATF6α, whose expression remains unaltered upon exposure to α-MSH, it would be expected to observe similar levels of $uXbp1^U$ mRNA in both animals [153, 209]. Thus, the diminished levels of s*Xbp1* mRNA are suggested to be intrinsically related with IRE1α RNase activity, which were not evaluated in the present study. On one side, it can be postulated that due to the lower levels of s*Xbp1* mRNA, IRE1α phosphorylation should be diminished in α-MSH- treated mice. However, in the obese condition, it has been determined that only a small portion of IRE1α proteins are hyper-phosphorylated, even though s*Xbp1* mRNA are 2 times higher when in comparison with leaner counterparts [179]. Furthermore, it has been demonstrated that IRE1α RNase activity can be maintained even in the absence of trans-autophosphorylation, and that splicing of u*Xbp1* can also be triggered through IRE1α-independent mechanisms [149, 210]. Thus, further studies should be carried out to comprehend the role of α-MSH in the regulation of the mechanisms responsible for the splicing of *Xbp1*.

Lastly, the ATF6 arm of the UPR dynamically interacts with the others ER-stress signalling pathways, PERK and IRE1α [211]. ATF4 is known to promote the transcription of ATF6, as well as to promote the trafficking of ATF6 to the GC for subsequent proteolytic activation, by site-1 protease (SP1) and site-2 protease (SP2) [150, 212].

Attending that α-MSH seems to modulate both PERK and IRE1α pathway, a variation in ATF6α pathway would have been expected to be observed. However, levels of active p50 ATF6 were similar in both experimental groups. Previously, it was demonstrated that ATF6α pathway impairment significantly alters the expression of adipogenic genes, thus impairing the adipogenesis process, and reducing lipid accumulation [213]. In this line, maintenance of ATF6α cellular levels, alongside with the modulation of the PERK and IRE1α pathway, can indeed present beneficial effects in obesity (Figure 22).

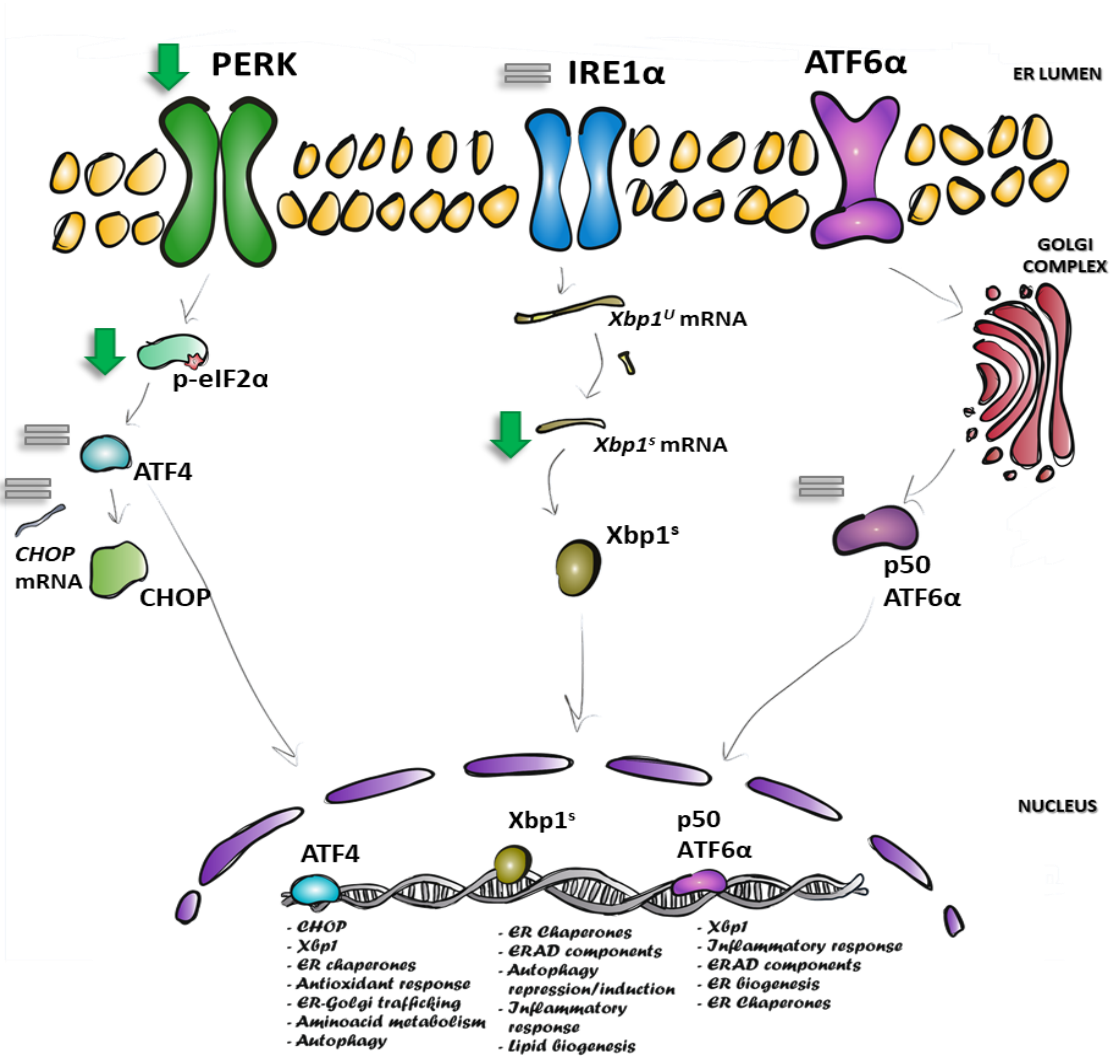

Figure 22 | Melanocortin α-MSH affects distinctly the three main ER-stress signalling pathways in ingWAT of obese mice. Melanocortin α-MSH significatively attenuated the expression of PERK expression, and downstream phosphorylation of its target – eIF2α. Albeit this significative attenuation, ATF4 expression levels remained unaltered as well as Chop mRNA levels. Furthermore, α-MSH does not significatively alters the expression of IRE1α protein, although significatively diminishing *Xbp1* splicing. Regarding ATF6 pathway, protein levels of p50-ATF6α remain unalters by α-MSH in ingWAT of obese mice.

5.2 Oxidative Stress

In this study, it was observed diminished levels of carbonylated proteins in ingWAT from α-MSH-treated mice, suggesting that α-MSH indeed contributes to the

relieve of ER-load. Thus, we sought to comprehend if levels of molecular chaperones were also dissimilar in ingWAT of treated animals. Neither HSP90 nor CLU presented altered expression levels in α-MSH-treated mice. HSP90 is expressed constitutively in eukaryotic cells, making it less prone to stimulation, unless upon pathological conditions. Maintenance of its expression levels present several benefits, since HSP90 has been recognized as an important stress-response regulator in adipocytes, with a litany of regulatory kinases depending on its interaction for stability and function [214]. Within these are included PERK and IRE1α ER-stress transducers, whose cytosolic domains are known to interact with HSP90, further contributing to its stabilization [214]. Furthermore, HSP90 plays an important role in adipogenesis, and thus important for the maintenance of AT homeodynamics in obesity [215]. Regarding extracellular molecular chaperone CLU, it has been demonstrated that it remains significantly increased in obesity, suggestive of a role in AT remodelling [216]. In obesity, apoptosis mechanisms are enhanced, with the increased expression of CLU in this circumstances being associated with cellular survival of non-apoptotic cells [217]. Thus, maintenance of CLU levels in ingWAT of obese mice could also aid in the reestablishment of AT homeodynamics.

Attending that melanocortin α-MSH contributed to the upkeep of ingWAT homeodynamics through the modulation of ER-stress signalling pathways and the maintenance of molecular chaperones expression, we aimed to comprehend the role of this neuropeptide in oxidative stress signalling pathways. In fact, we observed a tendency of α-MSH to diminish the levels of H_2O_2 in ingWAT of obese mice although statistical significance was not achieved. Intriguingly, we found that α-MSH modulate the expression of important antioxidant enzymes distinctly: while it was unable to alter GPx-1 and SOD1 protein expression levels, it significantly diminished protein levels of SOD2. SOD isoforms have been demonstrated to have distinct regulatory mechanisms. In the case of SOD1, it is known that this enzyme is expressed constitutively, even being considered by some authors as a “housekeeping” protein [218]. Consequently, induction of SOD1 is lower when compared to other SOD isoforms, namely SOD2, which is a possible explanation for α-MSH's inability to alter its expression. By contrast, expression of the SOD2 isoform is known to be induced by oxidative stress, mainly through NF-κB pathway [219]. HFD-mice with a specific deletion of $SOD2^{-/-}$ on adipocytes present an increased mitochondrial biogenesis and oxygen consumption rates, and exhibit less adiposity when in comparison with control animals (due to the increased energy expenditure rates) [220]. Moreover, previous studies demonstrated that α-MSH is also

capable of inducing mitochondrial biogenesis and increase mitochondrial respiration rates in ingWAT of DIO-mice [1]. On the other hand, the diminished levels of SOD2 can be associated with the diminished need of the cell to detoxify $O_2^{\bullet-}$, due to an ameliorated redox status in ingWAT of obese animals treated with α-MSH. Previous studies demonstrated that a synthetic analogue of α-MSH [Nle^4,D-Phe^7]-α-MSH increased both mRNA and protein levels of SOD2 in HUVEC cells [221]. Albeit the observed effect in ingWAT is contrary, it is worth noting that the cellular characteristics of the study are distinct, as well as the biological context. Albeit levels of $O_2^{\bullet-}$ were not measured in the present work, we demonstrated that concentration levels of H_2O_2 tended to be lower in this group and that levels of oxidized proteins and lipids (unpublished data) were diminished upon α-MSH-treatment. Altogether our data suggest that α-MSH lowers the levels of $O_2^{\bullet-}$, reflective of an ameliorated redox profile in ingWAT of obese mice.

Detoxification of cellular H_2O_2 and lipid peroxides can be in part carried out by the antioxidant enzyme GPx-1. Attending the diminished expression of SOD2, and the lower levels of peroxidised lipids (unpublished data) in α-MSH-treated mice, it would be expected to observe a diminished expression of GPx-1 in ingWAT of obese mice, although similar levels were obtained in both experimental groups. However, it should be noted that GPx activity was not evaluated in this study. Indeed, it was demonstrated that obese mice present lower GPx-1 activity, which is considered to be protective against HFD-induced insulin resistance [222].

Furthermore, levels of antioxidant enzyme HO-1 were also similar in ingWAT of both control and α-MSH-treated animals. HO-1 has been implicated in the reestablishment of sirtuin 1 activity, thus improving adipocyte function and cellular redox status, consequently ameliorating insulin profile and inflammation in murine adipocytes [223]. For this reason, HO-1 has been nominated by many as a target for the amelioration of the deleterious effects of obesity and associated metabolic complications. Induction of HO-1 expression can be carried out by distinct transcription factors, however Nrf2 plays a prominent role in its regulation. The latter can be induced by PERK transducer, where it promotes cell survival upon ER-stress [224]. The low levels of PERK/peIF2α in ingWAT of α-MSH-treated mice could be suggestive of lower activation levels of Nrf2 and consequently of HO-1 protein. However, our results point towards to the modulation of other mechanisms independently of the Nrf2 pathway, which are responsible for the maintenance of HO-1 levels in ingWAT by α-MSH.

Intriguingly, of all the antioxidant enzymes here tested, the melanocortin α-MSH was only capable of attenuating the expression of SOD2, while the levels of the

remainders stayed unaltered. Thus, it can be questioned: If the redox profile of these animals is indeed ameliorated, why would the cell spend vital resources in the expression of these antioxidant enzymes? Attending that the treatment with α-MSH occurs in a small period, maintenance of these levels could indeed serve as a second layer of protection for AT homeostasis. If conditions in AT regress to those exhibited prior to the treatment of α-MSH, the cell could quickly adapt to the new conditions and prevent cellular damage. As for the particular case of SOD2, attenuation of SOD2 expression appears to be beneficial attending the physiological conditions previously reported, and its inhibition would not crucially prejudice cell homeodynamics upon regression, since other enzymes responsible for the processing of $O_2^{\bullet-}$ have their expression maintained.

Both PERK and IRE1α are known to induce NF-κB activation upon ER-stress [225, 226], in which the extent of translational inhibition conducted by PERK/peIF2a signaling is proportional to the levels of NF-κB activation [225, 226]. Furthermore, NF-κB is also implicated in SOD2 regulation [219]. In the present study, it was demonstrated that α-MSH diminished the levels of eIF2α phosphorylation, attenuated the IRE1α signalling pathway and diminished the expression of SOD2 enzyme. We observed that total levels of NF-κB tended to decrease in α-MSH-treated mice, although significance was not achieved due to the large standard deviation observed in the control group. Still, it was clear that the levels of the phosphorylated form of NF-κB were significantly diminished in these animals. Furthermore, although the levels of pNF-κB/NF-κB ratio were similar in both experimental conditions, it is postulated that α-MSH can indeed attenuate both phosphorylation and expression levels of NF-κB. Due to the higher standard deviation present in this analysis, interpretation of these data can be tricky. However, the diminished levels of phosphorylated NF-κB induced by α-MSH in the present work, could potentially reflect an amelioration of the redox profile in ingWAT of obese animals.

Further supporting an ameliorated redox profile in ingWAT of obese mice by α-MSH is the diminished levels of carbonylated proteins found in this study, together with a similar decreased in lipid peroxidation also verified previously by our group (unpublished data). In contrast to oxidized proteins and lipids, we demonstrated here that α-MSH was unable to reduce DNA damage as the levels of p-H2AX in ingWAT of α-MSH-treated mice remained unaltered. However, phosphorylation of H2AX has been known to occur in association with other DNA lesions, such as stalled replication forks, or even in the absence of DNA damage [227, 228]. Due to the short period of α-MSH administration, it is possible that the damage in DNA could have in fact diminished, but the de-phosphorylation of H2AX has occurred inefficiently, due to the non-stimulation of

phosphatases responsible to the elimination of p-H2AX (such as phosphatase 1α) [229]. Even so, further studies will be needed to clarify if α-MSH has the ability to modulate effectors responsible for DNA damage repair. Nevertheless, acting on antioxidant enzymes, ER stress effectors and on the general stress transcription factor NF-kB, α-MSH favours an ameliorated redox profile in ingWAT, which is mainly observed by the diminished levels of damaged biomolecules (Figure 23).

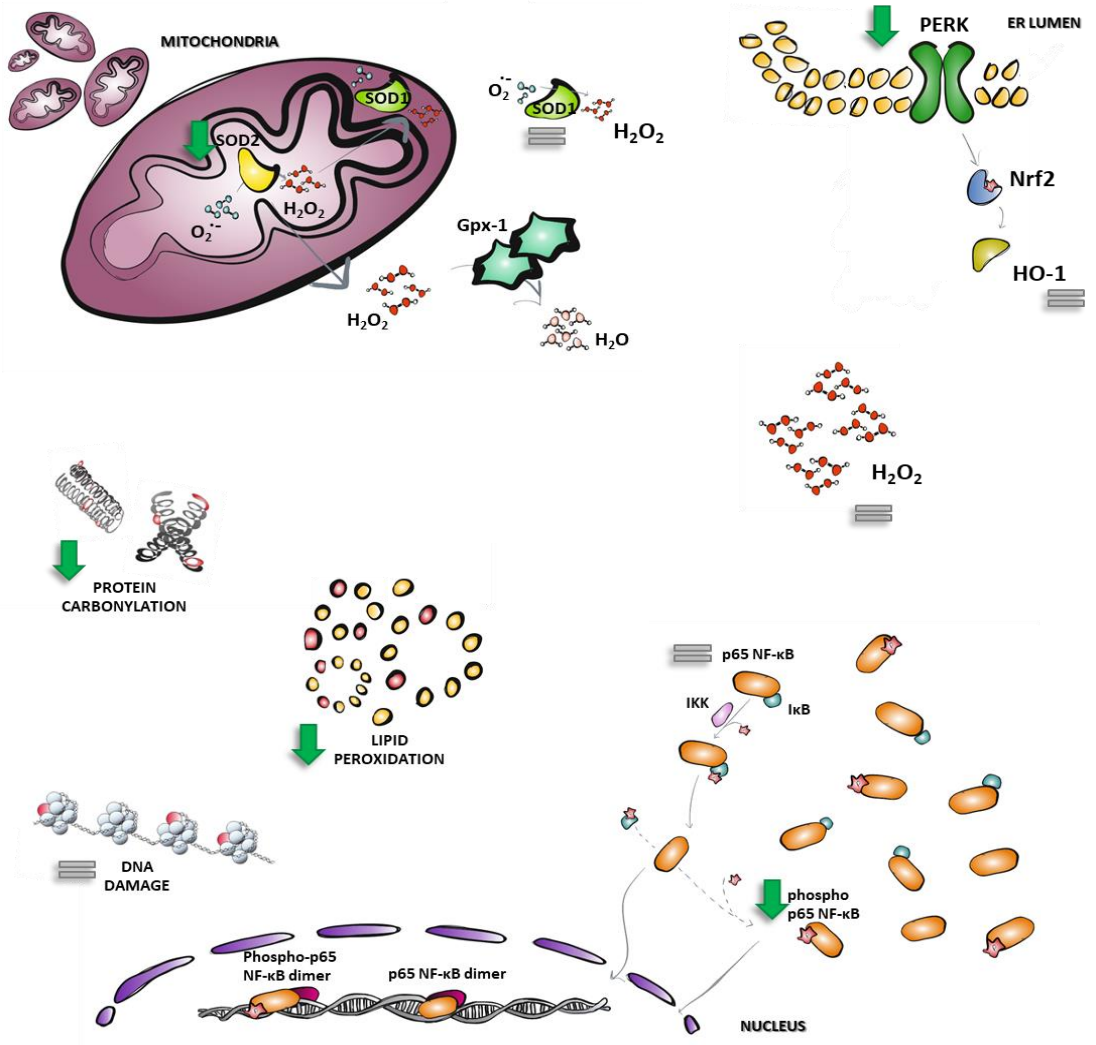

Figure 23 | The melanocortin α-MSH aids in the restitution of an ameliorated redox profile in ingWAT of obese mice. Melanocortin α-MSH diminish the expression of antioxidant enzyme SOD2, while it maintained unaltered levels of SOD1 and Gpx-1 in ingWAT of obese mice. Although it may seem like a paradox, the diminished expression of antioxidant enzymes, suggests a diminished requirement for the cell to produce these enzymes. Further supporting the idea of an ameliorated redox profile in ingWAT is the tendency of the H_2O_2 levels to decrease in α-MSH-treated mice. In agreement, this melanocortin also significatively diminished the levels of general stress transcription factor NF-κB.

5.3 Autophagy recycling mechanisms

It has been recognized that oxidative stress and autophagy are highly interconnected, although how this relation occurs is still debated in the literature. Autophagy presents an important role in obesity development and related comorbidities since it allows the cellular clearance of damaged or long-lived biomolecules. Attending the ameliorated oxidative profile observed in ingWAT from obese mice treated with α-MSH, we aimed to understand if autophagy responses were also regulated by this melanocortin. We found that α-MSH appears to inhibit to some extent autophagy mechanisms. Our data are not in accordance with published results by *Cai and colleges*, which reported that suppression of autophagy in mature adipocytes induced whole-body insulin resistance independently of adiposity and diet (236). Intriguingly, although the inhibitory effect of α-MSH in autophagy found in our study, obese mice treated with α-MSH still present an ameliorated glycaemic and lipid profile [1, 230].

Here, it was demonstrated that α-MSH did not significantly alter the expression of Beclin-1, a mediator of early autophagosome biogenesis, in ingWAT of obese mice. Son *et al.* observed that specific deletion of beclin-1 in adipocytes significantly impaired lipolysis and energy expenditure, while exhibiting an increased loss of mitochondrial mass [231]. Attending to the increased mitochondrial biogenesis observed previously in ingWAT of α-MSH-treated mice [1], together with all the beneficial effects of α-MSH on adipocyte metabolism described earlier [1, 100], it is somehow understandable that α-MSH do not alter beclin-1 expression although downregulation of autophagy process occurs. Indeed, maintenance of Beclin-1 protein levels can be beneficial to the cell, since depletion of Vsp34-Beclin-1 complex compromises cellular homeodynamics through the inhibition of autophagosome nucleation [136]. Furthermore, it has been described that beclin-1-mediated autophagy inhibits apoptosis promoting cell survival during stress [232].

Upon autophagy initiation, autophagosome elongation and maturation are regulated by many ATG proteins in a complex and still incompletely known series of events (see introduction). Autophagosome membrane elongation is known to involve two important conjugation systems, the ATG12 and the LC3 conjugation system.

Regarding the ATG12 conjugation system, it was observed that this melanocortin was unable to significantly alter the levels of ATG5, ATG7 and ATG16L1α. However, the expression levels of ATG16L1β are remarkably repressed in the ingWAT of α-MSH-treated obese mice. It was proven that specific ablation of ATG16L1 in WAT is

responsible for a significant reduced autophagic flux, as evidenced by the reduced lipidation of LC3-I to LC3-II, and increased accumulation of p62 [230]. Depletion of ATG16L1 has been also implicated in AT inflammation, insulin resistance and mitochondrial dysfunction [230]. However, other studies have demonstrated that overexpression of ATG16L1 is known to impair autophagosome biogenesis [233]. *Lystad and colleagues* demonstrated that ATG16L1β is involved in LC3B lipidation mechanisms, independently of canonical autophagy mechanisms [234]. Moreover, we were unable to fully understand the biological significance of maintaining the levels of ATG16L1α while diminishing the levels of ATG16L1β.

As for the LC3 conjugation system, it was demonstrated that this melanocortin significantly did not altered the expression of LC3-I protein. Likewise, expression levels of LC3 conjugate with PE (LC3-II), as well as of the enzymes involved in this conjugation process (ATG7 and ATG3) also remained similar in both experimental conditions. Maintenance of the levels of these enzymes can in fact explain why the levels of LC3-II do not considerably change. Curiously, $ATG7^{-/-}$ mice exhibit several characteristics in common with α-MSH-treated mice, even though its expression was not altered in ingWAT of these animals. It was observed that $ATG7^{-/-}$ mice present higher β-oxidation rates, an increased insulin sensitivity, an increased mitochondrial mass, and ultimately were resistant to HFD-induced obesity [235]. Attending the latter similarities, other methodologies should be applied, in an attempt to evaluate if ATG7 is indeed activated/modulated by MSH.

Even though LC3-II is degraded after autophagosome-lysosome fusion, its levels correlate with autophagosome number and autophagy-related structures, serving as a good indicator of autophagy activation [236]. Thus, it can be hypothesised that autophagosome number is similar in both control and α-MSH experimental groups, although autophagy flux is not necessarily the same. Previous works support this hypothesis, in which α-MSH binding to MC5R can stimulate the cAMP/PKA signaling pathway in adipocytes [192], which have been implicated in the induction of autophagy flux [231]. Albeit the support from the literature, interpretation of these results should be carried out carefully. Not only the inter-animal variations are significative, but also the assessment of autophagy flux through WB evaluation of LC3 protein levels is problematic. On one side, the use of anti-LC3 antibodies induces a bias in the analysis, as it presents a higher cross-reactivity for LC3-I than for LC3-II. On the other, LC3-I and LC3-II present distinct degradation rates [237]. Furthermore, levels of LC3-II are

significantly increased by both autophagy activation and inhibition of autophagy degradation [238] .

Thus, further studies using distinct methods are needed to unravel the role of α-MSH on the modulation of autophagy flux. More reliable methods to evaluate autophagy activation rely on the use of lysosome inhibitors, as the increased LC3 concentration in this case would reflect the autophagosome number that would have been degraded during a treatment period [238].

A common marker used to measure autophagy influx is p62, since it is almost uniquely degraded by autophagy through interaction with LC3 [239, 240]. Here we found that α-MSH does not alter the protein expression levels of p62 although it significantly diminished the levels of *p62* mRNA (unpublished results). Thus, α-MSH through unknown mechanism can stimulate the translation of p62 mRNA, allowing the maintenance of similar protein levels to those observed in the control. Perhaps, the discrepant differences found can even be explainable attending the intrinsic characteristics of the used method. The qPCR technique is much more sensible than WB, and thus small differences can pass undetected by the later. Nonetheless, the reason behind this apparent contradiction is still unclear. Still, p62 is known to play an important role in obesity progression through the regulation of adipogenesis, allowing the healthy expansion of AT [196]. Thus, maintenance of p62 expression levels could indeed be beneficial in obese ingWAT, since it could ameliorate the negative effects associated with obesity development. Notwithstanding, similar levels of both LC3 and p62 could also indicate similar accumulation of early autophagosomes in AT in both experimental groups.

However, results should be analysed carefully since expression of these autophagy markers can be either be enhanced or repressed through autophagy-independent mechanisms, since almost all autophagy related proteins exhibit non-autophagy roles (e.g. LC3 is also responsible for cytokine secretion and p62 is involved in pathogen control) [241]. Furthermore, evaluation of autophagy activity though LC3- and p62-based assays fail to detect residual autophagy, as these require the formation of LC3-II, which depend on conjugation systems [238].

The final step of autophagy involves the fusion of autophagosomes with lysosomes, a mechanism mediated by the LAMP family of proteins. The present study demonstrated that α-MSH significantly diminishes the levels of LAMP-1 glycosylated protein, while it maintained unaltered the levels of its non-glycosylated form. Additionally,

α-MSH can also significantly decreased the levels of *Lamp2* mRNA in ingWAT of DIO-mice (unpublished data). It is known that Lamp-1$^{-/-}$ mice presents conserved lysosomal properties, since compensatory mechanisms exist in the cells in a tissue-specific manner, in which upon LAMP1 depletion, expression of LAMP-2 is induced [242]. Although levels of LAMP2 protein were not accessed, these are expected to be reduced in α-MSH. Thus, our results suggest that the maintenance of LAMP1 levels, could be result from the attempt to compensate the expression of LAMP-2 protein. Although the LAMP proteins pay an important role on the endocytic pathway, the physiological significance of the obtained results remains unknown, since its absence seems to not fully impair this process. However, it is possible that α-MSH impairs the post-translational regulation of LAMP-1, through the regulation of endoglycosidases, not evaluated in the present study. Through the impairment of LAMP-1 glycosylation, this melanocortin could in fact attenuate the fusion of lysosomes with autophagosomes, thus attenuating the autophagy flux. Furthermore, clearance of autophagosomes is not known to be enhanced or repressed in this study and would deserve to be further investigated in consequent studies.

In conclusion, it was demonstrated in the present study that autophagy mechanisms are attenuated in obese ingWAT upon exposure to α-MSH (Figure 24). Attenuation of the autophagy mechanisms are concordant with the diminished levels of peroxidised lipids observed in ingWAT of α-MSH-treated mice (unpublished results), as lipid peroxidation derived aldehydes are known to stimulate this pathway. Furthermore, the attenuation of autophagy mechanisms also supports the activation of the mTORC1 pathway, whose stimulation by melanocortin α-MSH needs to be further confirmed in ingWAT. It seems clear that autophagosome accumulation is similar in both experimental groups, although fusion with lysosomes may be impaired in α-MSH-treated mice, attending the diminished levels of LAMP proteins. Even though autophagosome accumulation remain unaltered, its clearance can be compromised in obesity and thus affecting autophagy response. Further studies are needed, to fully comprehend the autophagy process modulated by this melanocortin, and respective physiological effects resulting from it.

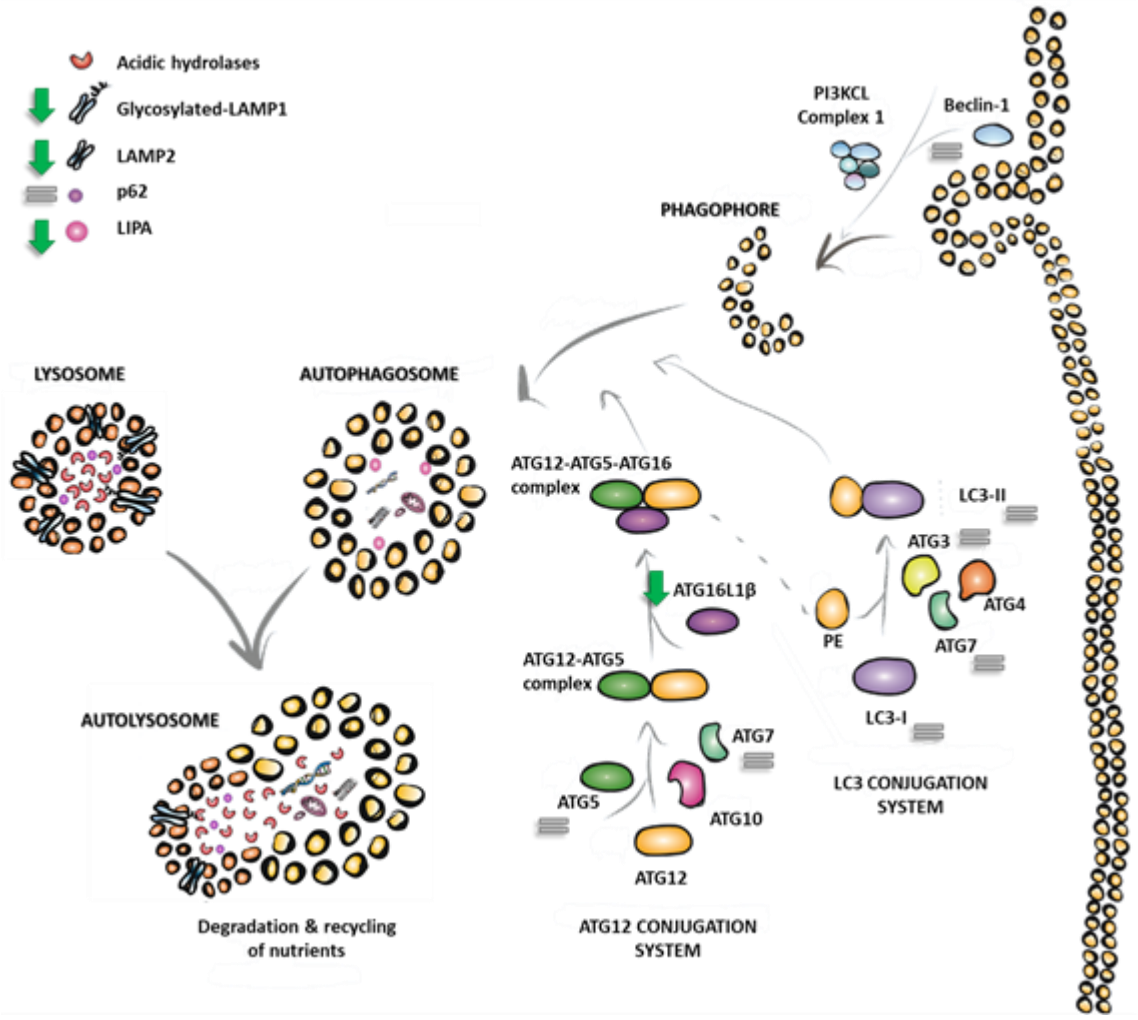

Figure 24 | Autophagy responses are suggested to be attenuated by α-MSH in ingWAT of obese mice. Although autophagy initiation is not suggested to be altered in both experimental groups, the expression of some key proteins in the LC3 and ATG12 conjugation systems are observed. It was demonstrated that levels of ATG16L1β levels were significantly decreased in ingWAT of α-MSH treated animals.

6. CONCLUDING REMARKS

The present study highlights a novel role for the melanocortin α-MSH, as a modulator of cellular stress responses and autophagy mechanisms in obese ingWAT (Figure 25).

α-MSH propensity the fine-tuning of the ER-stress response, through the direct modulation of both PERK and IRE1α signalling pathways, being able to maintain the expression of ATF4, a known inducer of cytoprotective genes. Presumably, and here firstly hypothesized, this effect could be due to the stimulation of the mTORC1 pathway. Alongside, attending that α-MSH significantly diminishes the splicing of Xbp1 (unpublished results), the IRE1α pathway is additionally suggested to be modulated. Similarly, α-MSH decreased oxidative stress in ingWAT, as demonstrated by the reduced expression of mitochondrial enzyme SOD2 and phosphorylation of p65 NF-κB. Moreover, preliminary data revealed that levels of H_2O_2 in ingWAT tended to decrease in obese mice treated with α-MSH. Concordantly with the amelioration of both ER-stress and oxidative stress responses in ingWAT, α-MSH is here suggested to also attenuate autophagy mechanisms. Notwithstanding, first and foremost, the modulatory effect of α-MSH on cellular stress responses is reflected in a significant decline of the levels of carbonylated proteins and peroxidised lipids (unpublished results), further supporting the denouement that α-MSH induces an ameliorated redox profile of ingWAT.

In sum, the present work proposes a model in which α-MSH aids in the improvement of redox homeodynamics in obese AT; by integrating several signalling pathways involved in ER-stress, oxidative stress and autophagy mechanisms. A novel therapeutical role for the melanocortin α-MSH can possibly emerge in the obesity field aiming the direct targeting of dysfunctional AT. Furthermore, knowledge obtained in the scope of this work could bestow to the development of safer drugs targeting obese AT, putting AT anew under the spotlight in the battle against obesity pandemic.

Obesity is one of the most visible, yet neglected, pathologies of our century. The health, sociological and socioeconomic impacts of obesity cannot continue to be overlooked.

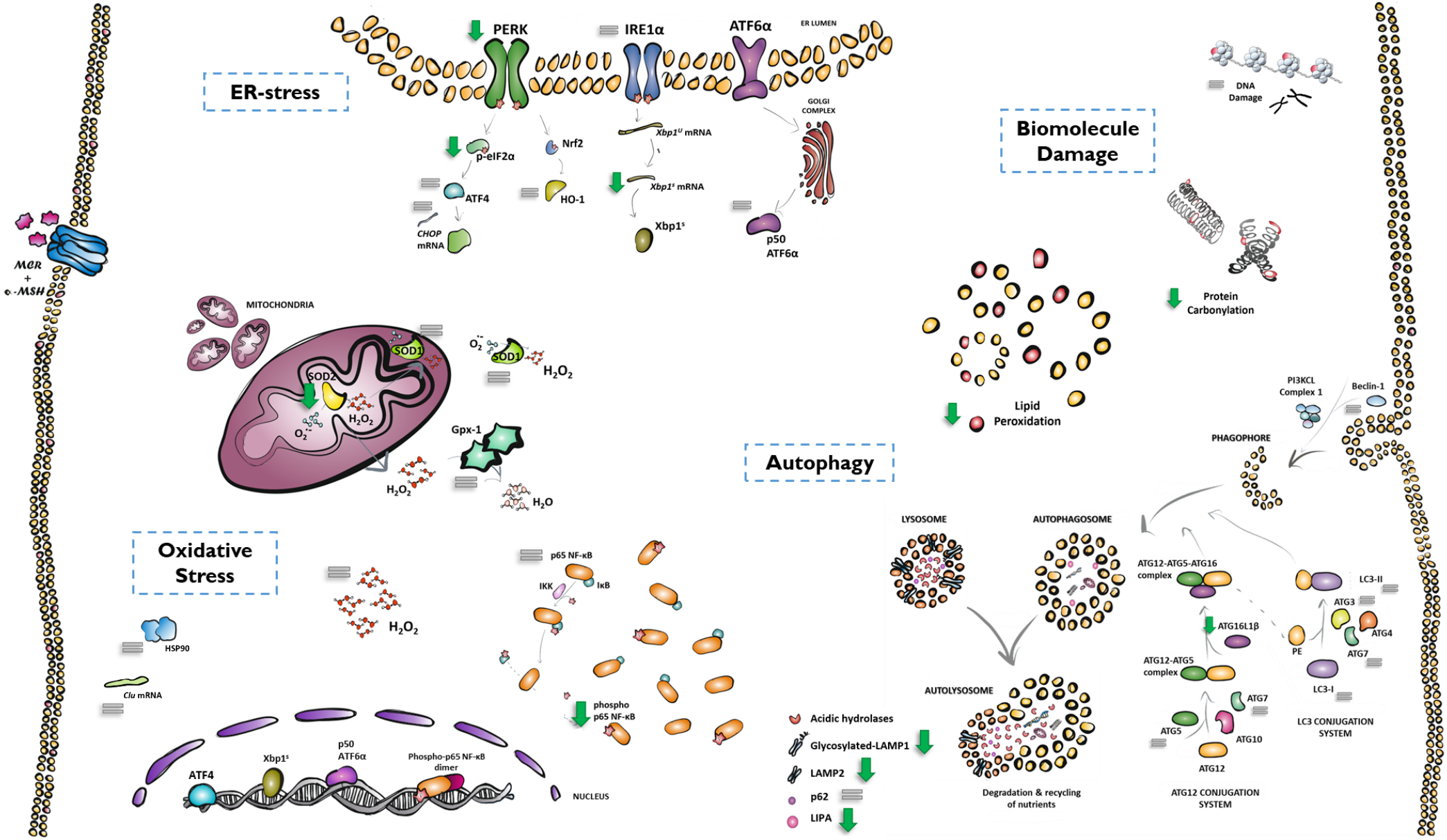

Figure 25 | α-MSH is suggested to aid in the reestablishment of obese AT redox homeodynamics through the modulation of cellular stress auto phagy signalling pathways.

7. FUTURE PERSPECTIVES

Obese individuals experience in first-hand the difficulty to lose excess body weight. Several strategies have been used to tackle obesity at the individual and public level, such as: caloric restriction, pharmacotherapy, bariatric surgery and even through educational physical and dietary programmes [11, 12]. Notwithstanding, weight loss promoted by these methods is still discouraging and disappointing, with most patients regaining weight in the long run. Primary causes of weight regain can be elicited by two distinct disorders: metabolic, which causes an elevation of body-weight set point; and hedonic, which causes an impaired activity of the hedonic regulation system, also known as "the cognitive and emotional brain" [6, 243]. Additionally, improper remodelling of AT after weight loss contributes *per se* to weight re-gain, by contributing to increased appetite and lower expenditure energy levels [244]. Discussions about which are the main problems and best approaches to contra-balance the aforementioned mechanisms have been addressed in the literature.

Attending the increased prevalence of this disease worldwide, questions regarding the effectiveness of the current approaches used to combat it have been raised. Most anti-obesity drugs have non-compensatory results owning to its undesirable side effects and the reduced efficacy (3-7%, calculated by net weight loss). Most of the negative side effects observed, are due to the modulatory effects of anti-obesity drugs on the activity and function of the CNS. Moreover, administration of these drugs continues to be challenging attending individual variation [245].

Unfortunately, in the past couple of years no major progress in the design and development of safer and efficient anti-obesity drugs has been made [243]. The development of safer drugs is thus obligatory. Emerging evidence suggests that direct targeting of AT by anti-obesity drugs is a safer approach to combat obesity, since adverse secondary effects resultant from their activity in the CNS are avoided to the fullest. Some authors suggest the exploitation of AT metabolic plasticity, as a strategy to follow in order to tackle obesity [246]. Others defend that improvement of the immune response is a better therapeutic option, as repression of this response is thought to be the explanation behind the inefficiency of anti-inflammatory therapeutics in obesity and metabolic disorders. Although the believe that inflammatory signals have deleterious effects on cellular metabolism, acute inflammatory responses have been suggested to have a protective role in AT of HFD-fed mice, allowing the healthy expansion and

remodelling of this organ, besides protecting other organs from ectopic deposition of fat [247]. Also, the initial inflammatory response is thought to have evolved as a defence mechanism against the excessive storage of nutrients in AT, through the blockage or counteracting of insulin action, which over time evolved into a maladaptive one [243]. Other authors highlight the complexity aetiology of obesity and the amount of cellular pathways affected, claiming that treatment strategies should be as complex as the disease itself. It is suggested by some authors that only a combinatory approach could have a positive effect on obesity treatment, perhaps through the use of drugs capable of increasing energy expenditure and appetite suppressants [243]. However, it is widely accepted by the scientific community, that deciphering AT biology, will represent a great step forward in the war against obesity.

The present study brought light into AT dynamics, through the assessment of the stress and signalling pathways triggered in obese ingWAT by α-MSH. Further studies should also ascertain the impact of the other melanocortins in obese AT. For example, the effect of deacetyl- and diacetyl- α-MSH in AT should also be evaluated, as acetylation of this peptide significantly impacts (1) the melanotropic potency *in vitro*, (2) the lipolytic potency *in vivo* and (3) the kinetics *in vivo* (acetylation has been shown to reduce the degradation rates of this peptide inside and outside circulation) [67]. Elucidation of the physiological roles of all these three melanocortins would be far-reaching, as in the past 20 years, as observed by doing a simple PubMed research, almost no research in this specific area has been made.

The present dissertation highlighted a novel role therapeutic role for melanocortin α-MSH, which through the modulation of cellular stress signalling pathways and autophagy mechanisms; appears to contribute to the overall amelioration of the metabolic profile observed previously in obesemice. Indeed, thinking that this specific melanocortin exhibits a therapeutic role against obesity is very ambitious, and thus this hypothesis needs to be further confirmed in more comprehensive studies.

Follow-up studies not only would need to evaluate the effect of this specific peptide in other fat depots (namely visceral depots, which are more intrinsically associated with the metabolic abnormalities observed in obesity), but also in other tissues. A more comprehensive study would allow us to evaluate the effect of this melanocortin globally, and thus access potential risk associated with its exogenous administration. It cannot be forgotten that the concentration of α-MSH administered is significantly higher than the one considered to be natural physiologically. Furthermore,

the current study relied on the intraperitoneally administration of α-MSH in ingWAT, during a short period of time (2 weeks) in obese mice. Thus, further studies should also access which would be the most favourable method for α-MSH administration and treatment duration (as the modification induced by obesity in AT are long-lasting and nefarious).

Also, this dissertation has focused on the effect of this melanocortin in obese C57BL/6 mice, which are commonly used as animal models for DIO. Indeed, this model is adequate for the evaluation of anti-obesity drugs and therapies, as these animals mimic metabolic syndrome in Humans [248]. However, as reflected in the results presented in this dissertation, this animal model presented a significative variance for the assessed proteins; thus limiting the study by making it harder to evaluate the obtained results, and consequently, to comprehend the physiological implications of α-MSH action. Furthermore, the melanocortin system presents species-specific characteristics, which could affect cell- and tissue-cellular signalling pathways differently in both rodents and humans. Thus, it would also be interesting to evaluate the effect of α-MSH on distinct model systems, to defuse the limitations imposed by our system.

Follow-up studies should attempt to clarify the role of α-MSH on general cellular signalling pathways, as well as the reassessment of the stress signalling pathways and recycling mechanisms here evaluated. Regarding the cellular pathways here examined, it would be enriching the evaluation of distinct effectors of the pathways here tested, as these present important roles in obesity pathophysiology.

Generally speaking, not only it would be interesting to evaluate the expression levels of distinct protein biomarkers upon treatment with α-MSH, but also if these suffer post-translational modifications which are key fine-tunning of its activity and physiological function (e.g. mass spectrometry). Further relevant for the evaluation of global changes in post-translational modification profiles, WB and immunofluorescence techniques may also be a rewarding approach. Also, protein localization, as well as protein-protein interactions, are pivotal to the understanding of protein dynamics. Cellular localization can be evaluated in situ through immunofluorescence or immunohistochemistry. Protein-protein interactions can be evaluated through proximity ligation assays (which at the same time allows the determination of cellular location) or through fluorescence resonance energy transfer assays. Additionally, to establish the link between protein and genome regulation, evaluation of epigenetic and protein-DNA interactions would also be interesting. This assessment could be carried out through chromatin

immunoprecipitation assays, followed up by DNA identification (e.g. PCR, microarrays or DNA sequencing). Also, though RNA immunoprecipitation techniques followed by PCR or cDNA sequencing, would allow on the determination of RNA-protein interactions. Through the employment of these techniques, we would have a more comprehensive view of cellular homeodynamics upon α-MSH treatment.

Obviously, the list of work above presented is very long. However, taking into consideration the results obtained in the scope of this dissertations, determining the influence of this melanocortin on some pathways would be especially crucial. As for the signalling pathways to be evaluated in further works, it would be interesting to evaluate the pathways here suggested to be activated by this melanocortin. Furthermore, assessment of the signalling pathways known to be unregulated in obesity and more intrinsically correlated with the development of related comorbidities should be evaluated.

Attending the diminished levels of carbonylated proteins and peroxidised lipids in ingWAT of α-MSH-treated mice, the specific oxidative modifications occurring in these biomolecules should be analysed. Also, cellular recycling mechanisms responsible for its clearance should be evaluated, as the repair/elimination of specific oxidative modifications is carried out through specific mechanisms (e.g. carbonylated proteins are specifically degraded by the proteasome). Among these, autophagy repair mechanisms would necessarily need to be re-evaluated attending the reasons discussed in the discussion section.

The employment of distinct techniques, as well as the testing of other cellular biomarker would be enriching, as it would lessen the limitations associated with our study. Having into consideration the suggested beneficial effect of α-MSH, not only in AT but also in systemic metabolism; deciphering of the molecular mechanisms by it affected in AT would shed light into the most beneficial signalling pathways to be pharmacologically modulated in obesity treatment. Thus, this work will contribute to the development of safer anti-obesity drugs, which would target the dysfunctional obese adipose tissue directly. Still, a deeper knowledge in adipocyte biology and obesity pathophysiological molecular mechanisms is necessary to strengthen the foundations for the development of new efficient therapeutic strategies.

8. REFERENCES

1. Rodrigues, A.R., et al., *Peripherally administered melanocortins induce mice fat browning and prevent obesity.* Int J Obes (Lond), 2019. **43**(5): p. 1058-1069.
2. Organization, W.H. *Obesity and Overweight*. 2020 [cited 2020; Available from: https://www.who.int/news-room/fact-sheets/detail/obesity-and-overweight.
3. NCD-RisC, *Trends in adult body-mass index in 200 countries from 1975 to 2014: a pooled analysis of 1698 population-based measurement studies with 19·2 million participants.* The Lancet, 2016. **387**(10026): p. 1377-1396.
4. Gaio, V., et al., *Prevalence of overweight and obesity in Portugal: Results from the First Portuguese Health Examination Survey (INSEF 2015).* Obes Res Clin Pract, 2018. **12**(1): p. 40-50.
5. Oliveira, A., et al., *Prevalence of general and abdominal obesity in Portugal: comprehensive results from the National Food, nutrition and physical activity survey 2015-2016.* BMC Public Health, 2018. **18**(1): p. 614.
6. Yu, Y.-H. and J. Kaberi-Otarod, *Primary Causes of Adipose Tissue Weight Gain.* 2019: p. 157-172.
7. Roy B, G.S., Sathian B, Banerjee I., *Genetic basis of obesity: a review.* Journal of Biomedical Sciences, 2016. **3**(2): p. 24-28.
8. Bluher, M., *Obesity: global epidemiology and pathogenesis.* Nat Rev Endocrinol, 2019. **15**(5): p. 288-298.
9. Nicolaidis, S., *Environment and obesity.* Metabolism, 2019. **100S**: p. 153942.
10. Abete, I., et al., *Genetic Regulation of Energy Homeostasis.* 2020: p. 175-180.
11. Gonzalez-Muniesa, P., et al., *Obesity.* Nat Rev Dis Primers, 2017. **3**: p. 17034.
12. Oussaada, S.M., et al., *The pathogenesis of obesity.* Metabolism, 2019. **92**: p. 26-36.
13. De Lorenzo, A., et al., *Why primary obesity is a disease?* Journal of Translational Medicine, 2019. **17**(1).
14. Fosbol, M.O. and B. Zerahn, *Contemporary methods of body composition measurement.* Clin Physiol Funct Imaging, 2015. **35**(2): p. 81-97.
15. Heymsfield, S.B., et al., *Multi-component molecular-level body composition reference methods: evolving concepts and future directions.* Obes Rev, 2015. **16**(4): p. 282-94.
16. Jastreboff, A.M., et al., *Obesity as a Disease: The Obesity Society 2018 Position Statement.* Obesity (Silver Spring), 2019. **27**(1): p. 7-9.

17. Gepstein, V. and R. Weiss, *Obesity as the Main Risk Factor for Metabolic Syndrome in Children.* Front Endocrinol (Lausanne), 2019. **10**: p. 568.
18. Ortega-Loubon, C., et al., *Obesity and its cardiovascular effects.* Diabetes Metab Res Rev, 2019. **35**(4): p. e3135.
19. Fuster, J.J., et al., *Obesity-Induced Changes in Adipose Tissue Microenvironment and Their Impact on Cardiovascular Disease.* Circ Res, 2016. **118**(11): p. 1786-807.
20. Chan, G. and C.T. Chen, *Musculoskeletal effects of obesity.* Curr Opin Pediatr, 2009. **21**(1): p. 65-70.
21. Quail, D.F. and A.J. Dannenberg, *The obese adipose tissue microenvironment in cancer development and progression.* Nat Rev Endocrinol, 2019. **15**(3): p. 139-154.
22. Avgerinos, K.I., et al., *Obesity and cancer risk: Emerging biological mechanisms and perspectives.* Metabolism, 2019. **92**: p. 121-135.
23. Rey-López, J.P., et al., *The prevalence of metabolically healthy obesity: a systematic review and critical evaluation of the definitions used.* Obesity Reviews, 2014. **15**(10): p. 781-790.
24. Weyer, C., et al., *Enlarged subcutaneous abdominal adipocyte size, but not obesity itself, predicts Type II diabetes independent of insulin resistance.* Diabetologia, 2000. **43**: p. 1498-1506.
25. Antonopoulos, A.S. and D. Tousoulis, *The molecular mechanisms of obesity paradox.* Cardiovasc Res, 2017. **113**(9): p. 1074-1086.
26. Chait, A. and L.J. den Hartigh, *Adipose Tissue Distribution, Inflammation and Its Metabolic Consequences, Including Diabetes and Cardiovascular Disease.* Front Cardiovasc Med, 2020. **7**: p. 22.
27. Berry, D.C., et al., *The developmental origins of adipose tissue.* Development, 2013. **140**(19): p. 3939-49.
28. Luong, Q., J. Huang, and K.Y. Lee, *Deciphering White Adipose Tissue Heterogeneity.* Biology, 2019. **8**(2): p. 23.
29. Kahn, C.R., G. Wang, and K.Y. Lee, *Altered adipose tissue and adipocyte function in the pathogenesis of metabolic syndrome.* J Clin Invest, 2019. **129**(10): p. 3990-4000.
30. Hassan, M., N. Latif, and M. Yacoub, *Adipose tissue: friend or foe?* Nat Rev Cardiol, 2012. **9**(12): p. 689-702.

31. Dichamp, J., et al., *3D analysis of the whole subcutaneous adipose tissue reveals a complex spatial network of interconnected lobules with heterogeneous browning ability.* Sci Rep, 2019. **9**(1): p. 6684.
32. Lee, M.J., Y. Wu, and S.K. Fried, *Adipose tissue heterogeneity: implication of depot differences in adipose tissue for obesity complications.* Mol Aspects Med, 2013. **34**(1): p. 1-11.
33. Coelho, M., T. Oliveira, and R. Fernandes, *Biochemistry of adipose tissue: an endocrine organ.* Arch Med Sci, 2013. **9**(2): p. 191-200.
34. Mizuno, H., et al., *Adipose-Derived Stem Cells in Regenerative Medicine.* 2017: p. 459-479.
35. Luong, Q. and K.Y. Lee, *Adipose Tissue*, L. Szablewski, Editor. 2018, Intechopen. p. 177-206.
36. Gesta, S. and C.R. Kahn, *Adipose Tissue Biology*, M.E. Symonds, Editor. 2017, Springer Science. p. 170-171.
37. Longo, M., et al., *Adipose Tissue Dysfunction as Determinant of Obesity-Associated Metabolic Complications.* Int J Mol Sci, 2019. **20**(9).
38. Cinti, S., *White, brown, beige and pink: A rainbow in the adipose organ.* Current Opinion in Endocrine and Metabolic Research, 2019. **4**: p. 29-36.
39. Wajchenberg, B.L., et al., *Depot-Specific Hormonal Characteristics of Subcutaneous and Visceral Adipose Tissue and their Relation to the Metabolic Syndrome.* Horm Metab Res, 2002. **34**: p. 616-621.
40. Tchkonia, T., et al., *Different fat depots are distinct mini-organs.* Current Opinion in Endocrinology & Diabetes, 2001. **8**: p. 227-234.
41. Smith, S.R., et al., *Contributions of total body fat, abdominal subcutaneous adipose tissue compartments, and visceral adipose tissue to the metabolic complications of obesity.* Metabolism, 2001. **50**(4): p. 425-35.
42. Mulya, A. and J.P. Kirwan, *Brown and Beige Adipose Tissue: Therapy for Obesity and Its Comorbidities?* Endocrinol Metab Clin North Am, 2016. **45**(3): p. 605-21.
43. Ikeda, K., P. Maretich, and S. Kajimura, *The Common and Distinct Features of Brown and Beige Adipocytes.* Trends Endocrinol Metab, 2018. **29**(3): p. 191-200.
44. Wang, W. and P. Seale, *Control of brown and beige fat development.* Nat Rev Mol Cell Biol, 2016. **17**(11): p. 691-702.
45. Cinti, S., *Pink Adipocytes.* Trends Endocrinol Metab, 2018. **29**(9): p. 651-666.

46. Giordano, A., et al., *White, brown and pink adipocytes: the extraordinary plasticity of the adipose organ.* Eur J Endocrinol, 2014. **170**(5): p. R159-71.
47. Giordano, A., et al., *Mammary alveolar epithelial cells convert to brown adipocytes in post-lactating mice.* J Cell Physiol, 2017. **232**(11): p. 2923-2928.
48. Li, L., et al., *Brown adipocytes can display a mammary basal myoepithelial cell phenotype in vivo.* Mol Metab, 2017. **6**(10): p. 1198-1211.
49. Stenkula, K.G. and C. Erlanson-Albertsson, *Adipose cell size: importance in health and disease.* Am J Physiol Regul Integr Comp Physiol, 2018. **315**(2): p. R284-R295.
50. Arner, P., et al., *Dynamics of human adipose lipid turnover in health and metabolic disease.* Nature, 2011. **478**(7367): p. 110-113.
51. Jernas, M., et al., *Separation of human adipocytes by size: hypertrophic fat cells display distinct gene expression.* FASEB J, 2006. **20**(9): p. 1540-2.
52. Skurk, T., et al., *Relationship between Adipocyte Size and Adipokine Expression and Secretion.* The Journal of Clinical Endocrinology & Metabolism, 2007. **92**(3): p. 1023-1033.
53. Mraz, M. and M. Haluzik, *The role of adipose tissue immune cells in obesity and low-grade inflammation.* Journal of Endocrinology, 2014. **222**(3): p. R113-R127.
54. Cildir, G., S.C. Akincilar, and V. Tergaonkar, *Chronic adipose tissue inflammation: all immune cells on the stage.* Trends Mol Med, 2013. **19**(8): p. 487-500.
55. Weisberg, S.P., et al., *Obesity is associated with macrophage accumulation in adipose tissue.* Journal of Clinical Investigation, 2003. **112**(12): p. 1796-1808.
56. Catrysse, L. and G. van Loo, *Adipose tissue macrophages and their polarization in health and obesity.* Cell Immunol, 2018. **330**: p. 114-119.
57. Marcelin, G., et al., *Deciphering the cellular interplays underlying obesity-induced adipose tissue fibrosis.* Journal of Clinical Investigation, 2019. **129**(10): p. 4032-4040.
58. Sun, K., C.M. Kusminski, and P.E. Scherer, *Adipose tissue remodeling and obesity.* J Clin Invest, 2011. **121**(6): p. 2094-101.
59. Garfield, A.S., et al., *Role of central melanocortin pathways in energy homeostasis.* Trends Endocrinol Metab, 2009. **20**(5): p. 203-15.
60. Hillebrand, J.J., M.J. Kas, and R.A. Adan, *To eat or not to eat; regulation by the melanocortin system.* Physiol Behav, 2006. **89**(1): p. 97-102.
61. Gantz, I. and T. Fong, *The melanocortin system.* Am J Physiol Endocrinol Metab, 2003. **284**: p. E468–E474.

62. Nogueiras, R., et al., *The central melanocortin system directly controls peripheral lipid metabolism.* J Clin Invest, 2007. **117**(11): p. 3475-88.

63. Shen, W.J., et al., *Melanocortin neurons: Multiple routes to regulation of metabolism.* Biochim Biophys Acta Mol Basis Dis, 2017. **1863**(10 Pt A): p. 2477-2485.

64. Cawley, N.X., Z. Li, and Y.P. Loh, *60 YEARS OF POMC: Biosynthesis, trafficking, and secretion of pro-opiomelanocortin-derived peptides.* J Mol Endocrinol, 2016. **56**(4): p. T77-97.

65. Cortes, R., et al., *Evolution of the melanocortin system.* Gen Comp Endocrinol, 2014. **209**: p. 3-10.

66. Dores, R.M., *Adrenocorticotropic hormone, melanocyte-stimulating hormone, and the melanocortin receptors: revisiting the work of Robert Schwyzer: a thirty-year retrospective.* Ann N Y Acad Sci, 2009. **1163**: p. 93-100.

67. Rudman, D., et al., *Three types of alpha-melanocyte-stimulating-hormone: bioactivities and half-lives.* American Journal of Physiology, Endocrinology and Metabolism, 1983. **245**(1): p. E47-E54.

68. Emeson, R.E. and B.A. Eipper, *Characterization of Pro-ACTH/Endorphin-Derived Peptides in Rat Hypothalamus.* The Journal of Neuroscience, 1986. **6**(3): p. 837-849.

69. Mountjoy, K.G., et al., *Desacetyl-alpha-melanocyte stimulating hormone and alpha-melanocyte stimulating hormone are required to regulate energy balance.* Mol Metab, 2018. **9**: p. 207-216.

70. Abbott, C.R., et al., *Investigation of the melanocyte stimulating hormones on food intake Lack of evidence to support a role for the melanocortin-3-receptor.* Brain Research, 2000. **869**(203-210).

71. Yang, L.K. and Y.X. Tao, *Biased signaling at neural melanocortin receptors in regulation of energy homeostasis.* Biochim Biophys Acta Mol Basis Dis, 2017. **1863**(10 Pt A): p. 2486-2495.

72. Rodrigues, A.R., H. Almeida, and A.M. Gouveia, *Intracellular signaling mechanisms of the melanocortin receptors: current state of the art.* Cell Mol Life Sci, 2015. **72**(7): p. 1331-45.

73. Sun, Y., D. McGarrigle, and X.Y. Huang, *When a G protein-coupled receptor does not couple to a G protein.* Mol Biosyst, 2007. **3**(12): p. 849-54.

74. Cai, M. and V.J. Hruby, *The Melanocortin Receptor System: A Target for Multiple Degenerative Diseases.* Curr Protein Pept Sci., 2016. **17**(5): p. 488-498.

75. Cerda-Reverter, J.M., et al., *Involvement of melanocortin receptor accessory proteins (MRAPs) in the function of melanocortin receptors.* Gen Comp Endocrinol, 2013. **188**: p. 133-6.

76. Sebag, J.A. and P.M. Hinkle, *Regions of melanocortin 2 (MC2) receptor accessory protein necessary for dual topology and MC2 receptor trafficking and signaling.* J Biol Chem, 2009. **284**(1): p. 610-8.

77. Asai, M., et al., *Loss of function of the melanocortin 2 receptor accessory protein 2 is associated with mammalian obesity.* Science, 2013. **341**(6143): p. 275-8.

78. Sebag, J.A., et al., *Developmental control of the melanocortin-4 receptor by MRAP2 proteins in zebrafish.* Science, 2013. **341**(6143): p. 278-81.

79. Takeuchi, S., *Agouti Family*, in *Handbook of Hormones*. 2016. p. 66-67.

80. Miller, M.W., et al., *Cloning of the mouse agouti gene predicts a secreted protein ubiquitously expressed in mice carrying the lethal yellow mutation.* Genes & Development, 1993. **7**: p. 454-467.

81. Ollmann, M.M., et al., *Antagonism of Central Melanocortin Receptors in Vitro and in Vivo by Agouti-Related Protein.* Science, 1997. **278**.

82. Hill, J., *Gene Expression and the Control of Food Intake by Hypothalamic POMC/CART Neurons.* Open Neuroendocrinol 2010. **3**: p. 21-27.

83. Anderson, E.J., et al., *60 YEARS OF POMC: Regulation of feeding and energy homeostasis by alpha-MSH.* J Mol Endocrinol, 2016. **56**(4): p. T157-74.

84. Wang, D., et al., *Whole-brain mapping of the direct inputs and axonal projections of POMC and AgRP neurons.* Front Neuroanat, 2015. **9**: p. 40.

85. Balthasar, N., et al., *Leptin receptor signaling in POMC neurons is required for normal body weight homeostasis.* Neuron, 2004. **42**(6): p. 983-91.

86. Cowley, M.A., et al., *Leptin activates anorexigenic POMC neurons through a neural network in the arcuate nucleus.* Nature, 2001. **411**(6836): p. 480-484.

87. Challis, B.G., et al., *Mice lacking pro-opiomelanocortin are sensitive to high-fat feeding but respond normally to the acute anorectic effects of peptide-YY3–36.* PNAS, 2004. **101**(34): p. 4695–4700.

88. Hinney, A., et al., *Systematic Mutation Screening of the Pro-Opiomelanocortin Gene: Indentification of Several Genetic Variants Including three Different Insertions, one Nonsense and two Missense Point Mutations in Probands of Different Weight Extremes.* Journal of Clinical Endocrinology and Metabolism., 1998. **83**(10): p. 3737-3741.

89. Hill, J.W. and L.D. Faulkner, *The Role of the Melanocortin System in Metabolic Disease: New Developments and Advances.* Neuroendocrinology, 2017. **104**(4): p. 330-346.

90. Tao, Y.X., *Chapter 6 Mutations in Melanocortin-4 Receptor and Human Obesity.* 2009. **88**: p. 173-204.

91. Farooqi, I.S., et al., *Clinical Spectrum of Obesity and Mutations in the Melanocortin 4 Receptor Gene.* The new england journal of medicine, 2003. **348**(12): p. 1085-1096.

92. Farooqi, I.S., et al., *Dominant and recessive inheritance of morbid obesity associated with melanocortin 4 receptor deficiency.* J. Clin. Invest., 2000. **106**: p. 217-279.

93. Chen, A.S., et al., *Inactivation of the mouse melanocortin-3 receptor results in increased fat mass and reduced lean body mass.* Nature America, 2000. **26**: p. 97-102.

94. Yoshiuchi, I., *Evidence for natural selection at the melanocortin-3 receptor gene in European and African populations.* Acta Diabetol, 2016. **53**(4): p. 583-7.

95. Baron, M., et al., *Loss-of-function mutations in MRAP2 are pathogenic in hyperphagic obesity with hyperglycemia and hypertension.* Nat Med, 2019. **25**(11): p. 1733-1738.

96. Liang, J., et al., *Pharmacological effect of human melanocortin-2 receptor accessory protein 2 variants on hypothalamic melanocortin receptors.* Endocrine, 2018. **61**(1): p. 94-104.

97. Jackson, D.S., et al., *Melanocortin receptor accessory proteins in adrenal disease and obesity.* Front Neurosci, 2015. **9**: p. 213.

98. Murphy, K.G. and S.R. Bloom, *Peripheral influences on central melanocortin neurons.* Peptides, 2005. **26**(10): p. 1744-52.

99. Rohde, K., et al., *Genetics and epigenetics in obesity.* Metabolism, 2019. **92**: p. 37-50.

100. Rodrigues, A.R., H. Almeida, and A.M. Gouveia, *Alpha-MSH signalling via melanocortin 5 receptor promotes lipolysis and impairs re-esterification in adipocytes.* Biochim Biophys Acta, 2013. **1831**(7): p. 1267-75.

101. Gan, L., et al., *alpha-MSH and Foxc2 promote fatty acid oxidation through C/EBPbeta negative transcription in mice adipose tissue.* Sci Rep, 2016. **6**: p. 36661.

102. Gutteridge, J.M.C. and B. Halliwell, *Mini-Review: Oxidative stress, redox stress or redox success?* Biochem Biophys Res Commun, 2018. **502**(2): p. 183-186.

103. Sies, H., *On the history of oxidative stress: Concept and some aspects of current development.* Current Opinion in Toxicology, 2018. **7**: p. 122-126.

104. Mittal, M., et al., *Reactive oxygen species in inflammation and tissue injury.* Antioxid Redox Signal, 2014. **20**(7): p. 1126-67.

105. Phaniendra, A., D.B. Jestadi, and L. Periyasamy, *Free radicals: properties, sources, targets, and their implication in various diseases.* Indian J Clin Biochem, 2015. **30**(1): p. 11-26.

106. Ursini, F., M. Maiorino, and H.J. Forman, *Redox homeostasis: The Golden Mean of healthy living.* Redox Biology, 2016. **8**: p. 205-215.

107. Lee, J.-C., et al., *Oxidative stress and metal carcinogenesis.* Free Radical Biology and Medicine, 2012. **53**(4): p. 742-757.

108. Leonard, S.S., G.K. Harris, and X. Shi, *Metal-induced oxidative stress and signal transduction.* Free Radical Biology and Medicine, 2004. **37**(12): p. 1921-1942.

109. Dickinson, B.C. and C.J. Chang, *Chemistry and biology of reactive oxygen species in signaling or stress responses.* Nat Chem Biol, 2011. **7**(8): p. 504-11.

110. Balaban, R.S., S. Nemoto, and T. Finkel, *Mitochondria, oxidants, and aging.* Cell, 2005. **120**(4): p. 483-95.

111. Berg, J., et al., *Biochemistry*, W.H.F.a. Company, Editor. 2015. p. 523-563.

112. Viscomi, C. and M. Zeviani, *Strategies for fighting mitochondrial diseases.* Journal of Internal Medicine, 2020.

113. Muller, F.L., Y. Liu, and H. Van Remmen, *Complex III Releases Superoxide to Both Sides of the Inner Mitochondrial Membrane.* Journal of Biological Chemistry, 2004. **279**(47): p. 49064-49073.

114. Andreyev, A.Y., Y.E. Kushnareva, and A.A. Starkov, *Mitochondrial Metabolism of Reactive Oxygen Species.* Biochemistry, 2005. **70**(2): p. 200-214.

115. Veith, A. and B. Moorthy, *Role of Cytochrome P450s in the Generation and Metabolism of Reactive Oxygen Species.* Curr Opin Toxicol, 2018. **7**: p. 44-51.

116. Zeeshan, H.M., et al., *Endoplasmic Reticulum Stress and Associated ROS.* Int J Mol Sci, 2016. **17**(3): p. 327.

117. Tu, B.P. and J.S. Weissman, *Oxidative protein folding in eukaryotes: mechanisms and consequences.* J Cell Biol, 2004. **164**(3): p. 341-6.

118. Hudson, D.A., S.A. Gannon, and C. Thorpe, *Oxidative protein folding: From thiol–disulfide exchange reactions to the redox poise of the endoplasmic reticulum.* Free Radical Biology and Medicine, 2015. **80**: p. 171-182.

119. Zito, E., *ERO1: A protein disulfide oxidase and H2O2 producer.* Free Radical Biology and Medicine, 2015. **83**: p. 299-304.

120. Shergalis, A.G., et al., *Role of the ERO1-PDI interaction in oxidative protein folding and disease.* Pharmacol Ther, 2020: p. 107525.

121. Cao, S.S. and R.J. Kaufman, *Endoplasmic Reticulum Stress and Oxidative Stress in Cell Fate Decision and Human Disease.* Antioxidants & Redox Signaling, 2014. **21**(3): p. 396-413.

122. Nordzieke, D.E. and I. Medrano-Fernandez, *The Plasma Membrane: A Platform for Intra- and Intercellular Redox Signaling.* Antioxidants (Basel), 2018. **7**(11).

123. Repetto, M., J. Semprine, and A. Boveris, *Lipid Peroxidation: Chemical Mechanism, Biological Implications and Analytical Determination.* 2012.

124. Nimse, S.B. and D. Pal, *Free radicals, natural antioxidants, and their reaction mechanisms.* RSC Advances, 2015. **5**(35): p. 27986-28006.

125. Schilstra, M.J., G.A. Veldink, and J.F.G. Vliegenthart, *Kinetic Analysis of the Induction Period in Lipoxygenase Catalysis.* Biochemistry, 1993. **32**: p. 7686-7691.

126. Bacellar, I.O.L. and M.S. Baptista, *Mechanisms of Photosensitized Lipid Oxidation and Membrane Permeabilization.* ACS Omega, 2019. **4**(26): p. 21636-21646.

127. Cai, Z. and L.-J. Yan, *Protein Oxidative Modifications: Beneficial Roles in Disease and Health.* J Biochem Pharmacol Res., 2013. **1**(1): p. 15--26.

128. Stadtman, E.R. and R.L. Levine, *Protein Oxidation.* Annals of the New York Academy of Sciences, 2006. **899**(1): p. 191-208.

129. Sitte, N., *Oxidative Damage to Proteins.* Aging at the Molecular Level, 2003: p. 27-45.

130. Araújo, R.F.F.d., D.B.G. Martins, and M.A.C.S.M. Borba, *Oxidative Stress and Disease.* 2016.

131. Pacifici, R.E. and K.J.A. Davies, *Protein, Lipid and DNA Repair Systems in Oxidative Stress: The Free-Radical Theory of Aging Revisited.* Gerontology, 1991. **37**(1-3): p. 166-180.

132. Steenken, S. and S.V. Jovanovic, *How Easily Oxidizable Is DNA? One-Electron Reduction Potentials of Adenosine and Guanosine Radicals in Aqueous Solution.* J. Am. Chem. Soc., 1997. **119**: p. 617-618.

133. Bruner, S.D., D.P.G. Norman, and G.L. Verdine, *Structural basis for recognition and repair of the endogenous mutagen 8-oxoguanine in DNA.* Nature, 2000. **403**: p. 859/866.

134. Pisoschi, A.M. and A. Pop, *The role of antioxidants in the chemistry of oxidative stress: A review.* Eur J Med Chem, 2015. **97**: p. 55-74.

135. McMurray, F., D.A. Patten, and M.E. Harper, *Reactive Oxygen Species and Oxidative Stress in Obesity-Recent Findings and Empirical Approaches.* Obesity (Silver Spring), 2016. **24**(11): p. 2301-2310.

136. Choi, A.M., S.W. Ryter, and B. Levine, *Autophagy in human health and disease.* N Engl J Med, 2013. **368**(7): p. 651-62.

137. Kołodziej, U., M. Maciejczyk, and A. Zalewska, *Oxidative stress – repair systems of oxidatively damaged biomolecules.* Prog Health Sci 2018. **8**(1): p. 145-154.

138. Mohammadyani, D., et al., *Molecular speciation and dynamics of oxidized triacylglycerols in lipid droplets: Mass spectrometry and coarse-grained simulations.* Free Radic Biol Med, 2014. **76**: p. 53-60.

139. Jarc, E. and T. Petan, *Lipid Droplets and the Management of Cellular Stress.* Yale Journal of Biology and Medicine, 2019. **92**: p. 435-452.

140. Ho, N., C. Xu, and G. Thibault, *From the unfolded protein response to metabolic diseases - lipids under the spotlight.* J Cell Sci, 2018. **131**(3).

141. Sampieri, L., P. Di Giusto, and C. Alvarez, *CREB3 Transcription Factors: ER-Golgi Stress Transducers as Hubs for Cellular Homeostasis.* Front Cell Dev Biol, 2019. **7**: p. 123.

142. Volmer, R., K. Ploeg, and D. Ron, *Membrane lipid saturation activates endoplasmic reticulum unfolded protein response transducers through their transmembrane domains.* PNAS, 2013. **110**(12): p. 4628–4633.

143. Tam, A.B., et al., *The UPR Activator ATF6 Responds to Proteotoxic and Lipotoxic Stress by Distinct Mechanisms.* Dev Cell, 2018. **46**(3): p. 327-343 e7.

144. Halbleib, K., et al., *Activation of the Unfolded Protein Response by Lipid Bilayer Stress.* Mol Cell, 2017. **67**(4): p. 673-684 e8.

145. Lin, J.H., et al., *Divergent effects of PERK and IRE1 signaling on cell viability.* PLoS One, 2009. **4**(1): p. e4170.

146. Harding, H.P., et al., *Perk Is Essential for Translational Regulation and Cell Survival during the Unfolded Protein Response.* Mollecular Cell, 2001. **5**(897-904).

147. Wek, R.C., H.-Y. Jiang, and A.T. G., *Coping with stress: eIF2 kinases and translational control.* Biochemical Society Transactions, 2006. **34**: p. 7-12.

148. Sha, H., et al., *Stressed out about obesity: IRE1alpha-XBP1 in metabolic disorders.* Trends Endocrinol Metab, 2011. **22**(9): p. 374-81.

149. Korennykh, A.V., et al., *The unfolded protein response signals through high-order assembly of Ire1.* Nature, 2009. **457**(7230): p. 687-693.

150. Nekrutenko, A. and J. He, *Functionality of unspliced XBP1 is required to explain evolution of overlapping reading frames.* Trends Genet, 2006. **22**(12): p. 645-8.

151. Haze, K., et al., *Mammalian Transcription Factor ATF6 Is Synthesized as a Transmembrane Protein and Activated by Proteolysis in Response to Endoplasmic Reticulum Stress.* Molecular Biology of the Cell, 1999. **10**: p. 3787-3799.

152. Shen, J., et al., *ER Stress Regulation of ATF6 Localization by Dissociation of BiP/GRP78 Binding and Unmasking of Golgi Localization Signals.* Developmental Cell, 2002. **3**: p. 99-111.

153. Yoshida, H., et al., *XBP1 mRNA Is Induced by ATF6 and Spliced by IRE1 in Response to ER Stress to Produce a Highly Active Transcription Factor.* Cell, 2001. **107**: p. 881-891.

154. Nishitoh, H., *CHOP is a multifunctional transcription factor in the ER stress response.* J Biochem, 2012. **151**(3): p. 217-9.

155. Song, S., et al., *Crosstalk of ER stress-mediated autophagy and ER-phagy: Involvement of UPR and the core autophagy machinery.* J Cell Physiol, 2018. **233**(5): p. 3867-3874.

156. Oeckinghaus, A. and S. Ghosh, *The NF-kappaB family of transcription factors and its regulation.* Cold Spring Harb Perspect Biol, 2009. **1**(4): p. a000034.

157. Johansen, T. and T. Lamark, *Selective autophagy mediated by autophagic adapter proteins.* Autophagy, 2011. **7**(3): p. 279-96.

158. Kaushik, S., et al., *Chaperone-mediated autophagy at a glance.* J Cell Sci, 2011. **124**(Pt 4): p. 495-9.

159. Oku, M. and Y. Sakai, *Three Distinct Types of Microautophagy Based on Membrane Dynamics and Molecular Machineries.* Bioessays, 2018. **40**(6): p. e1800008.

160. Shpilka, T., N. Mizushima, and Z. Elazar, *Ubiquitin-like proteins and autophagy at a glance.* J Cell Sci, 2012. **125**(Pt 10): p. 2343-8.

161. Mizushima, N., T. Yoshimori, and Y. Ohsumi, *The role of Atg proteins in autophagosome formation.* Annu Rev Cell Dev Biol, 2011. **27**: p. 107-32.

162. Manna, P. and S.K. Jain, *Obesity, Oxidative Stress, Adipose Tissue Dysfunction, and the Associated Health Risks: Causes and Therapeutic Strategies.* Metab Syndr Relat Disord, 2015. **13**(10): p. 423-44.

163. Vincent, H.K. and A.G. Taylor, *Biomarkers and potential mechanisms of obesity-induced oxidant stress in humans.* Int J Obes (Lond), 2006. **30**(3): p. 400-18.

164. Ejarque, M., et al., *Adipose tissue mitochondrial dysfunction in human obesity is linked to a specific DNA methylation signature in adipose-derived stem cells.* Int J Obes (Lond), 2019. **43**(6): p. 1256-1268.

165. Martinez-Reyes, I., et al., *TCA Cycle and Mitochondrial Membrane Potential Are Necessary for Diverse Biological Functions.* Mol Cell, 2016. **61**(2): p. 199-209.

166. Marchi, S., S. Patergnani, and P. Pinton, *The endoplasmic reticulum-mitochondria connection: one touch, multiple functions.* Biochim Biophys Acta, 2014. **1837**(4): p. 461-9.

167. Bournat, J.C. and C.W. Brown, *Mitochondrial Dysfunction in Obesity.* Curr Opin Endocrinol Diabetes Obes., 2010. **17**(5): p. 446-452.

168. Gregor, M.F. and G.S. Hotamisligil, *Thematic review series: Adipocyte Biology. Adipocyte stress: the endoplasmic reticulum and metabolic disease.* J Lipid Res, 2007. **48**(9): p. 1905-14.

169. Özcan, U., et al., *Endoplasmic Reticulum Stress Links Obesity, Insulin Action, and Type 2 Diabetes.* Science, 2004. **306**: p. 457-461.

170. Pagliassotti, M.J., et al., *Endoplasmic reticulum stress in obesity and obesity-related disorders: An expanded view.* Metabolism, 2016. **65**(9): p. 1238-46.

171. Kawasaki, N., et al., *Obesity-induced endoplasmic reticulum stress causes chronic inflammation in adipose tissue.* Sci Rep, 2012. **2**: p. 799.

172. Carlsen, H., et al., *Diet-induced obesity increases NF-kappaB signaling in reporter mice.* Genes Nutr, 2009. **4**(3): p. 215-22.

173. Baker, R.G., M.S. Hayden, and S. Ghosh, *NF-kappaB, inflammation, and metabolic disease.* Cell Metab, 2011. **13**(1): p. 11-22.

174. Hotamisligil, G.S. and R.J. Davis, *Cell Signaling and Stress Responses.* Cold Spring Harb Perspect Biol, 2016. **8**(10).

175. Goyal, P., et al., *Identification of novel Nox4 splice variants with impact on ROS levels in A549 cells.* Biochemical and Biophysical Research Communications, 2005. **329**(1): p. 32-39.

176. Marseglia, L., et al., *Oxidative stress in obesity: a critical component in human diseases.* Int J Mol Sci, 2015. **16**(1): p. 378-400.

177. Nunez, C.E., et al., *Defective regulation of adipose tissue autophagy in obesity.* Int J Obes (Lond), 2013. **37**(11): p. 1473-80.

178. Zhang, Y., J.R. Sowers, and J. Ren, *Targeting autophagy in obesity: from pathophysiology to management.* Nat Rev Endocrinol, 2018. **14**(6): p. 356-376.

179. Sha, H., et al., *The IRE1alpha-XBP1 pathway of the unfolded protein response is required for adipogenesis.* Cell Metab, 2009. **9**(6): p. 556-64.

180. Hillary, R.F. and U. FitzGerald, *A lifetime of stress: ATF6 in development and homeostasis.* J Biomed Sci, 2018. **25**(1): p. 48.

181. Kawamata, H. and G. Manfredi, *Import, Maturation, and Function of SOD1 and Its Copper Chaperone CCS in the Mitochondrial Intermembrane Space.* Antioxidants & Redox Signaling, 2010. **13**(9): p. 1375-1384.

182. Sturtz, L.A., et al., *A fraction of yeast Cu/Zn superoxide dismutase and its metallochaperone, CCS, localize to the intermembrane space of mitochondria: a physiological role for SOD1 in guarding against mitochondrial oxidative damage.* J Biol Chem, 2001. **276**(41): p. 38084-38089.

183. Abraham, N.G., J.M. Junge, and G.S. Drummond, *Translational Significance of Heme Oxygenase in Obesity and Metabolic Syndrome.* Trends Pharmacol Sci, 2016. **37**(1): p. 17-36.

184. Pratt, R., et al., *Mechanistic Insight of Na/K-ATPase Signaling and HO-1 into Models of Obesity and Nonalcoholic Steatohepatitis.* International Journal of Molecular Sciences, 2019. **21**(1): p. 87.

185. Li, M., et al., *Treatment of Obese Diabetic Mice With a Heme Oxygenase Inducer Reduces Visceral and Subcutaneous Adiposity, Increases Adiponectin Levels, and Improves Insulin Sensitivity and Glucose Tolerance.* Diabetes, 2008. **57**(6): p. 1526-1535.

186. Burgess, A., et al., *Adipocyte Heme Oxygenase-1 Induction Attenuates Metabolic Syndrome in Both Male and Female Obese Mice.* Hypertension, 2010. **56**(6): p. 1124-1130.

187. Schieber, M. and N.S. Chandel, *ROS function in redox signaling and oxidative stress.* Curr Biol, 2014. **24**(10): p. R453-62.

188. Moreno, R., et al., *Specification of the NF-kappaB transcriptional response by p65 phosphorylation and TNF-induced nuclear translocation of IKKepsilon.* Nucleic Acids Res, 2010. **38**(18): p. 6029-44.

189. Christian, F., E.L. Smith, and R.J. Carmody, *The Regulation of NF-kappaB Subunits by Phosphorylation.* Cells, 2016. **5**(1).

190. Pradere, J.P., et al., *Negative regulation of NF-kappaB p65 activity by serine 536 phosphorylation.* Sci Signal, 2016. **9**(442): p. ra85.

191. Geng, J. and D.J. Klionsky, *The Atg8 and Atg12 ubiquitin-like conjugation systems in macroautophagy. 'Protein modifications: beyond the usual suspects' review series.* EMBO Rep, 2008. **9**(9): p. 859-64.

192. DeVorkin, L., C. Choutka, and S.M. Gorski, *The Interplay between Autophagy and Apoptosis.* 2014: p. 369-383.

193. Tanida, I., T. Ueno, and E. Kominami, *LC3 conjugation system in mammalian autophagy.* Int J Biochem Cell Biol, 2004. **36**(12): p. 2503-18.

194. Mizushima, N. and T. Yoshimori, *How to interpret LC3 immunoblotting.* Autophagy, 2007. **3**(6): p. 542-5.

195. Eskelinen, E.L., *Roles of LAMP-1 and LAMP-2 in lysosome biogenesis and autophagy.* Mol Aspects Med, 2006. **27**(5-6): p. 495-502.

196. Moscat, J. and M.T. Diaz-Meco, *Feedback on fat: p62-mTORC1-autophagy connections.* Cell, 2011. **147**(4): p. 724-7.

197. Zhang, Z., et al., *Redox signaling and unfolded protein response coordinate cell fate decisions under ER stress.* Redox Biol, 2019. **25**: p. 101047.

198. Gan, L., et al., *Foxc2 enhances proliferation and inhibits apoptosis through activating Akt/mTORC1 signaling pathway in mouse preadipocytes.* Journal of Lipid Research, 2015. **56**(8): p. 1471-1480.

199. Mounir, Z., et al., *Akt Determines Cell Fate Through Inhibition of the PERK-eIF2a Phosphorylation Pathway.* Science Signalling, 2011. **4**(192): p. 1-11.

200. Wang, C., et al., *ATF4 regulates lipid metabolism and thermogenesis.* Cell Res, 2010. **20**(2): p. 174-84.

201. Chen, H., et al., *ATF4 regulates SREBP1c expression to control fatty acids synthesis in 3T3-L1 adipocytes differentiation.* Biochim Biophys Acta, 2016. **1859**(11): p. 1459-1469.

202. Harding, H.P., et al., *An Integrated Stress Response Regulates Amino Acid Metabolism and Resistance to Oxidative Stress.* Molecular Cell, 2003. **11**(3): p. 619-633.

203. Quiros, P.M., et al., *Multi-omics analysis identifies ATF4 as a key regulator of the mitochondrial stress response in mammals.* J Cell Biol, 2017. **216**(7): p. 2027-2045.

204. Munch, C. and J.W. Harper, *Mitochondrial unfolded protein response controls matrix pre-RNA processing and translation.* Nature, 2016. **534**(7609): p. 710-3.

205. Ben-Sahra, I., et al., *mTORC1 induces purine synthesis through control of the mitochondrial tetrahydrofolate cycle.* Science, 2016. **351**(6274): p. 728-733.

206. Duvel, K., et al., *Activation of a metabolic gene regulatory network downstream of mTOR complex 1.* Mol Cell, 2010. **39**(2): p. 171-83.

207. Palam, L.R., T.D. Baird, and R.C. Wek, *Phosphorylation of eIF2 facilitates ribosomal bypass of an inhibitory upstream ORF to enhance CHOP translation.* J Biol Chem, 2011. **286**(13): p. 10939-49.

208. Suzuki, T., et al., *ER Stress Protein CHOP Mediates Insulin Resistance by Modulating Adipose Tissue Macrophage Polarity.* Cell Rep, 2017. **18**(8): p. 2045-2057.

209. Yoshida, H., et al., *ATF6 Activated by Proteolysis Binds in the Presence of NF-Y (CBF) Directly to the cis-Acting Element Responsible for the Mammalian Unfolded Protein Response.* Molecular and Cellular Biology, 2000. **20**(18): p. 6755-6767.

210. Hollien, J., et al., *Regulated Ire1-dependent decay of messenger RNAs in mammalian cells.* J Cell Biol, 2009. **186**(3): p. 323-31.

211. Teske, B., et al., *The eIF2 kinase PERK and the integrated stress response facilitate activation of ATF6 during endoplasmic reticulum stress.* Molecular Biology of the cell, 2011. **22**(22): p. 4390-4405.

212. Ye, J., et al., *ER Stress Induces Cleavage of Membrane-Bound ATF6 by the Same Proteases that Process SREBPs.* Molecular Cell, 2000. **6**: p. 1355–1364.

213. Lowe, C.E., et al., *Investigating the involvement of the ATF6alpha pathway of the unfolded protein response in adipogenesis.* Int J Obes (Lond), 2012. **36**(9): p. 1248-51.

214. Marcu, M.G., et al., *Heat Shock Protein 90 Modulates the Unfolded Protein Response by Stabilizing IRE1α.* Molecular and Cellular Biology, 2002. **22**(24): p. 8506-8513.

215. Nguyen, M.T., P. Csermely, and C. Soti, *Hsp90 chaperones PPARgamma and regulates differentiation and survival of 3T3-L1 adipocytes.* Cell Death Differ, 2013. **20**(12): p. 1654-63.

216. Klouckova, J., et al., *Plasma concentrations and subcutaneous adipose tissue mRNA expression of clusterin in obesity and type 2 diabetes mellitus: the effect of short-term hyperinsulinemia, very-low-calorie diet and bariatric surgery.* Physiol Res, 2016. **65**(3): p. 481-92.

217. Koch-Brandt, C. and C. Morgans, *Clusterin: A Role in Cell Survival in the Face of Apoptosis?* Progress in Molecular and Subcellular Biology, 1996: p. 130-149.

218. Miao, L. and D.K. St Clair, *Regulation of superoxide dismutase genes: implications in disease.* Free Radic Biol Med, 2009. **47**(4): p. 344-56.

219. Dhar, S.K. and D.K. St Clair, *Manganese superoxide dismutase regulation and cancer.* Free Radic Biol Med, 2012. **52**(11-12): p. 2209-22.

220. Han, Y.H., et al., *Adipocyte-Specific Deletion of Manganese Superoxide Dismutase Protects From Diet-Induced Obesity Through Increased Mitochondrial Uncoupling and Biogenesis.* Diabetes, 2016. **65**: p. 2639-2651.

221. Rinne, P., et al., *alpha-Melanocyte-stimulating hormone regulates vascular NO availability and protects against endothelial dysfunction.* Cardiovasc Res, 2013. **97**(2): p. 360-8.

222. Asayama, K., et al., *Effect of Obesity and Troglitazone on Expression of Two Glutathione Peroxidases: Cellular and Extracellular Types in Serum, Kidney and Adipose Tissue.* Free Rad Res, 2001. **34**: p. 337-347.

223. Lakhani, H.V., et al., *Beneficial Role of HO-1-SIRT1 Axis in Attenuating Angiotensin II-Induced Adipocyte Dysfunction.* International Journal of Molecular Sciences, 2019. **20**(13): p. 3205.

224. Cullinan, S.B., et al., *Nrf2 is a direct PERK substrate and effector of PERK-dependent cell survival.* Mol Cell Biol, 2003. **23**(20): p. 7198-209.

225. Tam, A.B., et al., *ER stress activates NF-kappaB by integrating functions of basal IKK activity, IRE1 and PERK.* PLoS One, 2012. **7**(10): p. e45078.

226. Jiang, H.Y., et al., *Phosphorylation of the alpha subunit of eukaryotic initiation factor 2 is required for activation of NF-kappaB in response to diverse cellular stresses.* Mol Cell Biol, 2003. **23**(16): p. 5651-63.

227. Ward, I.M. and J. Chen, *Histone H2AX is phosphorylated in an ATR-dependent manner in response to replicational stress.* J Biol Chem, 2001. **276**(51): p. 47759-62.

228. Soutoglou, E. and T. Misteli, *Activation of the cellular DNA damage response in the absence of DNA lesions.* Science, 2008. **320**(5882): p. 1507-10.

229. Nazarov, I.B., et al., *Dephosphorylation of histone gamma-H2AX during repair of DNA double-strand breaks in mammalian cells and its inhibition by calyculin A.* Radiat Res, 2003. **160**(3): p. 309-17.

230. Cai, J., et al., *Autophagy Ablation in Adipocytes Induces Insulin Resistance and Reveals Roles for Lipid Peroxide and Nrf2 Signaling in Adipose-Liver Crosstalk.* Cell Rep, 2018. **25**(7): p. 1708-1717 e5.

231. Son, Y., et al., *Adipocyte-specific Beclin1 deletion impairs lipolysis and mitochondrial integrity in adipose tissue.* Mol Metab, 2020. **39**: p. 101005.

232. Xie, Y., R. Kang, and D. Tang, *Role of the Beclin 1 Network in the Cross-Regulation Between Autophagy and Apoptosis*, in *Autophagy: Cancer, Other Pathologies, Inflammation, Immunity, Infection, and Aging*. 2016. p. 75-88.

233. Fujita, N., et al., *The Atg16L Complex Specifies the Site of LC3 Lipidation for Membrane Biogenesis in Autophagy.* Molecular Biology of the Cell, 2008. **19**: p. 2092-2100.

234. Lystad, A.H., et al., *Distinct functions of ATG16L1 isoforms in membrane binding and LC3B lipidation in autophagy-related processes.* Nat Cell Biol, 2019. **21**(3): p. 372-383.

235. Zhanga, Y., et al., *Adipose-specific deletion of autophagy-related gene 7 (atg7) in mice reveals a role in adipogenesis.* PNAS, 2009. **106**(47): p. 19860-19865.

236. Loos, B., A. du Toit, and J.H. Hofmeyr, *Defining and measuring autophagosome flux-concept and reality.* Autophagy, 2014. **10**(11): p. 2087-96.

237. Mizushima, N., T. Yoshimori, and B. Levine, *Methods in mammalian autophagy research.* Cell, 2010. **140**(3): p. 313-26.

238. Yoshii, S.R. and N. Mizushima, *Monitoring and Measuring Autophagy.* Int J Mol Sci, 2017. **18**(9).

239. Kovsan, J., et al., *Altered autophagy in human adipose tissues in obesity.* J Clin Endocrinol Metab, 2011. **96**(2): p. E268-77.

240. Ichimura, Y., et al., *Selective turnover of p62/A170/SQSTM1 by autophagy.* Autophagy, 2008. **4**(8): p. 1063-6.

241. Galluzzi, L. and D.R. Green, *Autophagy-Independent Functions of the Autophagy Machinery.* Cell, 2019. **177**(7): p. 1682-1699.

242. Andrejewski, N., et al., *Normal Lysosomal Morphology and Function in LAMP-1-deficient Mice.* The Jornal of Biological Chemistry, 1999. **274**(18): p. 12692-12701.

243. Saltiel, A.R., *New therapeutic approaches for the treatment of obesity.* Science Translational Medicine, 2016. **8**(323): p. 323rv2.

244. Lofgren, P., et al., *Long-term prospective and controlled studies demonstrate adipose tissue hypercellularity and relative leptin deficiency in the postobese state.* J Clin Endocrinol Metab, 2005. **90**(11): p. 6207-13.

245. Srivastava, G. and C.M. Apovian, *Current pharmacotherapy for obesity.* Nat Rev Endocrinol, 2018. **14**(1): p. 12-24.

246. Lee, Y.H., E.P. Mottillo, and J.G. Granneman, *Adipose tissue plasticity from WAT to BAT and in between.* Biochim Biophys Acta, 2014. **1842**(3): p. 358-69.

247. Wernstedt Asterholm, I., et al., *Adipocyte Inflammation Is Essential for Healthy Adipose Tissue Expansion and Remodeling.* Cell Metabolism, 2014. **20**(1): p. 103-118.

248. Buettner, R., J. Schölmerich, and C. Bollheimer, *High-fat Diets: Modeling the Metabolic Disorders of Human Obesity in Rodents.* Obesity, 2007. **15**(4): p. 798-808.